2006

Radon in Ground Water: A Study of the Measurement and Release of Waterborne Radon and Modeling of Radon Variation in Bedrock Wells

Vincente E. Guiseppe

RADON IN GROUND WATER: A STUDY OF THE MEASUREMENT AND RELEASE OF WATERBORNE RADON AND MODELING OF RADON VARIATION IN BEDROCK WELLS

By

Vincente E. Guiseppe

B.S. Millersville University of Pennsylvania, 1999

A THESIS

Submitted in Partial Fulfillment of the

Requirements for the Degree of

Doctor of Philosophy

(in Physics)

The Graduate School

The University of Maine

December, 2006

Advisory Committee:

Charles T. Hess, Professor of Physics, Advisor

R. Dean Astumian, Professor of Physics

Richard A. Morrow, Professor of Physics

Andrew S. Reeve, Associate Professor of Geological Sciences

Charles W. Smith, Professor of Physics

LIBRARY RIGHTS STATEMENT

In presenting this thesis in partial fulfillment of the requirements for an advanced degree at The University of Maine, I agree that the Library shall make it freely available for inspection. I further agree that permission for “fair use” copying of this thesis for scholarly purposes may be granted by the Librarian. It is understood that any copying or publication of this thesis for financial gain shall not be allowed without my written permission.

Signature:

Date:

RADON IN GROUND WATER: A STUDY OF THE MEASUREMENT AND RELEASE OF WATERBORNE RADON AND MODELING OF RADON VARIATION IN BEDROCK WELLS

By Vincente E. Guiseppe
Thesis Advisor: Dr. Charles T. Hess

An Abstract of the Thesis Presented
in Partial Fulfillment of the Requirements for the
Degree of Doctor of Philosophy
(in Physics)
December, 2006

Naturally occurring radon gas (^{222}Rn) exists in ground water and drinking water supplies. Research involving radon in ground water requires the ability to accurately measure radon in water. In the absence of a national program, an intercomparison study of laboratories was sanctioned by the State of Maine. The University of Maine research laboratory supplied each laboratory with water samples of various radon concentrations, served as the reference laboratory, and analyzed the results presented here. The external review of the University of Maine laboratory and agreement with some of the participating laboratories verifies its accuracy in measuring radon in water. A study of nine elementary schools in Maine examined the release of waterborne radon during water use. The release of radon into the kitchen air was measured to be greater than the EPA action level of 0.150 Bq L^{-1} (4 pCi L^{-1}) in all schools but negligible concentrations of radon were found in adjacent classrooms. In two schools over a three-fold spatial radon variation was measured suggesting that multiple detectors are needed to accurately measure waterborne radon in air. During water use, the radon in water concentration was measured periodically and many of the schools showed an increase in the radon concentration by 200 Bq L^{-1} or more. To explore this effect, nine bedrock wells were studied in detail. Measurements

of the ambient and purged radon profiles in the wells showed variations of radon concentration of samples within the well. The rock chips removed during well-drilling were analyzed for radionuclides in the ^{238}U decay series. The ^{226}Ra concentrations in the rock chips do not explain the measured vertical variation of dissolved radon. The vertical flow and fracture locations were previously determined by borehole logging to determine location of ground water inflow. A mathematical model of the ground-water flow into and through the well with radon as a tracer was tested. The model was successfully fit to data obtained from the wells that had a variation in radon concentration.

ACKNOWLEDGEMENTS

First, I would like to thank my committee. Dr. Hess provided valuable advice, direction, and experience throughout my graduate education. His vision of this study's potential provided assurance when I had doubts. Dr. Reeve generously loaned well sampling equipment and furnished the wells. For that I am grateful. Dr. Smith, Dr. Astumian, and Dr. Morrow provided needed guidance and support.

I would like to thank Dr. Gesell of Idaho State University for reviewing this thesis and providing insightful comments. Thanks also to the editors and anonymous reviewers of *Health Physics* for their comments and suggestions made reviewing manuscripts.

Financial assistance for some of this work was provided by the U.S. Environmental Protection Agency grants #IW-2645-NAEX and #X-82918201-0, State of Maine grant #402076, and through University of Maine Graduate School awards. Bob Stilwell and Steven Sprengel of the State of Maine Radiation Control Program provided invaluable collaboration for the laboratory radon in water intercomparison. Field assistance from Mary Jo Norris, Jason Grant and Travis Gould was much appreciated. Thanks to Eric Rickert for providing geophysics data from the wells.

Many past and present graduate students, far too many to name here, offered friendship and made for a complete graduate experience. Special thanks go to Travis Gould for practical assistance at many stages of this study; Dan Breton for willingness to help solve any problem; Ross Brody for always baking up something good; Jim Kenneally for the LaTeX class file; and to Simon Krughoff for, among many other things, introducing me to Linux. For handling departmental/administrative hurdles, I thank Pat Byard.

I would like to thank my family for their continued support and teaching the importance of an education. Finally, I owe everything else to the patience and loving support of my wife, Kerry. Thank you.

TABLE OF CONTENTS

LIST OF TABLES

LIST OF FIGURES

Chapter 1

INTRODUCTION

1.1 Reasons to study radon in ground water

Radon (^{222}Rn) is a naturally occurring, radioactive gas formed within the ^{238}U decay series (Fig. 1.1). According to the U.S. Environmental Protection Agency (EPA), radon is a carcinogen and the second leading cause of lung cancer in the U.S. (EPA 1999). It is estimated that 3,000 - 33,000 lung cancer deaths in the U.S. are associated with radon (NRC 1999a). On average, radon accounts for roughly 55% of one's annual radiation dose with the remaining coming from medical (11%), internal (11%), terrestrial (8%), cosmic (8%), and other sources (NCRP 1987). Radon originates in the ground, where its radioactive parents are found. It can escape from the ground and build up in low concentrations in outside air and accumulate in basements and homes (Eisenbud and Gesell 1997). The EPA has set an action level of 0.15 Bq L^{-1} (4 pCi L^{-1}) for indoor air (EPA 1986).[1] A becquerel (Bq) is a measure of activity equal to one disintegration per second. One curie (Ci) is equal to 3.7×10^{10} Bq.

Since radon can dissolve and remain in ground water until dispensed and aerated, kitchen and bathroom appliances provide an additional pathway for radon into a building. Radon in water can raise the average indoor radon concentration and locally raise exposure near water-using appliances where high concentrations of radon occur (Prichard and Gesell 1981). This is due to radon being released when water is used for such things as cleaning, bathing, dish and clothes washing, and flushing toilets. Basements of homes usually have the largest concentrations of radon from entering soil gas; bathrooms can

[1] Action should be taken to lower indoor radon concentration to below this level

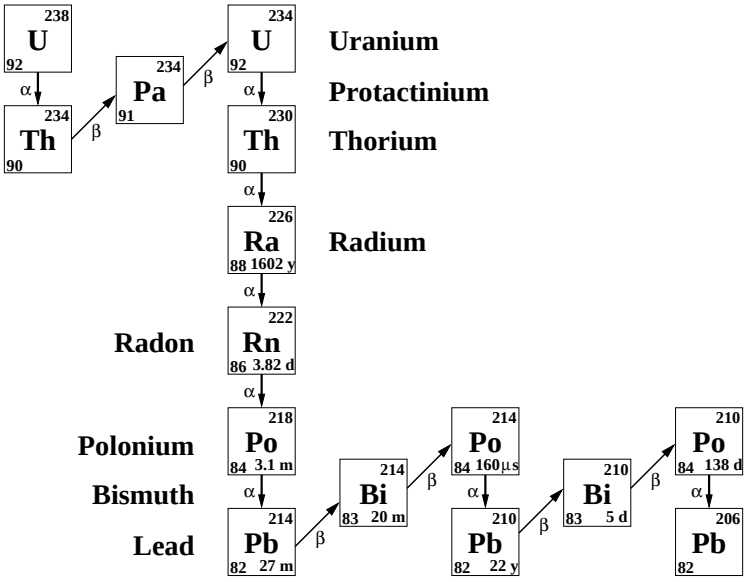

Figure 1.1: The U^{238} natural radioactive decay series (Baum et al. 2002).

have the highest concentrations of living areas[2] due to water use (Hess et al. 1985). Many studies have investigated the transfer of radon from water into air, and on average, there is 10^{-4} Bq L^{-1} in air per Bq L^{-1} in water as first proposed by Gesell and Prichard (1975). The EPA is concerned with the exposure due to radon in water and is working to set national standards on the amount of radon in water (EPA 1999, NRC 1999b).

1.2 Motivation

Previous studies have measured the average radon transfer coefficient from water to air to be between $1 \times 10^{-5} - 5 \times 10^{-4}$ in homes (NRC 1999b, Duncan et al. 1977, Prichard and Gesell 1981, Hess et al. 1982, Lachapelle 1988). An investigation identified radon transfer coefficients at rural schools in Maine that draw water from private wells (Norris et al. 2004). Schools were a logical progression from homes due to the large amounts of water used during the day and long exposure time for occupants. A model of the transfer coefficient was compared against the measured change in the radon concentration while

[2]Not the case where basements are used as living areas.

using water. The measurements of released radon did not agree within experimental uncertainty with those predicted by the model. At one school, four detectors were placed in a kitchen and a decrease of radon concentration with distance from the water faucet was observed. Norris et al. (2004) suggested that a variation of radon throughout the room could cause the discrepancy between the modeling and measurement of transfer coefficients but did not sufficiently demonstrate a variation. At one school, they measured the radon concentration in water several times while using running water. The radon increased in concentration during water usage. They suggested that a changing concentration of radon in water could provide another reason why the model did not agree with measurements.

The model used by Norris et al. (2004) attempts to predict the radon released while running water at a school. The model is given by

$$f = \frac{\Delta C_{air}}{C_w} = \frac{W\varepsilon}{VT\lambda} \tag{1.1}$$

where f is the transfer coefficient, ΔC_{air} [Bq L^{-1}] is the change in radon concentration in air, C_w [Bq L^{-1}] is the radon concentration in the water being used, W [L] is the total volume of water used in a duration of time T [min], $\overline{\varepsilon}$ is the total use-weighted emissivity of the faucets' running water, V [L] is the volume of the room and λ [min^{-1}] is the ventilation rate of the bulk room air. A faucet's emissivity is defined as the fraction of radon in water released into the air due to aeration. The derivation of this model can be found in Hess et al. (1987) and Hess and Haskell (1994). Generally, it predicts the radon release based on the amount of water used, the amount of radon aerated from the faucets running water, and the ventilation of room. However, the model was based on assumptions, which may be too simplistic. First, the radon released into a room was assumed to be well mixed. This assumption allowed the ventilation of the room to account for the loss of radon. An assumption of a uniform distribution allowed for a quantitative measurement of the released radon with a single detector anywhere in the room. If not uniform, a measurement of released radon would be dependent on the placement of a

detector. Secondly, the radon concentration of the water was assumed to remain constant over time T. If the radon concentration changes, the model will not be able to properly account for the amount released.

This study was designed to test the waterborne radon release model, determine if the assumptions used were justified, and validate how the measurements were made. Is the released radon well mixed (uniformly distributed) and can a non-uniform distribution cause the model to fail? Knowing how the radon mixes in the room impacts how the ventilation and radon release terms are incorporated into the model. A second consideration seeks to determine the extent radon can change over time during water usage and determine if the change can be explained in a predictable way. Finally, can the model disagreement be due to measurement errors caused by inadequate sample handling and analytical techniques in measuring radon in water? Measured radon in water concentration affects the calculation of the emissivities and radon in water measurement in the model. Radon in air detectors are routinely calibrated and are not as vulnerable to the protocol used as are measurements of radon in water.

1.3 Organization

This study is organized into three parts. The first part concerns validating the measurement and analytical techniques of radon in water. This study was intended to check nine laboratories against the University of Maine laboratory for their proficiency of measuring radon in water. The laboratories relied on their own methods and calibration procedures with no assistance or use of a common protocol. Even though serving as the reference laboratory, agreement with the other laboratories would also support the accuracy of the University of Maine laboratory. This part serves to confirm the overall quality of the university's measurements of radon in water.

The second part involves a study of waterborne radon in schools in Maine. The kitchens of the schools were studied to test a waterborne radon release model and measure a distribution of radon in air. Several measurements of radon in water were made while running water in the kitchen to detect any changes in concentration. This part confirmed the shortcomings of the model and discusses the impact of a spatial variation of radon in air and a temporal variation of radon in water.

The final part explores the variation of radon in ground water observed while pumping wells. Open bedrock wells were used instead of wells supplying water to homes or schools to fully eliminate any effects a plumbing system may play on radon variation. The factors controlling the presence of radon in ground water are reviewed. A mathematical model was proposed to explain the variation and was tested. Several series of experiments were conducted to develop and support the mathematical model. This part concludes by discussing the factors which cause the short term temporal variation and to what extent it can be predicted.

Chapter 2

A LABORATORY INTERCOMPARISON OF RADON IN WATER MEASUREMENTS

2.1 Introduction

2.1.1 Background

Many water testing laboratories provide measurements of radon in water for the public. However, no current federal government regulation exists to verify the accuracy of laboratories measuring radon in water. In 1993, the Maine Air and Water Radon Service Provider Registration Rules identified regulations which "...apply to all persons or companies ... that intend to conduct air or water radon services ... in the State of Maine." Specifically, it required water laboratories to "... measure radon in water according to the most recent method put forth by EPA, until EPA finalizes their radon in water measurements methods" (State of Maine 1993). Reference is made here to the US EPA Radon in Water Rule, authorized by the Safe Drinking Water Act Amendments of 1988, and first proposed in 1991 (EPA 1999). This rule, which is still proposed, would require a certification program for radon in water laboratories. All known radon in water intercomparison programs were terminated soon after the radon in water rule was proposed in anticipation that the rule and the associated certification program would soon be in place. However, after nearly a decade and a half, neither has come to pass due to disagreements over setting a maximum contaminant level (MCL), risk assessments and cost analysis (GAO 2002, CRCPD 2004). This leaves Maine, and the nation, with no current, active program to verify the accuracy or validity of radon in water analysis.

Due to indications that some laboratories had not done anything to verify radon in water analysis methods or results for over a decade, the Maine Radiation Control Program,

Radon/IAQ [Indoor Air Quality] Section (the agency responsible for overseeing Maine's radon service provider regulations) sent a questionnaire out to all laboratories registered with them for radon in water analysis. Of the twelve testing laboratories registered in Maine to measure the concentration of radon in water, two reported that they performed their own intercomparison while the remaining ten wished to know how they could participate in one. Based on these findings, the Maine Radiation Control Program, Radon/IAQ Section (Radon Section) decided to conduct an intercomparison with the University of Maine laboratory[1] serving as a reference laboratory. To ensure its ability to serve as a reference laboratory, the radon staff at the Radon Section evaluated and verified the quality assurance, protocols and storage and preparation of radionuclide standards at the University of Maine laboratory.

2.1.2 Radon in water measurement methods

Many methods have been developed to measure radon in water. In the de-emanation technique radon is bubbled from a water sample and counted in a scintillation cell or Lucas cell (Lucas 1957). Some modifications to the Lucas cell have been suggested (Mathieu et al. 1988) and the technique was made portable using a Pylon scintillation cell (Kitto et al. 1996). Alternatively, a NaI gamma spectroscopy system can be used to detect the gamma emissions of radon progeny from a water sample (Lucas 1964) and can be used with a shielded, modified Marinelli container to increase counting efficiency (Countess 1978). Another method uses an electret ion chamber to measure radon released from water to the air chamber of an electret passive environmental radon monitor (E-PERM) in order to determine the original radon concentration in water (Kotrappa and Jester 1993). The primary advantages of the E-PERM method include its low cost and minimal user training.

[1]The Environmental Radiation Laboratory, 5709 Bennett Hall, University of Maine, Orono, ME 04469

In the liquid scintillation method, introduced by Prichard and Gesell (1977), a water sample and scintillation cocktail (a solvent mixed with a fluor) are added to a low background glass vial and counted in a commercial liquid scintillation counter. This technique makes use of the high solubility of radon in some liquid scintillation cocktails and the near 100% counting efficiency of the radon and progeny. With the high solubility, the radon becomes trapped in the cocktail. Its decay, and the decay its first 4 progeny, interact with the cocktail causing it to fluoresce (emit light). The light is detected in two photo-multiplier tubes operating in coincidence counting. The decay of radon and its short-lived progeny ($t_{1/2}$ <27 min) result in three alpha particles at 5.49 MeV (^{222}Rn), 6.0 MeV (^{218}Po), and 7.69 MeV (^{214}Po). The decay of ^{214}Bi and ^{214}Pb result in two beta particles of endpoint energies ranging 0.67–3.27 MeV (Prichard and Gesell 1977, Baum et al. 2002). Many radon testing laboratories use this method due to the minimal preparation time, small sample volume, and automatic sample changing capabilities of the liquid scintillation counter.

In their 1999 proposed radon in water rule (EPA 1999), the EPA specified two analytical methods that fit EPA's criteria as compliance monitoring methods. These are the Lucas cell de-emanation method (Whittaker et al. 1987) and the liquid scintillation counting method using Standard Method 7500-RN (AWWA 1996). Additional liquid scintillation test procedures and documentation are readily available (ASTM 1998, Hess and Beasley 1990). The 1999 EPA proposed radon rule also states that other analytical methods had been evaluated, but failed at least one of the criteria used in their evaluation. The methods were all evaluated for accuracy, lack of bias, and precision over the range of maximum contaminant levels considered. The E-PERM method is listed as one of the methods failing at least one of the evaluation criteria.

2.1.3 History of radon in water laboratory intercomparison testing

In 1988, the Environmental Monitoring Systems Laboratory in Las Vegas, Nevada ran a national radon in water intercomparison study. The 28 participating laboratories (including the University of Maine and the laboratory designated 1B in this study) received standards and samples and measured the radon in water concentration using either (or both) the liquid scintillation or Lucas cell method. Both the supplied standards and samples contained a sealed radium (^{226}Ra) source supporting a constant of radon in water to eliminate any effects of long shipping times as compared to the half life of radon (3.82 days). From this intercomparison, Whittaker et al. (1987) concluded the two methods to be valid and equivalent, but with liquid scintillation more precise than the Lucas cell method. The American Society for Testing and Materials conducted a 15-laboratory collaborative study for evaluation of their liquid scintillation test procedures (ASTM 1998). The New Jersey State Department of Environmental Protection and the EPA Eastern Environmental Radiation Facility (Parsa and Horton 1990) ran a two year collaborative study. They found significant correlation between the two laboratories using the liquid scintillation measurement method with water samples measured in turn by both laboratories. Unlike previous studies, this study tests the individual calibrations, materials and methods used by the testing laboratories.

2.2 Procedure

Nine laboratories participated in the intercomparison studies, including laboratories from the states of Maine, New Hampshire, Massachusetts, New York and New Jersey. Each laboratory participated in a single round and there was a total of four study rounds completed between February and August of 2004. Each laboratory was asked to send 15 shipping vials normally issued to the public to the University of Maine. The Radon Section wanted to test the ability of the laboratories to accurately and precisely measure

three levels of radon concentration, henceforth referred to as low, medium and high level. Distilled water was used as the low level radon concentration. Local, municipal water supplied the medium level radon concentration of approximately 18.5 $\mathrm{Bq\,L^{-1}}$. The high level originated from a well in Dedham, ME with a typical radon concentration of 740 $\mathrm{Bq\,L^{-1}}$. The laboratory's shipping vials were filled with water from these three sources and returned for analysis. Except for the distilled water, the other two water sources were actual drinking water supplies and not radon standards. Therefore there were no "known" radon concentrations over the entire study. Instead, there was a reference result for each study round from the University of Maine laboratory to compare against the results of the testing laboratories.

2.2.1 Splitting samples

To ensure that each laboratory had a true split sample, we adhered to the following protocol.

1. When the shipping vials arrive, inspect the kits to ensure each vial has an assigned, unique sample identification number and paperwork to indicate sample date and time;

2. Prepare the University of Maine analysis vials by injecting 5 ml of mineral oil scintillation cocktail[2] into five 20 ml liquid scintillation glass vials with polyseal cone caps;[3]

3. Add three liters of water to be sampled (first the low level distilled water) into a clean four-liter beaker;

4. Submerge five of each testing laboratory's shipping vials in the beaker of water;

[2]Perkin Elmer Life and Analytical Sciences, Boston, MA
[3]Kimble # 74515-20; VWR International, West Chester, PA

5. While capping the submerged shipping vials, draw 10 ml of water from the beaker with a syringe[4] and inject under the mineral oil of the five prepared University of Maine liquid scintillation vials;

6. After filling five replicate samples for each laboratory, dry the shipping vials and put aside with a notation of date and time (all noted with the same time);

7. Rinse the beaker with distilled water several times;

8. Repeat steps 2-7 using the medium and high level radon water, respectively; and

9. Re-pack the shipping vials with paperwork indicating sample identification numbers, dates and time of sampling. Ship the packages that day using the shipping method specified by the laboratory providing the vials.

2.2.2 Counting samples

The 15 reference samples for each round were analyzed as follows.

1. Place the 15 prepared vials into a liquid scintillation counter[5] rack beginning with three liquid radium standards and two distilled water blanks (the standards and blanks contain 10ml of solution and 5ml of mineral oil cocktail in the same brand of glass vials and caps holding the samples);

2. Allow the samples to remain in the liquid scintillation counter for three hours before counting begins;

3. Count each sample for 55 minutes, three times; and

4. Analyze the counter's raw data to get the radon concentrations in the samples using

$$A = (SC - BC) \times K \times e^{0.000126\, min^{-1} \times T} \tag{2.1}$$

[4]The syringe was purged with distilled water, followed by a purge with the water sample and then a draw of the water sample from the beaker for collection.

[5]Packard Tri-Carb 1500; Perkin Elmer Life and Analytical Sciences, Boston, MA

where A [Bq L^{-1}] is the radon concentration, SC [counts min^{-1}] is the sample count rate, BC [counts min^{-1}] is the blank count rate, K [Bq L^{-1} min counts^{-1}] is the calibration factor from counting the radium standards, and T [min] is the elapsed time from sampling to counting. Since the samples, standards, and blanks all contain the same volume of sample and cocktail, the analysis requires no volume corrections. This analysis was performed by running custom computer code displayed in Appendix C.

The University of Maine laboratory uses liquid radium standards to calibrate the liquid scintillation counter with the radium solution supplied by the EPA Environmental Systems Laboratory in Las Vegas, NV. Standards are made by combining a weighed amount of radium solution and distilled water totaling 10 ml in a glass scintillation vial. Five ml of mineral oil scintillation cocktail was added to the solution and capped with polyseal caps. The standards rest for approximately a month so that the radon and radium achieve secular equilibrium.

2.3 Results

Table 2.1 lists the methods and materials used by each laboratory. Eight of the testing laboratories and the reference University of Maine laboratory used liquid scintillation to measure the radon in water; one used the E-PERM method. For those using liquid scintillation, Opti-fluor O (Perkin Elmer Life and Analytical Sciences, Boston, MA) was the most commonly used scintillation cocktail. All the laboratories used glass shipping vials of volumes ranging from 20-67 ml with either Teflon-lined rubber septum caps, Teflon-lined caps, or aluminum-lined caps. The liquid scintillation laboratories used glass scintillation vials with either polyseal (or similar polyethylene cone cap), Teflon-lined cap, or a foil lined cap. The volume of water used ranged from 8-15 ml and count times ranged from 5-55 min. All but one liquid scintillation laboratory claimed to use a radium stan-

dard. Through its quality assurance document, laboratory 3F claims to use equipment, methods and calculations consistent with the E-PERM method.

The laboratory's measurements of distilled water without any radon were expected to be less than their lower limit of detection (LLD). Fig. 2.1 shows the value of each laboratory's LLD. The results are separated by round and show an entry from the reference University of Maine (laboratory UM) laboratory for each round. Laboratory 2D measured one of the five samples below their stated LLD and the other four above. Fig. 2.2 shows the medium level concentration results. The spread among the five measurements can be seen by the plotted standard deviation. Laboratory 3F had one outlying measurement not shown. Fig. 2.3 shows the results from the high level samples. The high level water came from a well and had considerably less radon when it was sampled for the fourth round. Laboratory 1A reported outlying results for two samples.

Table 2.2 lists each laboratory's statistics for this study. The lower limit of detections ranged from 0.6-11 $\mathrm{Bq\,L^{-1}}$. A LLD at the 95% confidence interval was calculated for the reference University of Maine laboratory (Currie 1968). The percent variation, defined as the ratio of the standard deviation and sample mean, measures the spread of results among five samples. In the two cases noted, outliers (Proschan 1952) were removed from this calculation. The variations among the testing laboratories ranged from 1-23% and the University of Maine percent variations ranged from 1-4% over the four rounds. The percent discrepancy measures the deviation between a testing laboratory's average and the University of Maine's average. The sign of the percent indicates whether the average result fell below (-) or above (+) the reference result. The absolute percent discrepancies ranged from 1-100%. In order to determine a systematic bias in the results, averaging the medium and high level percent discrepancies in Table 2.2 gives an average of -6% and -7% discrepancy, respectively, showing an overall study-wide low bias.

Table 2.1: The materials and methods used by each laboratory to measure radon in water.

		LS cocktail		Shipping vial		Analysis vial		Sample	Count	^{226}Ra
Lab	Method	type	vol. (ml)	vol. (ml)	cap	vol. (ml)	cap	volume (ml)	time (min)	Standard
1A	LS	Opti-fluor O	5	20	Al-lined	20	Al-lined	10	20	✓
1B	LS	toluene	5	40	rubber/Teflon	20	polyseal	15	50	✓
1C	LS	Opti-fluor O	10	40	rubber/Teflon	20	polyseal	10	10	✓
2D	LS	Opti-fluor O	10	40	rubber/Teflon	27	polyseal	10	10	
2E	LS	Opti-fluor O	5	40	rubber/Teflon	20	polyseal	10	$>5^a$	✓
3F	E-PERM		–	67	Teflon-lined	3700	rubber collar	–	–	–
3G	LS	Instafluor	8	20	Al-lined	20	Teflon-lined	8	30	✓
3H	LS	Opti-fluor O	10	20	rubber/Teflon	20	polyseal	10	10	✓
4J	LS	Opti-fluor O	5	40	rubber/Teflon	20	foil-lined	15	50	✓
UM	LS	Mineral Oil	5	–	–	20	polyseal	10	55	✓

[a]Or until a statistically signifi cant number of counts have been recorded

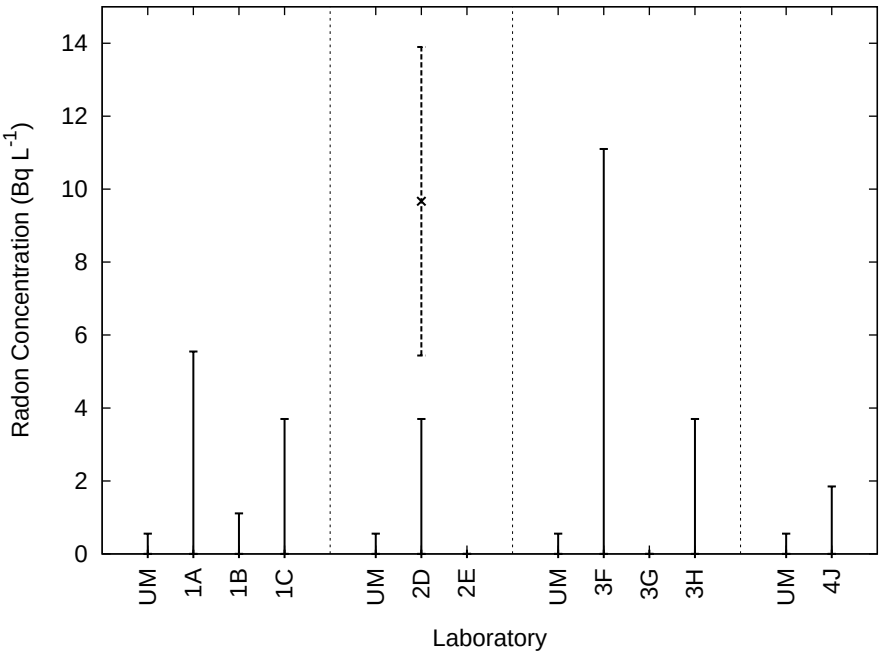

Figure 2.1: Low level radon results for distilled water. The top edge of the solid plotted range is the laboratory's lower limit of detection. The dashed line represents the average $\pm$ 1-σ standard deviation of the four samples laboratory 2D measured above their LLD. Laboratory 2E reported "zero" and laboratory 3G reported "non-detectable."

A general linear models analysis of variance using SAS [6] computer software was performed. This test grouped each round together and tested for significant differences between the laboratories at the 95% confidence interval. All laboratories are treated equally with no notion of a reference laboratory. Table 2.3 shows the results of the analysis of variance. In all but one case (round four, medium level) a significant difference exists between the results of the laboratories. A Duncan Multiple Range Test sorted the laboratories into subgroups sharing no significant difference. This analysis included the two outliers of laboratory 1A's high level results but not the lone outlier of laboratory 3F's medium level results due to its extremity. In general, laboratories with a percent variation or discrepancy greater than 10% showed significant difference with the University of Maine laboratory.

[6] SAS version 6.07; SAS Institute Inc, Cary, NC

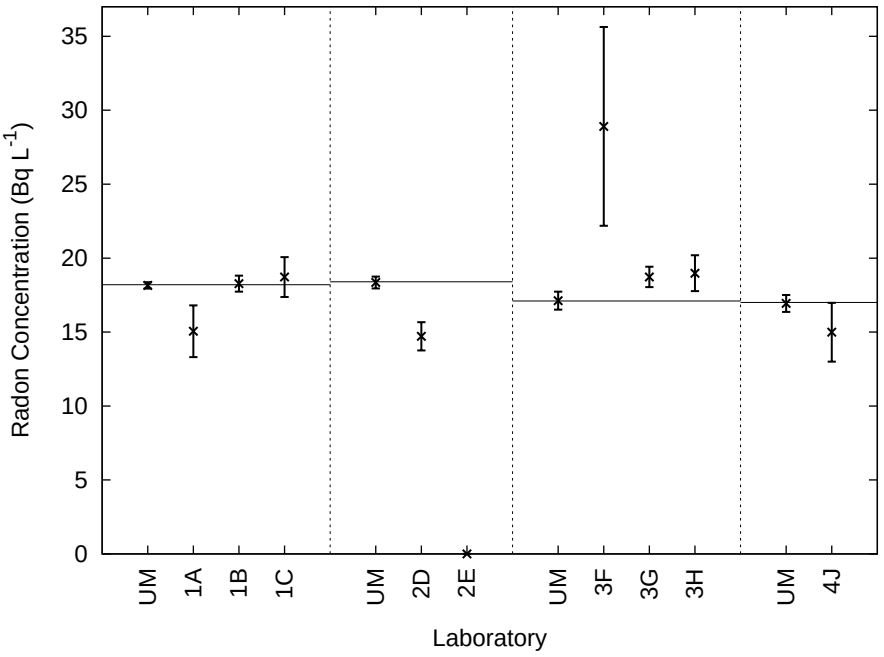

Figure 2.2: Medium level radon results. The plot shows the average of five radon measurements $\pm$ 1-σ standard deviation for each laboratory grouped by round. The results of the reference laboratory (UM) are indicated by the solid horizontal line for each round. Laboratory 2E reported zero for all five samples. Laboratory 3F has one outlying measurement at 310 $\mathrm{Bq\,L^{-1}}$ not included in the average or the plot.

2.4 Discussion

Four of the testing laboratories (1B, 1C, 3G, and 3H) had percent variations and absolute discrepancies less than 12% and results consistent with the reference laboratory. Even though laboratories 3G and 3H were not grouped with the reference laboratory in the analysis of variance for the high level measurements, their results are clearly consistent with the reference laboratory. The remaining five testing laboratories demonstrated an error somewhere in the measurement process with respect to the reference laboratory. The laboratories designated as 1A, 2D, 2E, and 4J all measured the radon to be less than that of the reference laboratory for either or both the medium and high level radon concentrations. This deviance signals the possibility of a radon loss somewhere throughout the testing process. Radon is known to easily escape from water and care must be taken

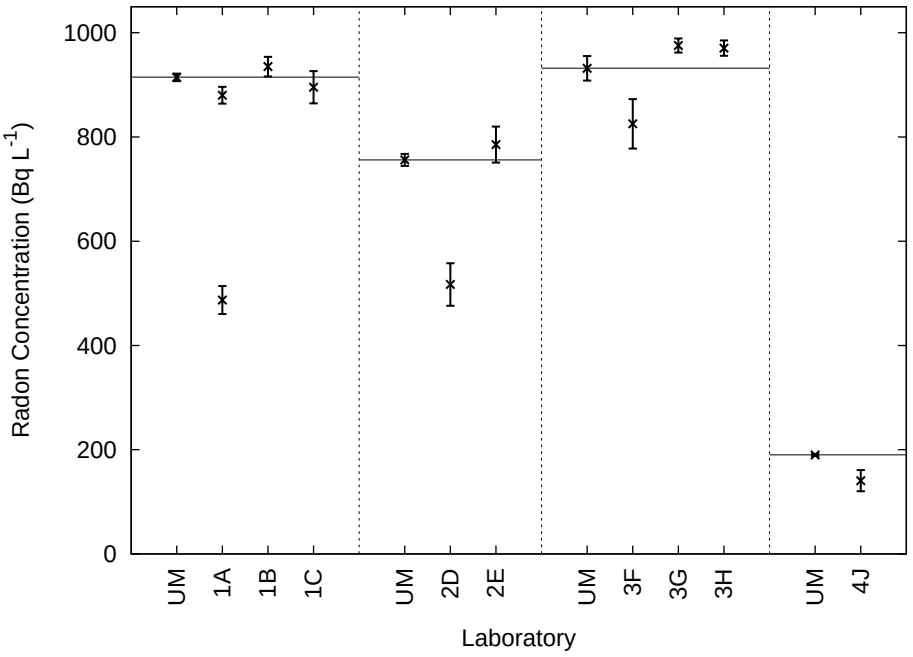

Figure 2.3: High level radon results. The plot shows the average of five radon measurements $\pm$ 1-σ standard deviation for each laboratory grouped by round. The results of the reference laboratory (UM) are indicated by the solid horizontal line for each round. Laboratory 1A measured two samples much lower than the other three so two data ranges are plotted.

to minimize this loss during sampling and measurement. (Freyer et al. 1997, Vitz 1991). Since these four laboratories all use the liquid scintillation method, they must open the shipping vial containing a water sample and transfer an aliquot to a liquid scintillation analysis vial. Depending on the speed and duration of this process, some radon may have been released. It is unlikely that radon was lost during shipping since all of the shipping vials were filled completely and capped with either a foil or Teflon lined caps (Vitz 1991, AWWA 1996). Further evidence of radon loss is shown in the high level measurements of laboratory 1A. Two of their five measurements were similar yet less than the results of the reference laboratory and the other two laboratories participating in that round. The reference laboratory prepared the samples for analysis directly without the extra steps of sample shipping and transfer from a shipping vial.

Table 2.2: The reported LLD, percent variation among five samples, and the percent discrepancy from the reference laboratory for the medium and high level radon measurements. Percentages in parentheses include noted outliers.

Lab	LLD	Percent Variation		Percent Discrepancy	
	($\mathrm{Bq\,L^{-1}}$)	med. (%)	high (%)	med. (%)	high (%)
1A	5.6	12	(30) 2	–17	(–21) –4
1B	1.1	3	2	1	2
1C	3.7	7	3	3	–2
2D	3.7	6	8	–20	–32
2E	—	—	4	–100	4
3F	11	(148) 23	6	(397) 69	–11
3G	—	4	1	9	5
3H	3.7	6	2	11	4
4J	1.9	13	14	–12	–26
UM	0.6	1–4	1–3	—	—

Table 2.3: The results of the analysis of variance test.

Round	Level	Significant difference		Duncan Grouping		
1	medium	yes	$p < 0.001$	UM,1B,1C	1A	
1	high	yes	$p = 0.028$	UM,1B,1C	1A	
2	medium	yes	$p < 0.001$	UM	2D	2E
2	high	yes	$p < 0.001$	UM,2E	2D	
3	medium	yes	$p < 0.001$	UM,3G,3H	3F	
3	high	yes	$p < 0.001$	UM	3G,3H	3F
4	medium	no	$p > 0.050$	UM,4J		
4	high	yes	$p < 0.001$	UM	4J	

Although the measurements of laboratory 2D for the medium and high level radon were less than the reference laboratory, four of their measurements of the blank low level radon concentrations were above their LLD. This laboratory is the only one who did not claim to use any radium standards for calibration, relying entirely on the ^{3}H and $^{1}4$C standards supplied with the detector. Although these two standards properly normalize and calibrate the detector, they do not set the efficiency for radon measurements alone. If the counting efficiency is lower than anticipated, a lower radon concentration will be calculated. It is likely that the lack of radium standards played a part in the discrepancy for laboratory 2D.

Laboratory 3F was the only laboratory to use the E-PERM method to measure radon in water. Although their high level results were not too far below those of the reference laboratory, their medium level results were significantly above the reference with one sample extremely high. This measurement inconsistency illustrates a possible error in their measurement procedure or calibration.

The other materials used by all the laboratories appear to be acceptable for testing of radon in water. All of the laboratories using liquid scintillation used common cocktails: two used the classic toluene and Insta-fluor[7] cocktails, while most opted for the safer Opti-fluor O or mineral oil cocktails. The vials used for analysis should be glass with a polyethylene cone cap (ASTM 1998, AWWA 1996) or any other tight-sealing cap like a Teflon-lined cap.[8] While the count times ranged from 5-55 min, a low count time yields a higher LLD and measurement uncertainty. Testing procedures recommend a count time of at least 50 min, or enough for a 2σ counting uncertainty of 10% (ASTM 1998, AWWA 1996).

It seems difficult to identify a point in a measurement protocol where an error occurred. In future intercomparison studies, testing laboratories using liquid scintillation could send their scintillation vials prepared with cocktail (if using a safe cocktail) and split water samples could be placed in both shipping and liquid scintillation vials. Based on the differences between the two measurements, systematic errors could be separated from random errors, such a radon loss during sample shipping or transfer. One laboratory (2E) reported receiving the water samples over their 4-day limit, which may have caused this and other laboratories to deal with a low counting signal. It was up to the testing laboratory to instruct any special shipping method much like they would while serving the public.

[7]Perkin Elmer Life and Analytical Sciences, Boston, MA

[8]Foil-lined caps on liquid radium standards can be a concern. The standard can be acidic and capable of corroding an aluminum lining and cause radon leakage. High measurements of radon can be a sign of leaking radium standards.

2.5 Summary and Conclusions

Nine laboratories each measured radon in 15 water samples over three different radon concentrations provided by the University of Maine. The University of Maine analyzed the split samples without the delay from shipping and the extra step of transferring a water sample from shipping to analysis vials. Eight of the laboratories used the liquid scintillation method of testing, while one used the E-PERM method. All laboratories used acceptable shipping and analysis materials, while one was without radium standards. The laboratories measured radon concentrations with variations between 1-23% among five replicate samples and discrepancies with the reference laboratory ranged between 1-100%. Those results inconsistent with the reference laboratory indicate a source of error somewhere throughout the process. Likely places of error can be loss of radon during sample shipping, transferring to analysis materials, or insufficient calibration. Most of the major discrepancies from the reference laboratory values (those $>$12%) occurred with measurements lower than the reference laboratory. We have notified the laboratories of their results and encouraged those with major discrepancies to individually repeat the test with the University of Maine. The Radon Section may repeat a similar study on a regular basis in the absence of a nationally run intercomparison program.

The agreement and consistency of the University of Maine laboratory with the testing laboratories 1B (the State of Maine Health and Environmental Testing Laboratory), 1C, 3G, and 3H suggests two conclusions from this work:

1. Those four testing laboratories are considered by the State of Maine to follow acceptable procedures for measuring radon in water.

2. The quality of the reference University of Maine laboratory has been established. The laboratory's methods, handling, calibration, and measurements have been verified to be accurate.

Chapter 3

SPATIAL VARIATION OF WATERBORNE RADON AND TEMPORAL VARIATION OF RADON IN WATER IN SCHOOLS

3.1 Introduction

Radon can dissolve and remain in ground water, subject to radioactive decay, until dispensed and aerated. Kitchen, laundry, and bathroom appliances provide a pathway in addition to soil gas for radon into a building. The EPA has proposed setting maximum contaminant levels for radon in ground water. The standard will be based on the fraction of radon that escapes the water during use (EPA 1999, NRC 1999b), which is defined as the radon transfer coefficient.

This study continued the investigation of radon in schools (Norris et al. 2004) with particular interest in spatial and temporal variations of radon concentrations. By measuring radon concentrations in air and water, transfer coefficients were determined experimentally and compared to predictions from a model. Multiple detectors were placed in kitchens to detect a variation of the released waterborne radon. Water samples were taken throughout water usage to detect any variation of radon concentration in water.

3.1.1 Radon release model

A model of radon release was applied where the radon transfer coefficient, f of a room is given by

$$f = \frac{\Delta C_{air}}{C_w} = \frac{W\overline{\varepsilon}}{VT\lambda} \tag{3.1}$$

where ΔC_{air} [Bq L^{-1}] is the change in radon concentration in air above background, C_w [Bq L^{-1}] is the radon concentration in the water being used, W [L] is the total volume

of water used in a time interval T [min], $\overline{\varepsilon}$ is the total use-weighted emissivity of the appliances running water, V [L] is the volume of the room and λ [min^{-1}] is the ventilation rate of the bulk room air. A faucet's emissivity is defined as the fraction of the radon in water released into the air due to aeration. The air is assumed to be well mixed while ventilating. The derivation of this model can be found in Hess et al. (1987) and Hess and Haskell (1994). The predicted transfer coefficients (f_{pred}) were calculated using W, $\overline{\varepsilon}$, V, T, and λ . For each radon detector in the kitchen, the measured transfer coefficient (f_{meas}) was found by the ratio of ΔC_{air} and C_w. The parameters in the model were measured over the course of a 1 hr simulation.

3.2 Materials and methods

Nine elementary/middle schools in Maine have been investigated to study water-use simulations with the intent to examine variations of radon in the water over time and spatially in each school kitchen. The schools were studied between August 2001 and August 2002. Simulations were performed at eight schools, school SW was studied twice, and only radon in water measurements were available for the ninth school MR.[1]

3.2.1 Simulations

In each school kitchen, the sinks and dish-washing sprayers were fully open to cause a burst of water and release of radon. Multiple water samples were collected over the 1 hr simulation from a sink running cold water with a faucet submerged in an overflowing beaker to prevent aeration. Using a syringe, a 10 ml sample from the beaker was injected under 5 ml of mineral oil cocktail[2] in a 20 ml glass scintillation vial with a polyseal cap.[3] The vials were returned to the laboratory and analyzed for radon using a liquid scintilla-

[1] A electrical power outage after the simulation caused a loss of radon in air data while the radon in water measurements taken during simulation were unaffected.

[2] Perkin Elmer Life and Analytic Sciences, Boston, MA

[3] Kimble # 74515-20, VWR International, West Chester, PA

tion detector[4] following the standard method recommended by the EPA (AWWA 1996) explained in Section 2.2.2. Water samples were also collected with a syringe from the drain of each sink and sprayer and transferred into scintillation vials in order to calculate emissivities. The sample from a drain contains the radon remaining after aeration, $C_w^{aerated}$, from the faucet. A non-aerated sample, using the overflowing beaker method, was taken at the same time to determine the original radon concentration. The emissivity is calculated from

$$\varepsilon = 1 - \frac{C_w^{aerated}}{C_w} \tag{3.2}$$

and the total use-weighted emissivity is the sum of the emissivities weighted by the fraction of water used.

The water usage was calculated from measured volumetric flow rates at each faucet. A beaker of known volume was filled and timed with a stopwatch. This procedure provided the amount of water passing through each sink/sprayer as well as the total water volume used during the simulation. These flow rates were measured at least six times during the simulation.

Radon in air measurements were made using Honeywell Professional Radon Monitors.[5] These detectors were placed in the kitchen and throughout the school to detect radon released in the kitchen accumulating in other rooms of the school. The detectors were started at least one hour before the simulation began and logged data for at least 24 hr. At school JS, 12 detectors were placed on a surface at mid-level throughout the kitchen (Fig. 3.1). During a repeat study at school SW, 15 detectors were placed at three vertical levels in the kitchen. There are five locations where the detectors were placed: at the floor, mid, and ceiling levels of the kitchen (Fig. 3.2). With an array of detectors in the kitchen at these two schools, a linear interpolation between known concentration was made to map the radon concentration throughout the room to illustrate a horizontal

[4]Packard Tri-Carb 1500; Perkin Elmer Life and Analytic Sciences, Boston, MA
[5]Sun Nuclear, Melbourne, FL

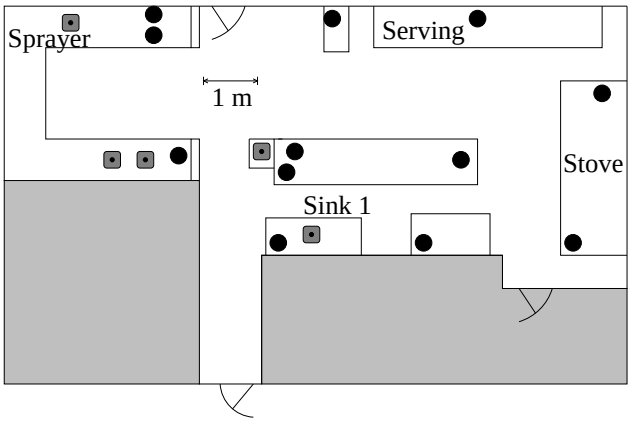

Figure 3.1: The floor plan at the school JS kitchen. The circles represent radon detectors and the squares are sinks or sprayers running water. All of the detectors are roughly at kitchen counter height.

and vertical variation. The map represents the spatial distribution of radon at one instant in time. The time chosen was the midpoint of the interval over which the detectors show an accumulation of radon due to water use. The known radon concentrations were placed in a two-dimensional grid and all the intermediate concentrations were estimated by iteratively taking the average of four nearest neighbors.

An injection of sulfur hexafluoride (SF_6) into the air provided a tracer gas to determine the bulk air ventilation in the room . The air flow patterns in the room were not measured. Air was periodically sampled into 10 L, SKC Mylar bags[6] and later analyzed in a Miran Infrared Gas Analyzer[7] to measure the SF_6 concentration in each bag. The concentrations are fitted to an exponential decay to calculate the ventilation (decay) rate. The volumes of the kitchens were measured directly.

3.2.2 Calibration

The radon in air detectors continuously monitor the radon concentration and log the radon concentration with no on-site calibration or analysis needed. The manufacturer recommends an annual calibration of the detectors. In July 2002, the detectors were cali-

[6]SKC Inc., Eighty Four, PA
[7]Invensys/Foxboro, Foxboro, MA

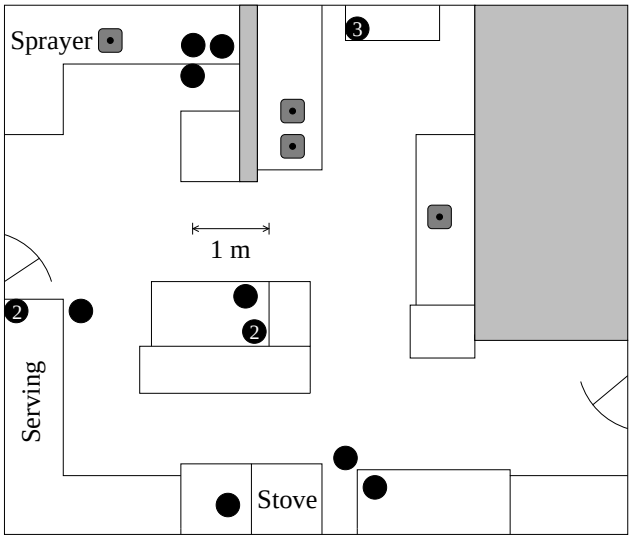

Figure 3.2: The floor plan at the school SW kitchen. The circles represent radon detectors and the squares are sinks or sprayers running water. Each detector is either at the floor, mid, or ceiling level and numbered circles represent the number of overlapping detectors in this aerial view.

brated by the manufacturer before the study began. Throughout the study, all the detectors were periodically placed in a radon chamber to check the calibration. The chamber was fed radon from a 6.7 kBq Pylon ^{226}Ra source.[8] Detectors with erroneous readings compared to the others were not used in the study.

3.3 Results

3.3.1 Radon in water

Table 3.1 lists the average radon in water concentrations and the range of variation from the start to the end of the simulation. The radon in water measurements increased by a factor of 4 at one school and increased by at least 200 $\mathrm{Bq\,L^{-1}}$ at six of the nine schools. No school showed a decrease of radon concentration in water over time. The radon in water concentrations at school JS illustrate the factor of 4 increase in radon during the simulation (Fig. 3.3). The two simulations at school SW were separated by 7 d

[8]Pylon Electronic Development Company, Ltd., Ottawa, Ontario.

and had similar radon in water measurements (Fig. 3.4) with a maximum level of 1780 Bq L^{-1}. Plots of radon in water measurements for the remaining schools can be found in Appendix A.

Table 3.1: The average, maximum, and minimum radon in water concentrations measured over 1 hr.

School	C_w Bq L^{-1})	C_w^{max} (Bq L^{-1})	C_w^{min} (Bq L^{-1})
JS	1140	1900	451
SL	740	1030	543
CR	703	839	524
DM	203	239	177
BR	250	300	219
SW11	1520	1780	974
SW18	1370	1730	1010
MR	616	733	472
BL	226	237	209
LS	768	843	624

3.3.2 Radon in air

The parameters used to determine the predicted transfer coefficients are listed in Table 3.2. For each school, the length of the simulation, T, was 60 min. The predicted transfer coefficients ranged from 1.6 $\times 10^{-4}$ to 665$\times 10^{-4}$. The average increase of radon among the detectors present in the kitchens and the measured transfer coefficient are listed in Table 3.3, which also presents the ratio of the predicted and measured transfer coefficients. The average amount of radon released ranged 0.096 to 1.96 Bq L^{-1} across all the school kitchens. Except for school BR, the predicted transfer coefficient was greater than the measured transfer coefficient. The build-up and decay of radon concentration in air for one detector in the kitchen and low concentrations of measured radon in adjacent classrooms can be illustrated by data from school JS (Fig. 3.5). Except for the kitchen-only study at SW18, the remaining schools had several detectors in other rooms of the school. Table 3.4 lists the average maximum and background radon in air concentration

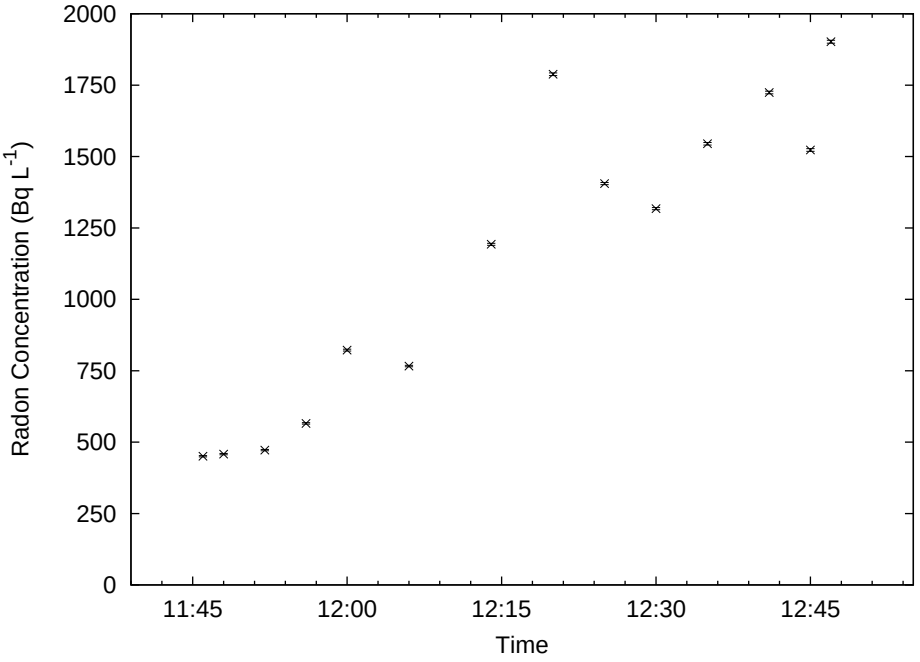

Figure 3.3: The radon in water during water usage at school JS as a function of time.

in the school's classrooms. The increase in radon in the classrooms was no more than 0.1 $\mathrm{Bq\,L^{-1}}$ above background during the 24 hr measurement period.

In each of the school kitchens, several radon detectors were utilized to measure a spatial variation of the increase of radon concentration in the air due to water usage. The spatial variation was evident in schools JS and SW where the kitchen was studied in detail. The interpolated results from the JS kitchen are contoured in Fig. 3.6. This figure demonstrates a horizontal variation of radon in the kitchen ranging from 0.75-4 $\mathrm{Bq\,L^{-1}}$. The vertical variation of released radon is evident at school SW. Fig. 3.7a shows the radon concentration at the dish-washing sprayer. The detector placed at the mid level (the same height as the sprayer itself) recorded the largest radon concentration of 1.1 $\mathrm{Bq\,L^{-1}}$. However at the stove, the furthest location from any water usage, the highest radon concentration measured was 0.65 $\mathrm{Bq\,L^{-1}}$ by the detector closest to the ceiling (Fig. 3.7b). The interpolated concentrations (Fig. 3.8) illustrate the variation of radon concentrations throughout the kitchen for the mid, 0.20–0.70 $\mathrm{Bq\,L^{-1}}$, and ceiling,

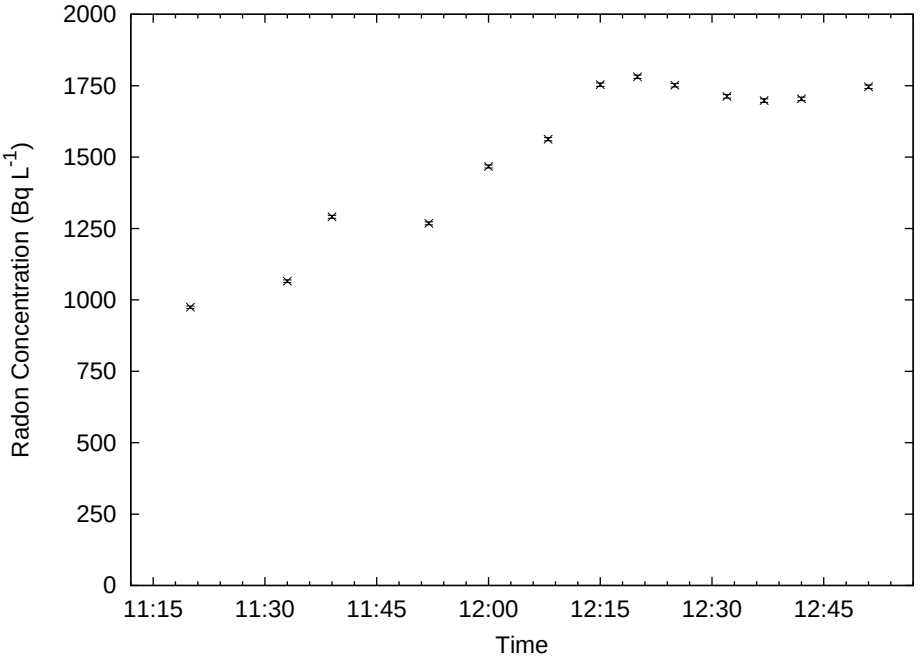

(a)

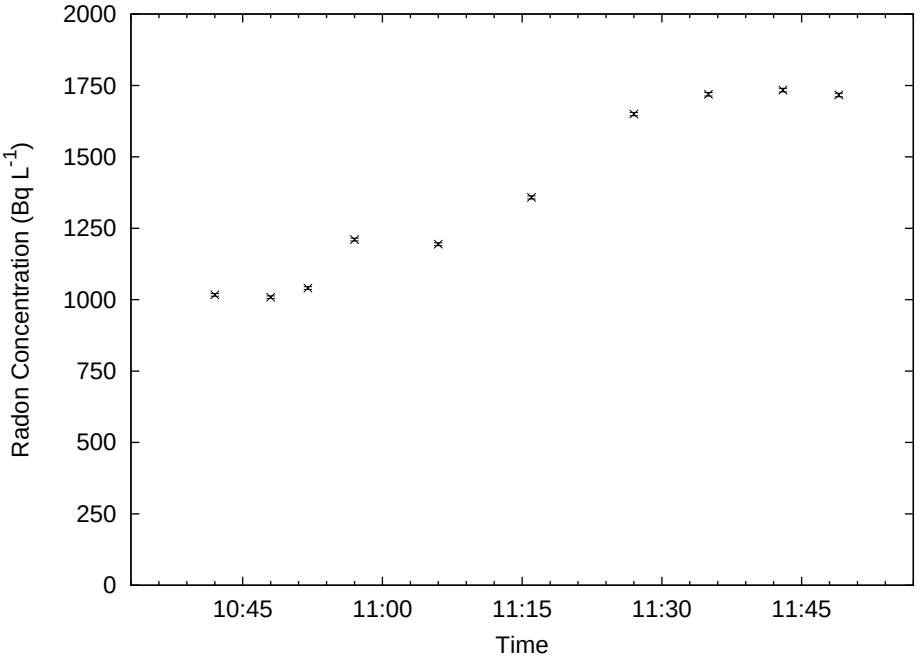

(b)

Figure 3.4: The ^{222}Rn in water concentrations during water usage at school SW as a function of time on (a) 11 July and (b) 18 July 2002.

Table 3.2: The parameters measured to predict the transfer coefficient. The volume V, ventilation rate λ, water used W, total use-weighted emissivity $\overline{\varepsilon}$, and the predicted transfer coefficient f_{pred}. The error is a 1-σ measurement uncertainty.

School	V (L)	λ (min^{-1})	W (L)	$\overline{\varepsilon}$	f_{pred} ($\times 10^{-4}$)
JS	137000	0.0183 ± 0.003	2369 ± 76	0.55 ± 0.02	86.7 ± 14.2
SL	169000	0.0481 ± 0.003	2582 ± 73	0.25 ± 0.01	13.4 ± 1.1
CR	14000	0.0302 ± 0.004	3271 ± 52	0.52 ± 0.01	665 ± 93
DM	163000	0.0604 ± 0.009	2010 ± 101	0.31 ± 0.03	10.7 ± 2.0
BR	74200	0.1076 ± 0.011	177 ± 5	0.42 ± 0.01	1.6 ± 0.2
SW11	131000	0.1786 ± 0.002	2707 ± 126	0.51 ± 0.02	9.9 ± 0.6
SW18	131000	0.1129 ± 0.022	2672 ± 66	0.44 ± 0.01	13.2 ± 2.6
BL	184000	0.1248 ± 0.026	2597 ± 163	0.53 ± 0.04	9.9 ± 2.3
LS	130000	0.2800 ± 0.078	2188 ± 45	0.57 ± 0.01	5.7 ± 1.6

Table 3.3: The radon released into the kitchens. The number of radon in air detectors placed in each kitchen with the average increase in radon concentration, the measured transfer coefficient, and the ratio of the predicted and measured transfer coefficients. The error is a 1-σ standard deviation of multiple measurements.

School	Number of Detectors	$\overline{\Delta C}_{air}$ (Bq L^{-1})	$\overline{f}_{meas}$ ($\times 10^{-4}$)	$\frac{f_{pred}}{\overline{f}_{meas}}$
JS	12	1.960 ± 0.971	17.2 ± 8.5	5.0 ± 2.6
SL	3	0.511 ± 0.122	6.9 ± 1.6	1.9 ± 0.5
CR	2	0.706 ± 0.315	10.0 ± 4.5	66.5 ± 31.0
DM	3	0.130 ± 0.032	6.2 ± 1.6	1.7 ± 0.5
BR	3	0.160 ± 0.130	6.5 ± 5.1	0.2 ± 0.2
SW11	4	0.330 ± 0.300	2.2 ± 2.0	4.5 ± 4.1
SW18	15	0.403 ± 0.320	3.0 ± 2.3	4.5 ± 3.6
BL	7	0.096 ± 0.096	4.2 ± 4.2	2.3 ± 2.4
LS	7	0.250 ± 0.170	3.3 ± 2.2	1.7 ± 1.3

0.35–0.55 Bq L^{-1}, levels. The detectors on the floor measured radon concentrations of 0.13–0.48 Bq L^{-1}.

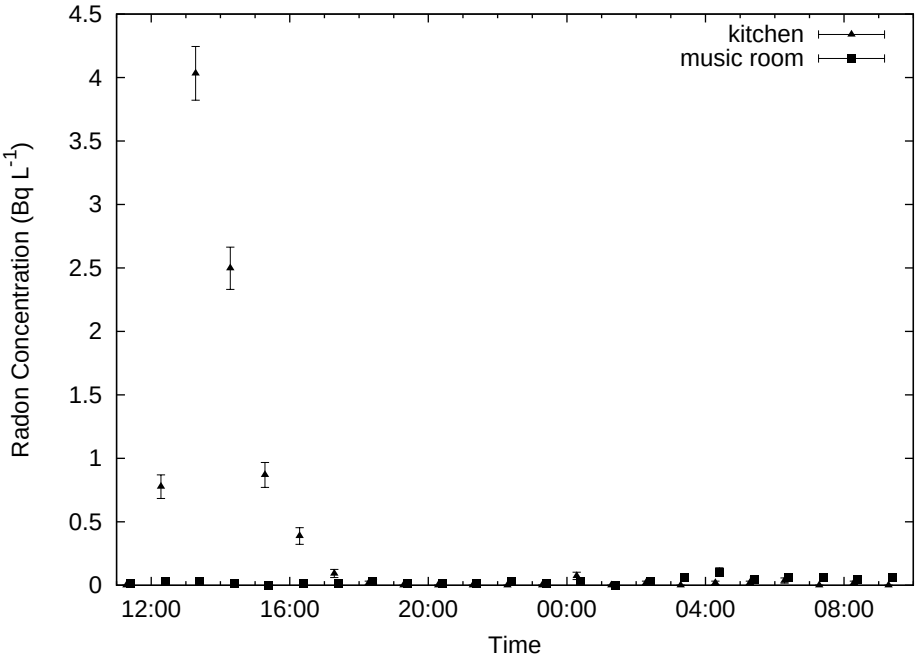

Figure 3.5: The radon in air concentration as a function of time from one detector in the kitchen and music room at school JS. The simulation used water from 11:45-12:45.

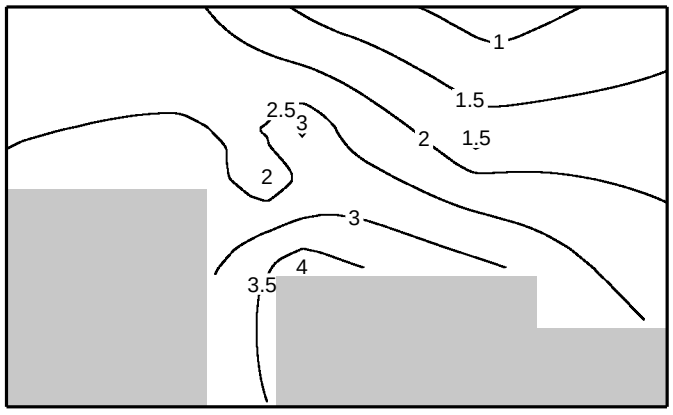

Figure 3.6: The interpolated radon in air measurements (in Bq L^{-1}) at 13:10 at the school JS kitchen.

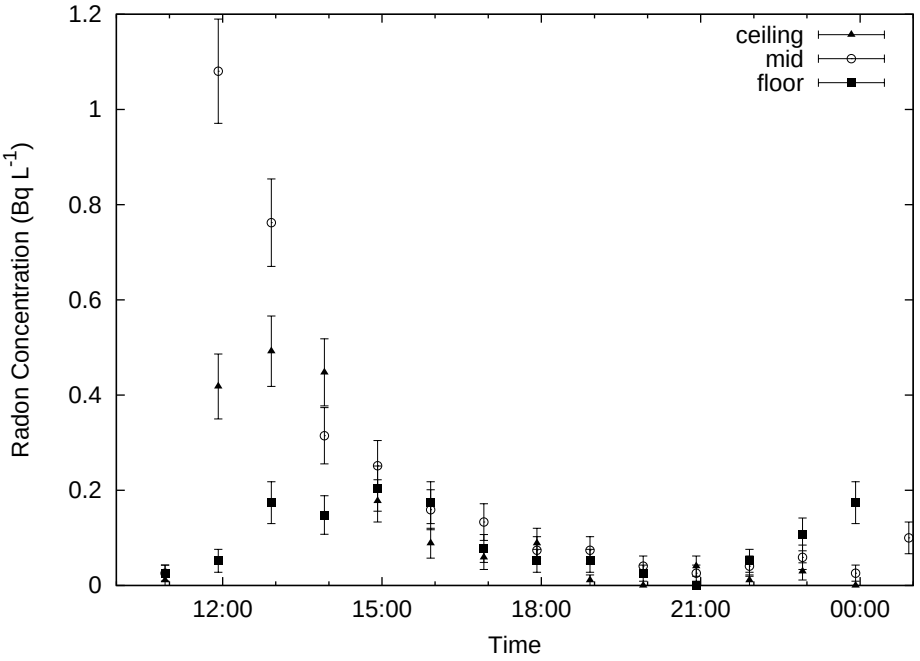

(a)

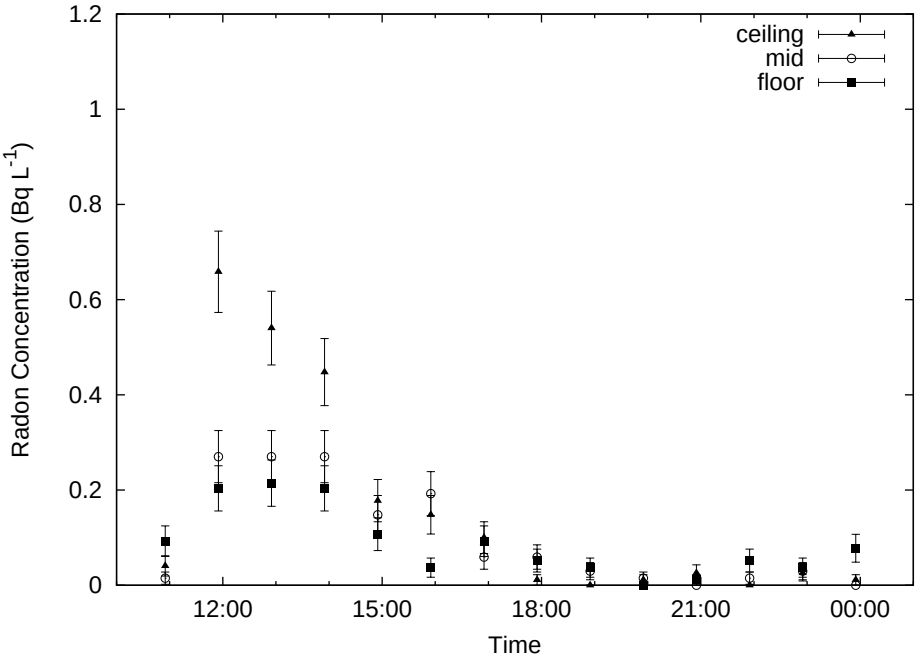

(b)

Figure 3.7: The radon in air concentration as a function of time from three detectors at separate levels (a) near the sprayer and (b) near the stove in the kitchen at school SW. The simulation used water from 10:45-11:45.

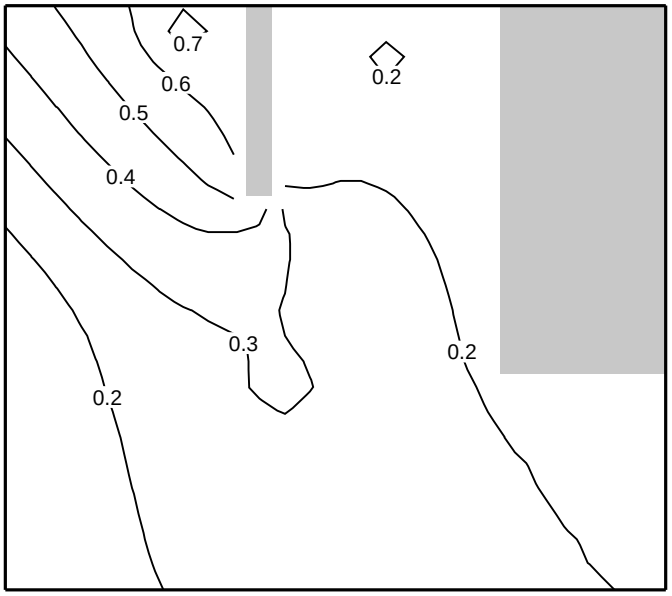

(a)

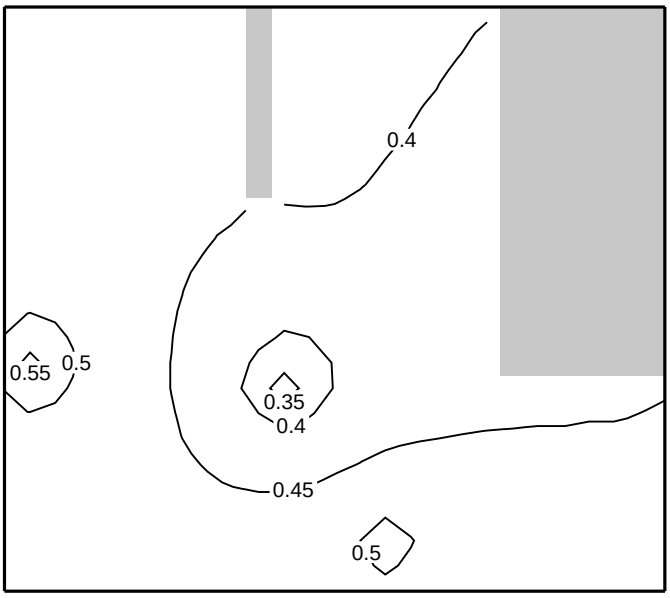

(b)

Figure 3.8: The interpolated radon in air measurements (in Bq L^{-1}) at 12:55 at the (a) mid and (b) ceiling level at the school SW kitchen.

Table 3.4: The number of rooms measured and their average maximum and background radon concentrations. The error is a 1-σ standard deviation of multiple measurements.

School	Number of rooms	$\overline{C}_{air}^{max}$ (Bq L^{-1})	$\overline{C}_{air}^{background}$ (Bq L^{-1})
JS	3	0.079 ± 0.023	0.024 ± 0.004
SL	9	0.110 ± 0.021	0.036 ± 0.008
CR	12	0.120 ± 0.040	0.032 ± 0.010
DM	10	0.220 ± 0.140	0.120 ± 0.090
BR	12	0.094 ± 0.026	0.031 ± 0.004
SW11	9	0.091 ± 0.072	0.030 ± 0.024
BL	8	0.070 ± 0.020	0.020 ± 0.006
LS	8	0.096 ± 0.034	0.028 ± 0.007

3.4 Discussion

The radon in water concentration significantly increased at six of the schools during the course of the simulation. A short-term temporal variation was reproduced at school SW, which was likely due to similar prior water-usage on the sample days. Though the plumbing in the school and mixing in water tanks could cause the observed increase in radon concentrations, this is unlikely. The measurements that demonstrate the radon variation were always collected from a dedicated sink by slowly drawing cold water. Within five minutes of starting the simulation, a thermometer indicated that the water temperature dropped and held constant at 11 °C, which indicates the origin of water to be solely ground water and not the warmer water within the schools plumbing system. This could be due to initially drawing older well water before reaching radon-rich ground water (see Chapter 4). The history of water usage affects the radon concentration indicating that if a measurement was made in these schools for a routine radon in water measurement, the results would heavily depend on how much water had been recently drawn from the well.

The spatial variation of radon observed at school JS indicates a movement of radon not predicted by the model. The largest radon concentration occurred at the location of sink 1,

which had the largest emissivity. The lowest concentration occurred in the furthest corner of the kitchen by the serving counter away from any water sources. It is clear that radon is not perfectly mixed within the kitchen and the largest concentrations are found near water sources. Since areas far from the water sources showed little radon concentration, the radon evidently did not spread out horizontally. The dual-level variations observed at school SW provide an explanation of the movement of radon through the kitchen. The largest radon concentration of 0.7 $\mathrm{Bq\,L^{-1}}$ was observed near the sprayer, while elsewhere at that level the concentration was near 0.2 $\mathrm{Bq\,L^{-1}}$, which indicates there was little horizontal movement of radon at the mid level. An intermediate amount of radon at 0.4–0.5 $\mathrm{Bq\,L^{-1}}$ covered most of the ceiling level. Radon concentrations at this level were more evenly distributed, which indicates that the waterborne radon is moving mainly upward, not horizontally, from the running water. These results suggest that studies of released radon from water are complicated by the heterogeneous distribution of radon and deserve multiple detectors throughout the room, both horizontally and vertically.

In all but one case (school BR), the predicted was higher than the measured transfer coefficient. This discrepancy suggests that either the model used to calculate the transfer coefficient overestimates the released radon or that not all of the released radon was measured. This latter point was the impetus for placing several detectors in the kitchen to ensure that all released radon was measured. It is clear from our results that heterogeneous distribution of radon exists in the kitchen after water usage. The model took into account a ventilation rate of the kitchen using SF_6 but it assumed the radon was well mixed. The actual air flow pattern in the room was not measured, however, if the radon was following the air flow pattern and exiting ventilation openings, instead of uniformly mixing, the radon loss due to ventilation would be greater than predicted. Therefore, the model would overestimate the radon release.

School BR was the only case with a measured transfer coefficient greater than the predicted value. At this school we were warned of a low yield well and used a lower amount

of water than typically used. Since the model assumed a large burst of waterborne radon in a short amount of time, it seemed to fail when the water usage was small over the duration of the simulation. School CR had a predicted transfer coefficient much higher than the measured, by a factor of 66. This school had the smallest kitchen volume compared to the others. It is possible that the released radon continued to occupy a larger volume of air in nearby spaces (above drop ceiling, closets). Mistakenly using a smaller room volume explained why the model predicted a higher radon concentration and transfer coefficient given the dependence on volume in equation (3.1).

In general, very little radon was measured in the adjacent and distant classrooms of the schools. This means that any radon leaving the kitchen was diluted with the air in the rooms measured. The average maximum radon concentrations generally were below the 0.150 $\mathrm{Bq\,L^{-1}}$ action level. At school DM, the maximum concentrations did measure higher than the action level in some classrooms, but the average background concentrations were also high. These maximum concentrations were found during the 24 hr measurement period after the simulation. Any radon from soil gas and building materials can build up in classrooms over night while the building is closed and inactive and the increase in concentration measured may not be entirely due to waterborne radon.

3.5 Summary and Conclusions

By placing radon in air detectors throughout a kitchen and school, the release of radon was tracked while running water provided a burst of radon in the kitchen. The key findings are:

1. Even though the amount of radon found in the kitchen after a water usage always exceeded the 0.150 $\mathrm{Bq\,L^{-1}}$ action level, little radon accumulation was found moving to the other, student-occupied rooms in the school.

2. Inside the kitchen, however, a spatial variation of the radon concentration existed throughout the room following water usage. For the two schools measured in detail, variations between 0.75 to 4.0 Bq L^{-1} and 0.2 to 0.7 Bq L^{-1} were found.

3. To accurately measure the radon accumulation in a room due to water usage, more than one detector is required.

4. Measurements of the air flow pattern would assist in making better conclusions about how well the room air mixes and where to place radon detectors.

5. Measuring SF_6 over time at one location of the kitchen is not sufficient to account for the ventilation of radon.

6. The model requires modification to incorporate the existence and ventilation of a non-uniform distribution of radon in air.

7. More than half of the schools studied showed significant ($>$200 Bq L^{-1}) increase in dissolved radon in water concentration during 1 hr of running water.

8. The model needs to account for a change in radon in water concentration.

9. It would be useful to understand why the radon concentration changes to predict the observed behavior and get a better representation of the ground water's radon concentration.

Chapter 4

MODELING RADON VARIATION IN BEDROCK WELLS

4.1 Introduction

4.1.1 Location of radon in ground water

Identifying strict geological determinants of the occurrence of radon in ground water is not easy. Radon concentrations differ among different rock types, however, it can also vary within the same geological formation (Sloto 2000, Hess et al. 1985). Radon concentrations in water up to 37,000 $\mathrm{Bq\,L^{-1}}$ in parts of the U.S. have been measured (Duncan et al. 1977, Hess et al. 1985). Radon concentrations in Maine have been identified by rock type with typical concentrations of ground water in granites of 810 $\mathrm{Bq\,L^{-1}}$ and 480 $\mathrm{Bq\,L^{-1}}$ in sillimanites (Brutsaert et al. 1981, Hess et al. 1985). It it generally accepted that high radon levels will be found in terrain of high grade metamorphic rock and granites (Brutsaert et al. 1981). This is primarily due to high concentrations of uranium in some of the minerals.

4.1.1.1 Influence of uranium

Naturally occurring uranium contains over 99% ^{238}U by mass (Baum et al. 2002). Radon is a member of the ^{238}U (henceforth referred to as uranium) decay series and ^{226}Ra (henceforth radium) is the immediate parent to radon. It is therefore expected that the presence of radium in rock will dictate the presence of radon.

When a radium nucleus decays, the resulting radon nucleus undergoes recoil from the emission of an alpha particle (a helium nucleus). Only a fraction of the radon produced in rock will be found in ground water or soil gas. The emanating power of a solid is defined

to be the fraction of the radon atoms that escape from the total number formed in the solid (Tanner 1980). There are many factors that control the emanating power of radium bearing rocks. The range of the recoiling radon atom is 20 to 70 nm, depending on the mineral densities (Quet et al. 1975). If the radium atom is close to pore space filled with water, the recoiled radon atom can come to rest in the water. The recoil range in air is greater, so if the pore is filled with air it is more likely that the radon atom will traverse the empty pore space and come to rest in the mineral grain. The effect of water-filled pore space is to increase the emanating power of the solid. Most of the emanated radon must come from radium found in shallow surface layers, up to a depth of the recoil range (Tanner 1964). Therefore, the presence of ground water enhances the release of radon from the solid ground. The water, which hydrates mineral surfaces, is able to absorb the kinetic energy of the radon atom formed during radioactive decay and carry it away instead of remaining adsorbed on rock surfaces (Tanner 1980).

Even though the presence of radium is a necessary requirement for radon production, the physical condition of the rock affects radon production more than the concentration of radium in the rock. Radon concentrations in water have been found to be thousands of times greater than dissolved radium and uranium concentrations (Hess et al. 1985). This is due to radium and uranium absorbtion on the host rock, usually on fracture walls. Others have found no correlation between radon and either dissolved radium (O'Connell and Kaufmann 1976, Davis and Watson 1990) or uranium (Veeger and Ruderman 1998, Gundersen 1989, Wanty and Nordstrom 1993, Gall et al. 1995). Radium is usually not homogeneously distributed in the rock. It is found mostly in films or crusts on the surface of rock pores. The secondary deposition of radium at the locations by its radioactive parents may be the cause of this non-homogeneity (Tanner 1964). It has been suggested that radium ions can diffuse into the fracture walls of bedrock causing a disproportionate amount of radon entering the adjacent water. This would explain why a lesser amount of uranium is found on fracture walls (Wood et al. 2004). It has been shown that the

radon concentration is inversely proportional to to bedrock fracture aperture (Torgerson et al. 1992, Folger et al. 1996, Nelson et al. 1983). For a large aperture, there is a low surface to volume ratio inside the fracture thereby producing dilute amounts of radon. Larger fractures generally have higher aquifer transmissivities, which would leave the water with less residence time with the surrounding radium in the rock. This correlation between high transmissivities and low radon concentration has been shown by Lawrence et al. (1991). However, others have found high aqueous radon concentrations within high hydraulic conductivity rock (Gall et al. 1995). In the study by Folger et al. (1996), they found differences of radon concentrations within and between well pairs hydraulically connected. The differences within well pairs have been explained by differences in hydraulic conductivities and fracture aperture measured in rock. The differences between well pairs were explained by differences in emanating power, ground water flow velocities and distribution of radium.

4.1.1.2 Chemical characteristics

Radon is an inert gas and therefore not chemically active. Radon concentrations in water do not correlate with pH, concentration of dissolved ions or solids, nor other chemical concentrations in the water (Senior et al. 1997, Davis and Watson 1990). In a study in Rhode Island, Veeger and Ruderman (1998) found some highly variable radon concentrations (20 to 3,000 $\mathrm{Bq\,L^{-1}}$) over 91 domestic wells. They discovered a positive correlation with alkalinity and fluoride content. They claimed the alkalinity would be a sign of weathering in the bedrock exposing the uranium deposits. The fluoride, reacting with uranium, would increase the uranium mobility to fracture surfaces.

4.1.1.3 Well characteristics

The type of well seems to have bearing on the amount of radon in ground water. Surface water generally has low radon concentration while deep bedrock water has high

radon concentrations. Public water typically has low radon since the high discharge wells usually draw from gravel aquifers to supply the high demand of water. With the high capacity wells, any radon is diluted with large volumes of water. However, private water supplies can have higher radon concentrations by a factor of 3 to 20 times (Hess et al. 1985). This is due to the low discharge of the wells, increasing the exposure of water to radium. Brutsaert et al. (1981) found some evidence high levels of sodium where the radon is low. High levels of sodium would be found in surface recharge water with a connection to road salt or septic system contamination. They also found that for wells drilled into granite, in general the radon level increased with depth to 30 m then remained constant with depth. The radon concentrations were negatively correlated well yield. High yield wells supplied water in the lowest radon concentrations, again suggesting a relationship between residence time and radon concentration.

4.1.2 Temporal Variations of Radon in Ground Water

4.1.2.1 Long term variations

Many researchers have discovered that the measured radon concentration in water varies between separate sampling times or while continuously sampling. In Southeastern Pennsylvania, Sloto (2000) noted that radon can change with time due to dilution by recharge. Changes in the contributing aquifer due to pumping and fluctuation in the water table can also drive the variation. They noted that there was no direct seasonal pattern of variation. Instead, the variation was directly related to changes in water depth, which can change seasonally. Farai and Sanni (1992) found significant variation when sampling over a year. Drane et al. (1997) questioned the ability of determining average annual radon concentrations by random grab samples. They found by taking five samples at each well, 97% of the radon measurements were within 30% of the annual mean.

4.1.2.2 Continuous sampling

Hightower and Watson (1995) sampled from nine wells for over seven months and found variation in the radon concentration. During sampling from a home spigot, they would purge the well to remove water from the well and pipes not representative of the ground water. For one of these sites, they sampled during a 140 min purge three times during the study. At the start of the purge they noted that the well had not been used recently. They found the radon concentration increased rapidly during the purge in an "S" shape curve; a low concentration followed by a rapid increase in radon concentration before leveling off. After reaching a maximum, the radon than declined slightly. The rapid increase was assumed to be due to an initial measurement of old, stagnant water in the well and pipes before reaching the fresh ground water. The later decrease was due to drawing from a source with a lower radon concentration. They concluded that the long term temporal variation they noticed over the seven months may not be due to a long term effect. Instead, it could be explained by inconsistent water usage or well pumping prior to water collection for those measurements. As shown by their 140 min sampling, the radon concentration is dependent on the amount of water recently removed. The U.S. EPA noted some of these studies and acknowledged that radon can vary on a daily basis or even longer. They acknowledged that long term variations (monthly, yearly) may simply be a reflection of the short term variations caused by well purging. They agreed that the local geology and specific operating condition during sampling may cause temporal variations, but the data supporting it is too limited to draw conclusions (EPA 1999).

Freyer et al. (1997) performed a study with similar results. When sampling for radon, they also found an "S" shaped curve. They concluded that this effect was due to an initial mixture of old, stagnant water from inside and immediately surrounding the well with entering radon-rich ground water. They noted that the moment in time of representative ground-water sampling is usually determined by water temperature, electrical conductiv-

ity, or pH but these may not be the most reliable indicators. Instead, they suggest that continuous sampling of radon while purging enables a better determination of representative sampling for other physical and chemical parameters. In 11 wells in an unconfined aquifer in Japan, Fukui (1985) also found a similar "S" shaped curve of radon concentration over time.

A study by McHone and Siniscalchi (1992) concluded that multiple sampling is needed to assess representative radon concentrations. They started with hourly test and stepped to longer sampling cycles. The 16 to 19 hourly tests were performed during a single day and found that early morning hours gave the lowest radon. Later in the day usually resulted in a 58% increase in radon concentration. Measurements of low radon concentrations early in the day before any water usage are consistent with previously noted studies. The period of stable radon concentration measured each day was used as the representative daily sampling period for daily sampling. The day of least variation was used for a weekly test.

4.1.2.3 Sampling protocol

The studies mentioned describe a fluctuation of radon concentration in water over a period of minutes to years. It was suggested that the long term variation may simply be a result of short term variation depending on the sampling protocols. Researchers have noted this effect and the importance of purging, they have either followed a predetermined purge time/volume or dispensed advice for future work. For instance, protocols include running water for 10 minutes (McHone and Siniscalchi 1992) or until water temperature is $11\,^{o}$C (Brutsaert et al. 1981), purge for at least 5 minutes (Drane et al. 1997), 15 minutes (EPA 1999), or remove $1\,\mathrm{m}^3$ (Fukui 1985). In order to truly assess the radon in ground water, it is worthwhile to completely understand the mechanism that cause such variations.

4.1.3 Radon as a tracer

Studies of radon concentrations in water have shown that it can be used as a tracer or signal of events. For instance, radon concentration in water increased by a factor of four several months before the 1995 Kobe, Japan, earthquake. The increase was more pronounced several days before the earthquake by a factor of ten. Since the earthquake, the radon concentrations have returned back to low concentration. It is believed that the increase in radon was due to precursor phenomena, such as the formation of strain-induced cracks in the rock, before the earthquake (Igarashi et al. 1995). Other cases of radon anomalies before earthquakes in the Soviet Union, China, and California are reviewed by Tanner (1980).

Radon in water can be used to signal areas of ground-water inflow into streams and rivers. Due to radon's short half life, contributions of snow melt and runoff, and aeration of radon, most surface water is low in radon concentration. However, by measuring various spots in a river or stream, areas with high radon concentrations could indicate ground-water seepage points (Ellins et al. 1990, Genereux et al. 1993, Lee and Hollyday 1993, Yoneda et al. 1991). Hoehn and von Gunten (1989) measured the radon concentration in a series of observation wells near a river. There was ground-water flow originating from the river. As ground water moved away from the river in radon-emanating rock, the radon concentration increased and ground-water residence times were estimated.

4.1.4 Radon in boreholes

It has been noted that radon concentration in water can vary for a number of reasons. However, the radon content in a borehole may provide the key to understanding the radon pumped out of the well. It is clear that the aquifer mineralogy (the presence and emissivity of the parent radium) establishes some baseline radon concentration in ground water. From there, the flow in and out and subsequent mixing in a borehole may control the variations noted over time.

In a borehole intersecting multiple bedrock fractures, each could have separate flow rates and radon concentrations supplying the well. This will affect the temporal variation of radon in water, especially if the water-table level or cone of depression drops thereby eliminating some fractures from supplying the well (Lawrence et al. 1991). The more fractures a well may have, with their separate flow rates and radon concentrations, may make the mixing problem a complicated one. Although for crystalline rock aquifers, it is common for only a few fractures to produce all the flow in the well (Folger et al. 1996).

Since the inflow points down a borehole may be signaled by a change in radon concentration, radon concentration profiles with depth may be a useful tool. This would show any differences or similarities in radon concentration in the vertical column of water in a well. This can be indirectly measured by a gamma-ray log of the well. A gamma-ray log measures naturally occurring gamma-ray radiation with a detector that is lowered down the well. Radon itself does not produce gamma rays, but a few of its short lived daughters do (^{214}Pb and ^{214}Bi). In a study by Nelson et al. (1983), they found the radon daughters dominated the gamma logs where the ground water flow was appreciable. They found the total gamma activity to increase near high radon concentration ground-water inflow and decrease along the flow inside the borehole. These gamma logs enabled a crude flow profile in the well.

It is possible to directly measure the radon content in the water by taking a water sample from discrete intervals in the well. A study by Gall et al. (1995) found a vertical variation of radon in the water column by using a straddle packer assembly. This method packs off an interval of the well column and allows a pump to draw water exclusively from one area. The areas with elevated radon levels (and also uranium in adjacent rock measured by neutron activation analysis) were correlated to fractures zones with high flow conductivity.

Another study took a more detailed look at the radon depth profile and correlations with temporal variations of radon while pumping a well. Cook et al. (1999) examined both

nested piezometers (small diameter pipes installed into the subsurface (Fitts 2002)) and an open borehole. The nested piezometers had a screen length (interval open to the ground (Fitts 2002)) between 0.5-5 m over 100 m for 10 discrete intervals in the ground. Samples were taken from the piezometers with pressurized stainless steel bailers. The goal was to make depth measurements before and after pumping (2 well volumes) to get horizontal ground-water flow. They hypothesized that the natural ground-water flow would be proportional to the ratio of the purged to unpurged radon concentrations. This would only be true in nested piezometers where the sample point is well mixed. Where there would be low flow, the stagnant water at that depth would have low radon concentration due to the decay of radon. At high flow areas, there would be newer, replenished water entering the well. From the radon measurements, the flow rates were determined, which agreed with other borehole logging parameters such as electrical conductivity and temperature gradients. In addition, they looked at the radon concentration over time while pumping from two of the 10 nested piezometers. For one, the radon concentration increased while pumping and after one well volume removed, the level became constant with time. The initial and final radon concentration even agreed with the concentration at that depth for the unpurged and purged measurements, respectively. For the other case, the increase was less, which led the authors to suggest that they may have been drawing water from greater distances.

The results from the nested piezometers verified a relation between radon depth profiles and temporal radon changes while pumping. The temporal effect has been clearly noted in open boreholes (much like private wells). Unlike nested piezometers with a small screen length (the part of the pipe open to the ground), open boreholes are screened or open most of their drilled length. A casing closes off a top portion of the borehole from the ground. Cook et al. (1999) conducted their experiment in open boreholes differently than with the nested piezometers. Unpurged water samples at 5 m intervals were taken with either the bailer or a dialysis membrane diffusion cell left in place for a period of

time. The open borehole was not pumped. From the unpurged profiles, a variation in radon was observed. They believe increases in radon concentration signals active areas of ground-water inflow and hydraulically active fractures. There may be vertical flow in the well, which was not accounted for in these studies. To rule out other causes of variation, they performed alpha spectroscopy on the drilling chips and found little variation of the parent radium as a function of borehole depth. They concluded the radium content in the surrounding rock must not dominate radon content of the enclosed water.

Borehole geophysicists send a variety of tools down a borehole to measure parameters to survey a well. Commons tools include temperature sensors, calipers (to measure diameter and locate fractures), flow meters (using either a impeller or heat pulse), gamma-ray detectors, and electrical conductivity probes (Folger et al. 1996, Fitts 2002). This last tool can be used to explore the inflow and outflow of water in a well. This is done by first replacing the well column with de-ionized water. Next, an electrical conductivity probe is continuously lowered and raised while the well is pumped. Since the well is being pumped, any inflow points will supply ground water of some salinity into the de-ionized water column. Running the electrical conductivity probe up and down the well will show the time evolution of fluid electrical conductivity. The hydraulically active zones will be evident as a peak in conductivity. Further, this peak will skew and spread in the direction of the water velocity under pumping condition. With a proper model, the individual flow rates from each inflow can be determined. This flowing electrical conductivity is explained in more detail in Doughty and Tsang (2005). The spirit of this experiment may work for with radon. The natural radon flowing into the well under pumping conditions and the mixing in the well that follows could provide the same information. The radon method would save the lengthy step in the flowing electrical conductivity method of replacing an entire well volume with de-ionized water.

4.1.5 Sampling a well

In order to study radon in ground water from an open borehole, it is necessary to adequately sample the water. Generally speaking, there are two basic means to collect a sample of water, either draw water out with a pump or send down a bailer to collect a sample. Clearly, these two methods have differing effects on the well. When water is pumped, the water in the well evacuates and/or new ground water is drawn from the surrounding aquifer. In the above studies, when the radon in water was observed over time to show temporal variations, it was performed by pumping water out of the well from some arbitrary depth. However, using a bailer only takes a small volume of water from a desired depth. Collecting a sample with a bailer will mix water in the well but has minimal effect on the aquifer.

There are commercial products available called discrete interval samplers for sampling at depth in a column of well water. Parker and Clark (2002) reviews a variety of these samplers. There are a few basic designs. One type is made from a stainless steel tube with a collection vial housed inside. It has inlet and exhaust ports designed such that the collection vial does not fill until it has remained stationary for a few seconds. Another bailer is made from a flexible polyethylene bag with a floating ball check valve. It can be maneuvered with proper up and down movements to fill the bag. A third type involves applying positive pressure (above the ambient pressure of the water to be sampled) to the sampling vessel while the sampler is lowered and raised. This involves running a tube from the sampler to the surface where an inert gas can be applied with an air pump or gas cylinder. The sampler is outfitted with floating check valves to allow water to flow under the desired pressure differences between the inside and ambient water. It is clear that the application of positive pressure to the sample will keep it from leaking and ensure a water sample from a discrete depth in the well. However, the unit is expensive and the application of a gas at a correct pressure before and after every sample adds to the labor

involved. A fourth type uses a diffusion bag lowered down to a depth in a well. It relies on the diffusion across the membrane. The obvious drawback of this method is the long (several days) waiting period for equilibrium across sampler membrane.

Aside from those samplers mentioned, a pump can also be used to take samples from a discrete interval. The pump (if submersible) or the tube from a surface driven (or peristaltic) pump can be lowered to discrete depths. This process can be aided by placing packers above and below the pump point. Typically these packers, like balloons, can be inflated when in position to block off other parts of the well. That interval can then be pumped to purge that portion of the well or simply pumped long enough to collect a sample at the surface.

The major drawback of all of these discrete interval samplers for measuring radon is the ability to collect a sample following the protocol for liquid scintillation analysis. The water collected for radon analysis must first be drawn into a syringe where a fixed volume can be obtained. It is also ideal for the water entering the syringe to have minimal radon loss due to degassing. In order to use these samplers for radon analysis, modifications would need to be made to allow a syringe to draw water from the collected water. Of the samplers mentioned, the pressurized sampler seems to be the most suited for the task of collecting water for radon analysis. The positive pressure applied during transit ensures no leaking of water into the empty sampler on the way down, as well as keeping the high pressure inside during removal of the sampler from the well. The other designs claim to resist the pressure changes while the sampler is in transit, but it remains to be shown how well they resist loss or out-gassing of radon.

A simpler sampler can be designed and built with the same principle of operation as the pressurized sampler, but with an easier operation. This study used a custom built sampler that electrically controls valves to open and seal a sampler at desired times during transit and collection (Section 4.3.1.1). Electrical control enables similar principles of operation by applying an electrical potential across the valves instead of applying and

releasing air pressure from an air pump or compressed air tank. In addition, since it is custom built, it was designed around a method to use a syringe to extract water samples without any distraction from the intended operation of the sampler.

4.1.6 Goals of this study

The short term temporal variation of radon in water may not be entirely due to changes in the aquifer mineralogy nor changes in the emanating power of radium in the rock. One or more fractures supply ground water to a well. The movement and mixture of water from these sources could cause a change in the radon concentration of a well while pumping. This investigation used an advection-dispersion model to fit the movement and mixing of radon-rich water in a well. At a collection of research wells, a custom built sampler was utilized to take a depth profile of the water before and after the wells were pumped to purge them of some stagnant water and draw water from the aquifer. The additional step of taking a depth profile both before and after pumping was essential in order to see changes in the radon profile and infer locations of water inflow. These inflow locations, or water bearing zones, were verified by borehole geophysical logging on the wells. The locations of inflow and estimates of inflow rates and initial radon concentrations allowed a test of the model.

4.1.7 Wells used

The wells used in this study are a collection of fractured bedrock wells on the University of Maine campus, Orono, ME, USA (Fig. 4.1). Five of the wells are 76 m deep, open boreholes drilled during the summer of 2003 exclusively for teaching and research purposes. Based on their locations around campus, a three-letter identification code has been assigned: BRY, FRW, FWD, RVR, and STW. Another four wells of depths 90-110 m were drilled for an aquaculture laboratory but not currently used: AWA, AWB, AWC, and AWD. The wells are ideal for this study since, except for other research, they are not used.

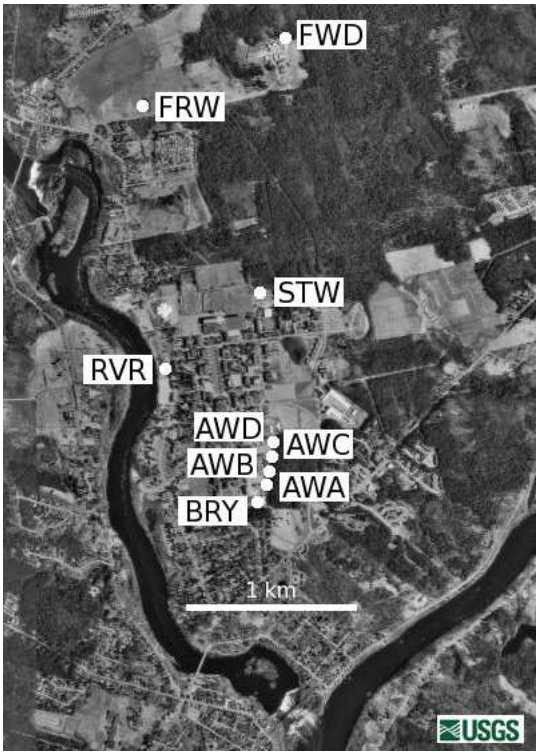

Figure 4.1: A map of the University of Maine campus in Orono, ME, USA showing the locations of the research wells.

Therefore, there will not be the question of prior usage or history that plagued studies by other researchers.

4.2 Theory

4.2.1 A conceptual well

A conceptual well model was developed to aid in construction of a mathematical model of the flow and mixing of radon enriched ground water through a well. Assume the borehole of the well is a perfect cylinder of cross-sectional area, A. Ground water feeds the well through discrete fracture locations (Fig. 4.2). The well is pumped from some spot in the well with discharge Q [L min^{-1}]. The fractures each provide a flow $q_i : i \in (1, 2, 3)$ into the well. If the water level in the well drops while pumping, an additional flow, q_h, is provided by the water stored in the well. The pumping sets up flow fields in the borehole

given by q_h, q_a, q_b, q_c. By mass balance,

$$Q = q_h + q_1 + q_2 + q_3 \tag{4.1}$$

$$q_a = q_1 + q_h \tag{4.2}$$

$$q_b = q_2 + q_3 \tag{4.3}$$

$$q_c = q_3 \tag{4.4}$$

Since all of the flow in the well exists over a fixed cross-sectional area, the flow is proportional to the velocity,

$$q_a = A(v_1 + v_h) \tag{4.5}$$

$$q_b = A(v_2 + v_3) \tag{4.6}$$

$$q_c = Av_3 \tag{4.7}$$

where v [m min^{-1}] is the average velocity.

As long as the water level in the well remains constant during pumping, $q_h \approx 0$ and q_i are assumed to remain constant. The flow of each fracture is linked to the change of head in the well. In the case where the water level drop in the well cannot be neglected and the only fractures were above the pump location, it is the flow of q_a which is assumed to remain constant while pumping.

4.2.2 Advection-dispersion model

An advection-dispersion model was applied to the wells studied. The intent was to describe the change in radon concentration as water was pumped out of a well. It will be assumed that, while pumping, ground water enters the well at one or more fractures with a particular radon concentration. The model used described the movement of radon out of these fractures carried by the moving water to the location of the pump. In general, the change in concentration is given by:

$$D\nabla^2 C - v\nabla C - \lambda C + S = \frac{\partial C}{\partial t}. \tag{4.8}$$

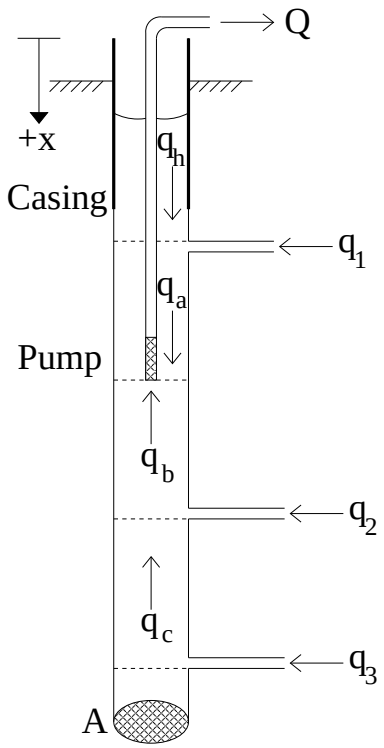

Figure 4.2: A conceptualized well showing inflow and outflow.

where C [Bq L^{-1}] is the radon concentration (Fitts 2002, Appelo and Postma 1996).

In the first term, D [m min^{-1}] governs mixing as the radon moves with the water:

$$D = D_{diff} + D_{disp} \tag{4.9}$$

where D_{diff} is the molecular diffusion coefficient and D_{disp} is the mechanical dispersion coefficient due to variations in the water velocity across the cross section of the well. The average velocity of the water is given by v. The second term represents the advective flow of the radon with the velocity of water. This advection is the primary means for transporting the radon through the well. The third term on the left is the radioactive decay of radon and the final term, S [Bq L^{-1} min^{-1}] represents sources of radon into the well. The sources will likely occur at discrete location where fractures supply the well with its primary source(s) of water.

The molecular diffusion of radon in water is quite small, $10^{-5}\,\mathrm{cm^2\,s^{-1}}$ (Tanner 1964), and the first term in equation 4.9 can be ignored for large enough flow velocities. Since the mechanical dispersion is velocity-driven, it is proportional to the velocity (Appelo and Postma 1996),

$$D_{disp} = \alpha v \tag{4.10}$$

where α is the dispersivity in the direction of v. The radioactive decay of radon follows the general decay law,

$$A(t) = A_0\, e^{-\lambda t} \tag{4.11}$$

where the half-life is given by,

$$\lambda = \frac{ln\,2}{t_{\frac{1}{2}}} \tag{4.12}$$

The half-life of radon is large enough, $t_{\frac{1}{2}} = 3.82\,\mathrm{days}$, that it can also be ignored for analyzing transport of radon for time intervals on the order of a 1 to 4 hours.

During pumping, most of the flow in the well will be vertical and horizontal velocity can be ignored. Therefore, a one-dimensional version of equation 4.8 can be used. With a sizeable cross section (∼15 cm diameter), a well is not one-dimensional, although the mechanical dispersion accounts for the horizontal non-uniformity of velocity and one-dimension flow will suffice in the model. The one-dimensional advection-dispersion model is given by,

$$\alpha\, v\frac{\partial^2 C}{\partial x^2} - v\frac{\partial C}{\partial x} + S(x) = \frac{\partial C}{\partial t} \tag{4.13}$$

Here x is the distance down the well measured from the well head.

4.2.3 Finite difference solution

A custom finite difference computer code (Appendix C) was written to model the wells studied. The method used employs a central difference of the dispersion term, backward difference on the advection term, and a forward difference in time, as shown

by,

$$\alpha\, v \frac{C_{i+1}^m - 2C_i^m + C_{i-1}^m}{(\Delta x)^2} - v\frac{C_i^m - C_{i-1}^m}{\Delta x} = \frac{C_i^{m+1} - C_i^m}{\Delta t} \tag{4.14}$$

where i and m represent a spatial and temporal location, respectively, and Δx and Δt are the space and time steps. The dispersivity and velocities are considered to be constant over each space step. Solving for the concentration at a particular location and forward in time is defined with respect to other location at the current time,

$$C_i^{m+1} = C_i^m + \frac{\alpha\, v_i\, \Delta t}{(\Delta x)^2}(C_{i+1}^m - 2C_i^m + C_{i-1}^m) - \frac{v_i\, \Delta t}{\Delta x}(C_i^m - C_{i-1}^m) : v > 0 \tag{4.15}$$

$$C_i^{m+1} = C_i^m - \frac{\alpha\, v_i\, \Delta t}{(\Delta x)^2}(C_{i+1}^m - 2C_i^m + C_{i-1}^m) + \frac{v_i\, \Delta t}{\Delta x}(C_i^m - C_{i+1}^m) : v < 0 \tag{4.16}$$

At locations of water inflows, an additional source term,

$$\frac{v_j\, \Delta t}{\Delta x} C_j \tag{4.17}$$

is added onto equations 4.15 and 4.16 for each source location, j, where v_j is the velocity of the water source. All of the velocities refer to the water velocities inside the borehole. It will suffice to model flow using only water velocity instead of volumetric flow rate.

The initial conditions are set from the radon concentrations measured as a function of depth in the well before pumping. Unless the space and time steps are set so that

$$\Delta x = v\, \Delta t \tag{4.18}$$

it has been shown that a finite difference code generates artificial numerical dispersion (Appelo and Postma 1996). The numerical dispersion amounts to a dispersivity of

$$\alpha_{num} = \frac{\Delta x}{2} - \frac{v\, \Delta t}{2} \tag{4.19}$$

and it can be eliminated by using an effective dispersivity found by subtracting the numerical from the actual dispersivity,

$$\alpha_{effective} = \alpha_{actual} - \alpha_{num} \tag{4.20}$$

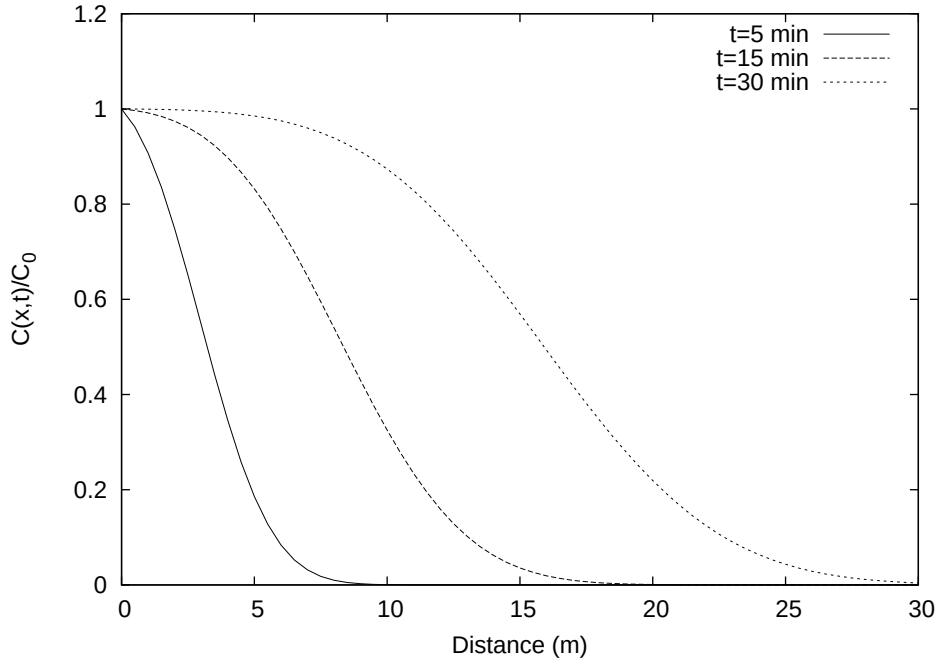

Figure 4.3: Normalized radon concentration vs. depth for a hypothetical well at three different times. An inflow of radon at $x = 0$ with fixed velocity, $v = 0.5$ m min^{-1}, and dispersivity, $\alpha = 1$ m.

4.2.4 Example of the model

To illustrate how the parameters in equation 4.13 change the theoretical radon concentrations, hypothetical solutions are generated for a column of water with a inflow of radon with concentration C_0 at $x = 0$ with initial concentration $C = 0$ everywhere being pumped at $x = 40$ m. The movement of the radon from a source flowing with the water for several times is shown in Fig. 4.3. The midpoint of the front, $C = C_0/2$, moves approximately as $x_{1/2} = v\,t$.

The effects of the water velocity in the water column are shown in Fig. 4.4. The radon concentration as a function of time at a distance of 15 m downstream of the inflow location is plotted. The effect of larger velocities results in a faster movement of the radon front. It also results in an increase spreading of the front.

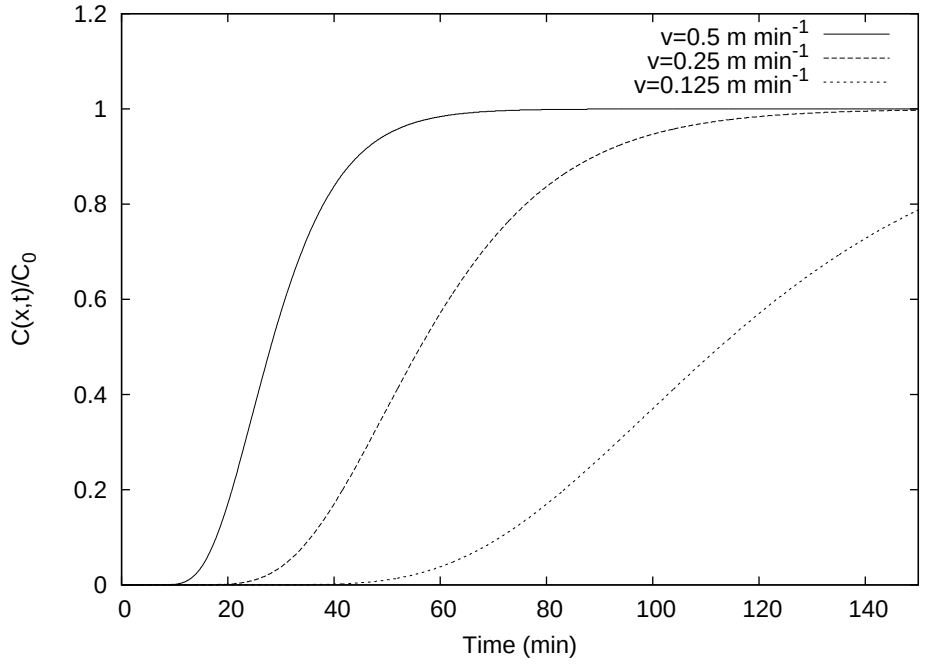

Figure 4.4: Normalized radon concentration vs. pump time for a hypothetical well for three water velocities. An inflow of radon at $x = 0$ at a fixed dispersivity, $\alpha = 1$ m.

Fig. 4.5 shows the effect of different dispersivities for a fixed water velocity. Lower dispersivities cause a front of radon closer to a square wave, while larger dispersivities cause more spreading of the radon front.

4.3 Materials and methods

4.3.1 Depth measurements

4.3.1.1 Construction of depth sampler

In order to measure the radon concentration in the water column in a well, a sampler was constructed (Fig. 4.6) out of common parts listed in Table 4.1.

It was important to use a water sampling vessel that was pressure tight, could easily be operated, and accessible to remove a pressurized water sample with a syringe. The major valve control was made by two direct current (DC) solenoid valves. The valves

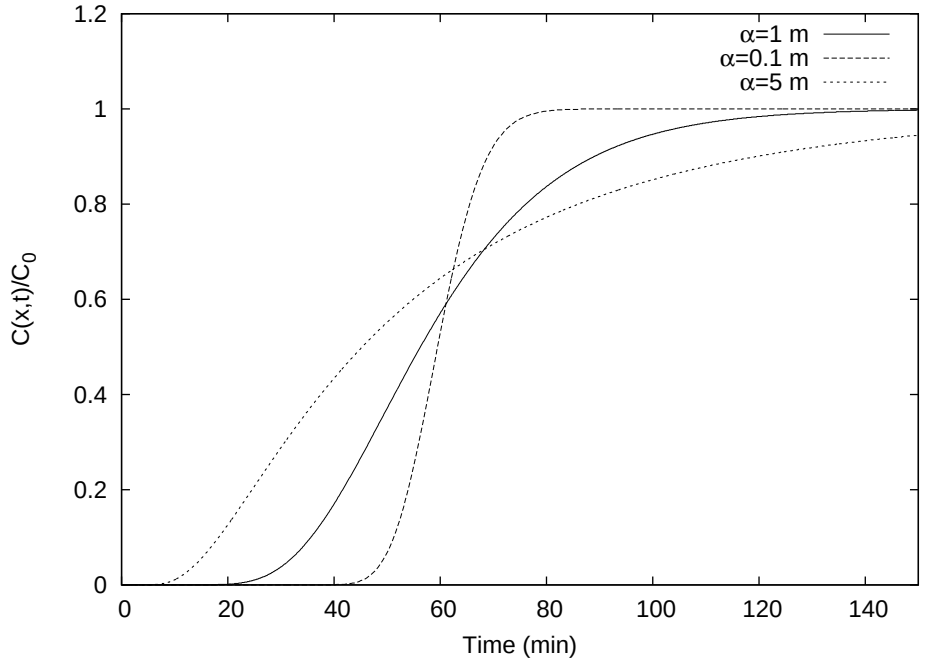

Figure 4.5: Normalized radon concentration vs. pump time for a hypothetical well for three dispersivities. An inflow of radon at $x = 0$ at a fixed velocity, $v = 0.25$ m min^{-1}.

are normally closed and will open when 24 V DC is applied. A system to remove a pressurized water sample was needed; the method used to pressurize a basketball was borrowed. When an air pump is used to fill a basketball with air, a special needle is attached to the pump and inserted into a rubber nipple in the ball. When inserted, the pump can inflate the ball, but when removed, the nipple holds the modest amount of air pressure. An air-filling needle was fastened to the tip of a syringe in place of the usual sharp needle. A basketball-filling nipple was removed from a basketball, turned down on a lathe to achieve the proper diameter and fastened inside a cord grip.

A pipe connects the two valves and serves as the sampler body for holding the water sample. One-way check valves are on either end of the pipe and valve assembly. These were needed since the DC valves only hold a pressure differential in one direction when closed. The addition of a check valve with the opposite sense of direction ensures the sampler will not leak when the inside is a different pressure than the outside. With this

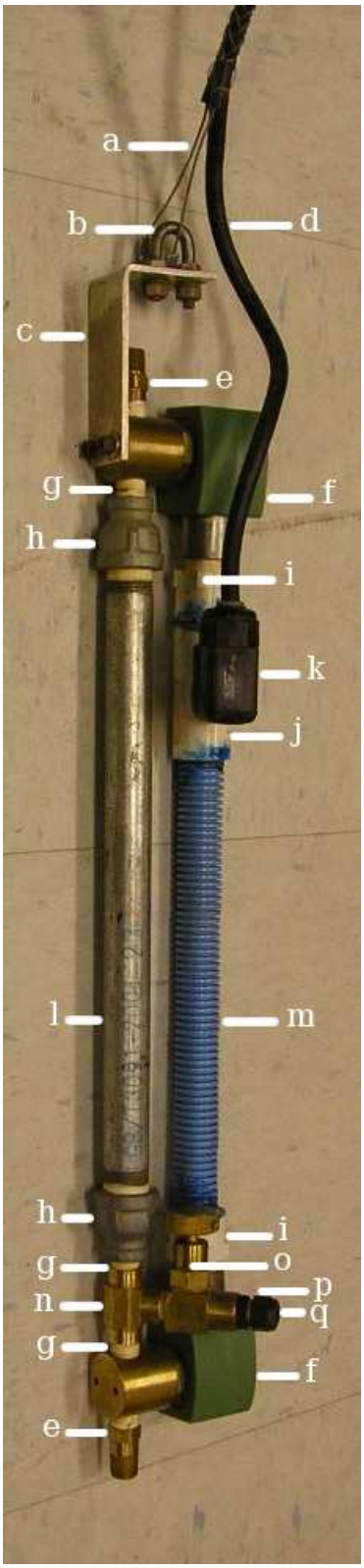

Figure 4.6: The discrete interval sampler constructed to remove water samples from a well. The labeled parts are listed in Table 4.1.

Table 4.1: The parts used to assemble the discrete interval sampler. Parts without a source are general hardware.

Part	Description	Source & Cat. Number
a	cable support grip	Grainger, Portland, ME 6C095
b	u-bolt	
c	aluminum support	manufactured
d	16/2 SJOOW cable 360 feet	Delco Wire & Cable, Oldsmar, FL
e	check valve 1/4” NPT male x male	McMaster-Carr, New Bruswick, NJ 7768K56
f	general service solenoid valve 1/4” NPT	ASCO, Florham Park, NJ 8262G20 24VDC
g	brass nipple 1/4” MPT	
h	galvanized reducing coupling 1/2” FPT x 1/4” FPT	
i	PVC male conduit adaptor 1/2” NPT	
j	PVC tee 1/2” x 1/2” x 1/2” MPT	
k	liquid-tight cord grip 1/2” MPT	McMaster-Carr, New Bruswick, NJ 7008 K73
l	12”galvanized pipe 1/2” MPT	
m	flexible electrical conduit 1/2”	
n	brass tee 1/2” NPT female x male x female	
o	brass needle valve 1/4” NPT male x female	McMaster-Carr, New Bruswick, NJ 7833K21
p	liquid-tight cord grip 1/4” MPT	McMaster-Carr, New Bruswick, NJ 69915 K47
q	rubber filling nipple	basketball

valve configuration, water can only enter through the bottom and exit from from the top when the DC valves open. In between the sampler body and the retrofitted basketball nipple is a flow control valve that can be manually opened and closed (see figure 4.7) .

Figure 4.7: A closeup of the discrete interval sampler showing the flow control valve and insertion of a syringe for sample removal.

This was needed as a redundant sealing point in case the basketball nipple leaked. More importantly, it allowed a manageable way to fill the syringe. When a water sample is taken deep in the well, it will be at a much higher pressure than atmospheric pressure at the surface of the earth. The pressure can be great enough to fill and blow out the plunger in the syringe upon inserting it through the nipple. The flow control valve allows a slow, controlled, filling of the syringe.

To electrically connect the DC valves and support the sampler, 110 m of 2-conductor, 16 gauge copper cable with a waterproof rubber sheath was used. The gauge chosen offers a low enough resistance to energize the valves and high enough breaking strength to support the sampler. The two DC valves are wired in parallel for simultaneous operation. The electrical connections on the sampler are made behind a water-tight flexible conduit between the two DC valves. The cable exits the sampler through a water tight cord grip and is fastened to the sampler body with a strain relief grip. At the surface, the cable is wound around a large reel mounted on a stand, which allows the sampler to be easily

Table 4.2: The dates when radon profiles were measured at the wells.

well	unpurged date	purged date	interval (days)
STW	5 May 05	1 Jun 05	57
FRW	5 May 05	20 Jun 05	26
BRY	31 Jun 04	21 Jun 06	355
FWD	8 Jul 05	13 Jul 05	5
RVR	8 Jul 05	12 Jul 05	4
AWA	3 Aug 05	2 Sep 05	30
AWB	3 Aug 05	4 Oct 05	62
AWC	4 Aug 05	22 Sep 05	49
AWD	4 Aug 05	20 Sep 05	47

lowered and raised through the well. The DC valves are powered by two rechargeable 12 V sealed lead-acid batteries wired in series.

4.3.1.2 Operation of depth sampler

The depth sampler is used to obtain water samples from discrete depths in the well's water column. The depth profile of radon was made twice at each well for a particular sampling run. It was first taken from an undisturbed well, one without any recent pumping. This profile represents the unpurged state of the well. The well then remained untouched for several days for the well to equilibrate from the disturbance of moving the sampler up and down the well. After this time, the well was pumped for some amount of time and a repeat depth profile was immediately made by taking samples of the water at multiple depths. These measurements represent the purged radon depth profile. These two measurements were made once on all nine wells. The dates and length of time between the unpurged and purged measured are listed in Table 4.2.

The sampler was operated by first placing the stand holding the spool of cable and the sampler over a well head. The wells are usually sampled starting at a depth of 15 m below the well head and continued every 6 m down the depth of the well until hitting bottom. The shallowest depth was sampled first, so that any water at a depth being sampled had not

previously been disturbed by lowering and raising the sampler. The sampler was lowered to the desired sampling location and the the reel was locked in place. The battery leads are connected to the cable to open the DC valves. Down inside the well, the air originally inside the sampler will escape out of the top due to the hydrostatic pressure outside of the sampler causing water to rush in the bottom until an equilibrium pressure has been reached. Trials have shown this process takes a few seconds. For consistency, the battery remained connected for 15 seconds. After disconnecting the battery, the sampler was raised by winding the cable around the reel. At the surface, the sampler was laid flat next to the reel. The syringe was inserted through the basketball nipple and the flow control valve was opened slightly to allow 5 ml of water into the 10 ml syringe. The water was used to flush the syringe and discarded. Next, two separate 10 ml samples were taken the same way using the flow control valve to regulate filling the syringe. While suspending the sampler in the up-side down direction, the DC valves were energized to allow the remaining water to drain out. The process was repeated for deeper samples until the bottom of the well was reached.

The sampler was cleaned between use with distilled water. A 1 L bottle with a pipe fitting on the lid and filled with distilled water was screwed to the bottom of the sampler. With the DC valves energized and the sampler upside-down, the bottle was squeezed which forced the distilled water to flush the inside of the sampler. The outside of the sampler was also rinsed with distilled water.

4.3.2 Measuring radon while pumping

Each of the nine wells studied were pumped in between the discrete interval sampling. While the pumping occurred, periodic samples of the pumped water were taken to measure the radon concentration. Pumping and measurement of radon were repeated at four of the wells, but on the repeat study there was not any corresponding depth profile

Table 4.3: The flow rate and duration of pumping at each well. The error is a 1-σ standard deviation of multiple measurements.

well	date	flow rate (L min^{-1})	duration (min)
STW	1 Jul 05	4.33 ± 0.34	134
FRW	20 Jun 05	5.12 ± 0.09	135
BRY	21 Jun 05	4.88 ± 0.09	132
FWD	13 Jul 05	4.39 ± 0.11	142
RVR	12 Jul 05	5.09 ± 0.13	140
AWA	2 Sep 05	4.97 ± 0.12	128
AWB	4 Oct 05	5.05 ± 0.12	122
AWC	22 Sep 05	5.13 ± 0.12	123
AWD	20 Sep 05	5.15 ± 0.10	124
STW	18 May 06	4.35 ± 0.38	187
FRW	25 May 06	5.10 ± 0.11	143
AWA	27 May 06	4.95 ± 0.11	257
AWC	31 May 06	5.02 ± 0.11	253

measurements. The flow rates and duration of pumping for each well are listed in Table 4.3.

4.3.2.1 Pumping the well

A 12 V submersible pump[1] was lowered down the well to a depth of 40 m measured from the well head. The pump was powered by a rechargeable 12 V lead-acid battery[2] at the surface. The pump was supported by a tube that delivered the water from the pump to the surface. The end of the tube was placed at the bottom of a 400 ml glass beaker and the flowing water was allowed to overflow from the beaker. The pump was run for at least 2 hr, and for some wells later in the study, as long as 4 hr.

When the pump was first started, a water sample was taken from the beaker. The tube was momentarily removed from the beaker to minimize agitation in the beaker. Using the 10 ml syringe, a water sample was taken and discarded to flush the syringe. Next, two consecutive, separate 10 ml samples were taken from the beaker. When sampling was

[1] Sampling Pump 81. Keck Instruments, Williamston, MI

[2] Die Hard Deep Cycle, Sears, Roebuck and Co., Hoffman Estates, IL

complete, the beaker water was discarded and the pump's tube was placed back in the beaker. Additional pairs of samples are taken the same way after 10 minutes, followed by intervals of 20 minutes until the pumping had ceased.

4.3.2.2 Temperature monitoring

While pumping occurred, the temperature of the water was logged. This was done by placing a glass thermometer[3] in the beaker with the overflowing pumped water. The temperature was noted periodically as the temperature changed and less often once it stabilized.

4.3.2.3 Flow rate determination

The flow rate of the pump was determined by timing the filling of the 400 ml beaker several times. The tube from the pump was removed from the beaker and the beaker water was discarded. Using a stop watch, the time it took to fill the beaker was measured with a stop watch. This process was immediately repeated two more times for a total of three measurements. This triplicate flow rate measurement was then repeated two more times throughout the duration of pumping the well.

4.3.2.4 Water level depth measurements

While pumping from the well, the water level in the well may drop. This was measured using a water-level meter[4] lowered from the surface down the well. The depth to the water was measured relative to the top of the well. Depth measurements were made often after pumping began to assess how quickly the water was dropping. Depth measurements were made periodically to achieve at least 15 measurements during pumping. If the water level dropped quickly, measurements were spaced to collect depth changes of no more than 0.5 m.

[3]Fisherbrand Laboratory Thermometer 14-997, -20^o C–110 C, Pittsburgh, PA
[4]Solinst 101-30MP4, Georgetown, ON

4.3.3 Radon measurements

The water samples obtained from the discrete interval sampling and while pumping were analyzed for radon concentration. The 20 ml glass scintillation vials with polyseal cone caps were prepared before sampling by adding 5 ml of mineral oil scintillation cocktail. In both sampling cases, 10 ml of water was collected with a syringe. While at the well, the syringe needle was placed in the vial and slowly injected underneath the mineral oil, which remains above the water. The vial was capped and brought back to the laboratory for counting in a liquid scintillation counter. The raw data from the counter was analyzed to calculate the radon concentration at the time sampled from the well following the procedure in Section 2.2.2.

4.3.4 Borehole logging

The wells studied were also logged using borehole geophysical instruments[5] by researchers in the Department of Earth Sciences, University of Maine. The tools used were a 3-arm caliper and a heat pulse flow meter. The spring loaded calipers measure the diameter of the borehole while being pulled up the length of the well. This measurement should respond to openings and cracks in the borehole wall, locating fractures in the bedrock. The heat pulse flow meter measures flow by firing a heat pulse into the water. Oriented above and below the heated location are temperature sensors that monitor the temperature and await the moving heat pulse. Water velocity in the borehole was measured by timing the movement of the heated pulse of water over a fixed distance. The measurement was made in a fixed cross-sectional area allowing the calculation of discharge. These measurements were made under ambient and pumped conditions.

[5]Mount Sopris Instrument Company, Inc., Golden, CO

4.3.5 Measurement of rock chips

Rock chips were collected at 6 m intervals during well drilling at five of the wells. These were counted in one of two high purity germanium detectors.[6] They were placed in the counter for 24 hr and analyzed for radium content by counting the 186.2 keV gamma peak using gamma spectroscopy. Liquid radium standards of approximately the same volume and shape of the rock samples were used to calibrate the analysis. ^{235}U emits gamma radiation with energy of 185.7 keV and can be incorrectly counted as a radium disintegration event. Other gamma radiation from ^{235}U was used to subtract the competing contribution at 186 keV. The content of ^{214}Pb and ^{214}Bi progeny were also measured using their 352 keV and 609 keV gamma radiation, respectively. The sample bags holding the rock chips were not air tight therefore gamma-producing radon daughters can only be used to set a lower limit for the original radium content of the rocks.

Rock samples from four of the wells and 2 rocks broken away from fractures in one well were analyzed for their radon bearing concentration. The rock samples were placed in a Teflon-lined glass vial with over 20 ml of distilled water. These vials were allowed to sit for over one month in order for the radon to grow in. After that time, they were opened and two, 10 ml water samples were drawn with a syringe and prepared for liquid scintillation radon analysis by liquid scintillation. From the mass of the rocks, volume of the distilled water, and measured radon concentration, the radon emanated per rock mass was determined and compared against the radium concentration. These two would be equal under complete emanation and secular equilibrium between the radium and radon.

4.3.6 Modeling radon measurements

The finite difference method was used to numerically solve the advection-dispersion equation and simulate radon transport in the pumped wells. The model was first given a proper domain defining the length of the well and the duration of the pumping. The initial

[6] Canberra Industries, Meriden, CT

radon concentration measured (the unpurged radon data) are used to define the initial concentration throughout the domains. A linear fit between adjacent measured points sets the concentration at every node between the first and last data point. The model accepts one or more inflow locations carrying water, and radon, into the borehole and towards the pump. The number of sources was estimated from the radon profiles and the borehole geophysics flow data. From the radon profiles, locations where the unpurged and purged data deviate from each other are likely inflow locations. If that location also shows an onset of flow in the flow logs, it was considered a source in the model. The radon concentration of each water source was estimated from the change in the radon profile after pumping. The relative flow rate of each source entering the borehole was estimated from the pump flow rate, following mass conservation. For those wells where the water level in the well dropped considerably ($>$0.5 m) while pumping, the model including the velocity resulting from the storage flow contribution, q_h.

Simulations were calibrated by adjusting the source terms (inflow and radon concentration) until simulated radon concentrations fit measured radon concentrations. Once the parameters were optimized, a sensitivity analysis was performed to determine uncertainties. This was done by finding the range over which the source flow rates and radon concentration remained within $\pm 2\sigma$ of the measured data.

4.4 Results

The results from the STW, FWD, FRW, RVR, AWA, and AWC wells represent the major features of the wells and are presented here and discussed. The results from the remaining wells are given in Appendix B and not discussed. Well AWB showed little variation with depth and time; the profiles of well BRY were separated by almost a year

but had a response similar to AWA; and the AWD well purged profile measurements were faulty.[7]

4.4.1 Radon measurements with depth

The wells were measured using the depth sampler to obtain a water sample and analyzed for radon following the liquid scintillation method. The following results represent the radon profile in the standing water column in the well's borehole.

The radon profiles (Figs. 4.8-4.13) show that a variation of radon concentration exist throughout the depth of a well. The unpurged profile represents ambient well conditions. The purged profile reveals the change in radon concentration immediately after the well has been pumped. The results of the advection-dispersion model at the end of pumping each well were plotted. In particular, wells STW and FWD show a region of the well with a remarkably low radon concentration (<3 Bq L^{-1}). In all cases, there were one or more spatial regions in the well that show a change in radon concentration after pumping. This change was evident on either side of the 40 m depth, where the pump was placed.

4.4.2 Pumping the well

Figures 4.14-4.23 show the radon concentration of the water pumped out of the well and the radon concentration predicted by the model. The temperature of the pumped wells stabilized to a temperature between 7-8.5 °C within 7 ± 5 min of pumping. While pumping, the water level in the FWD, FRW, RVR, and AWC wells dropped less than 0.2 m while the STW and AWA wells dropped over 2 m while pumping (Appendix B, Figs. B.6-B.8).

The STW, and FWD wells resemble the skewed "S" shaped response (Figs. 4.14, 4.15, 4.16). The radon rises from its initial value before reaching a terminal concentration. This response was also observed in both cases of well FRW (Figs. 4.17, 4.18) with a small,

[7]The sampler was not retrieving full water samples. It was discovered that debris was clogging the valves.

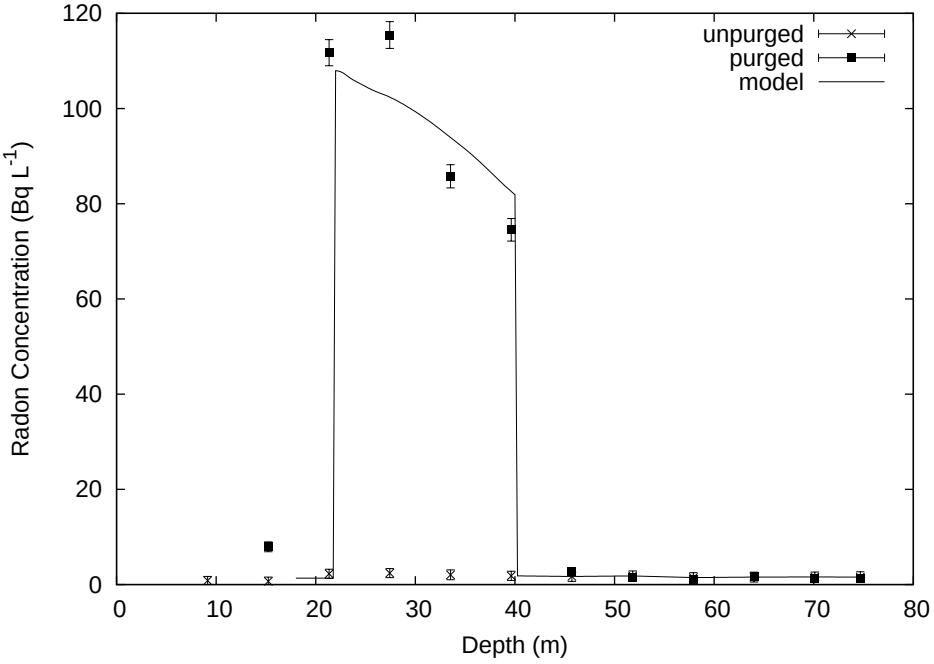

Figure 4.8: The unpurged and purged radon profiles in well STW with a 2-σ measurement uncertainty. The solid line represents the purged radon profile replicated by the model.

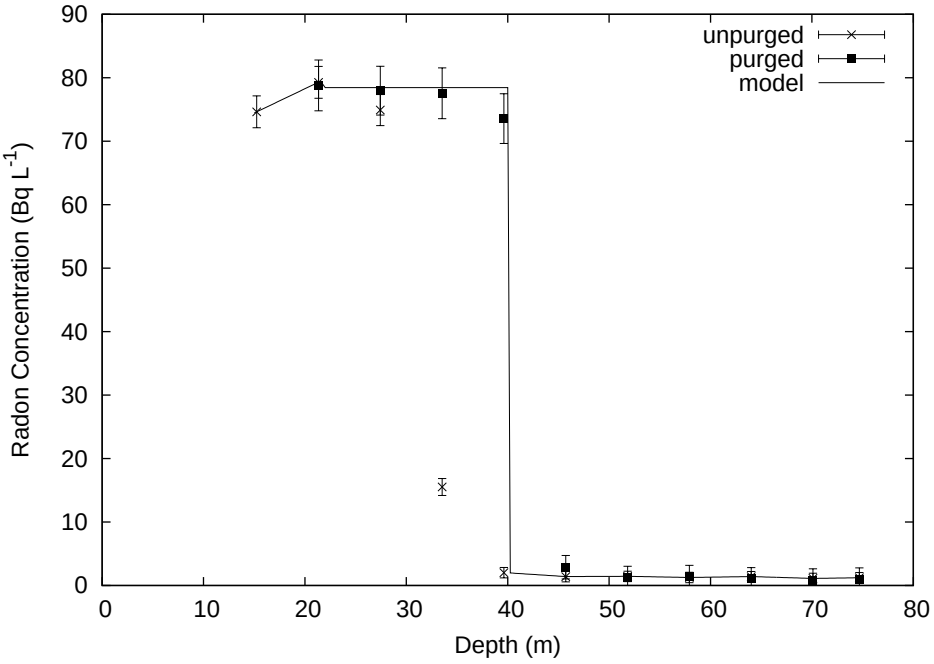

Figure 4.9: The unpurged and purged radon profiles in well FWD with a 2-σ measurement uncertainty. The solid line represents the purged radon profile replicated by the model.

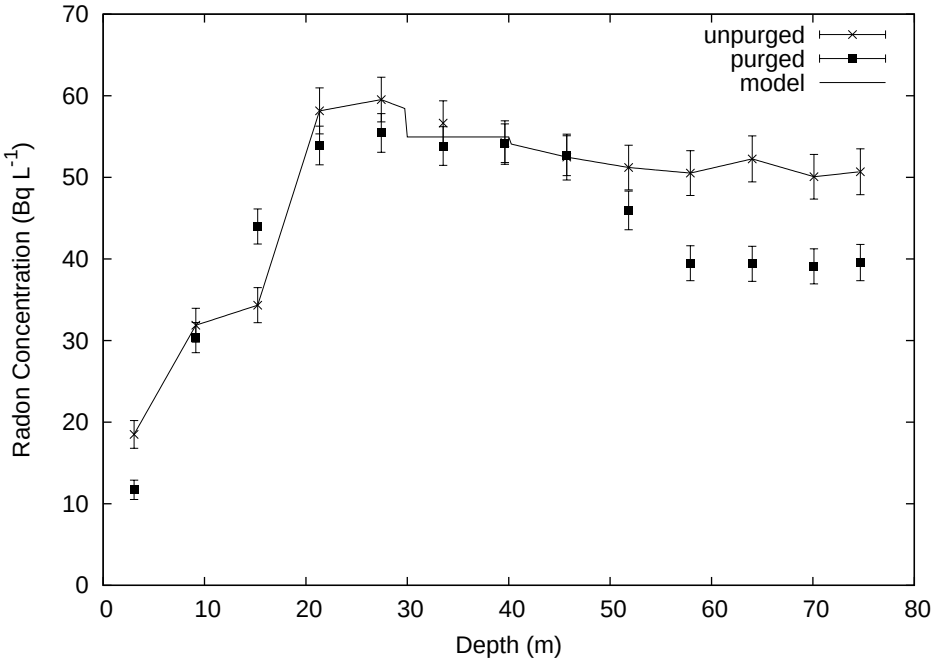

Figure 4.10: The unpurged and purged radon profiles in well FRW with a 2-σ measurement uncertainty. The solid line represents the purged radon profile replicated by the model.

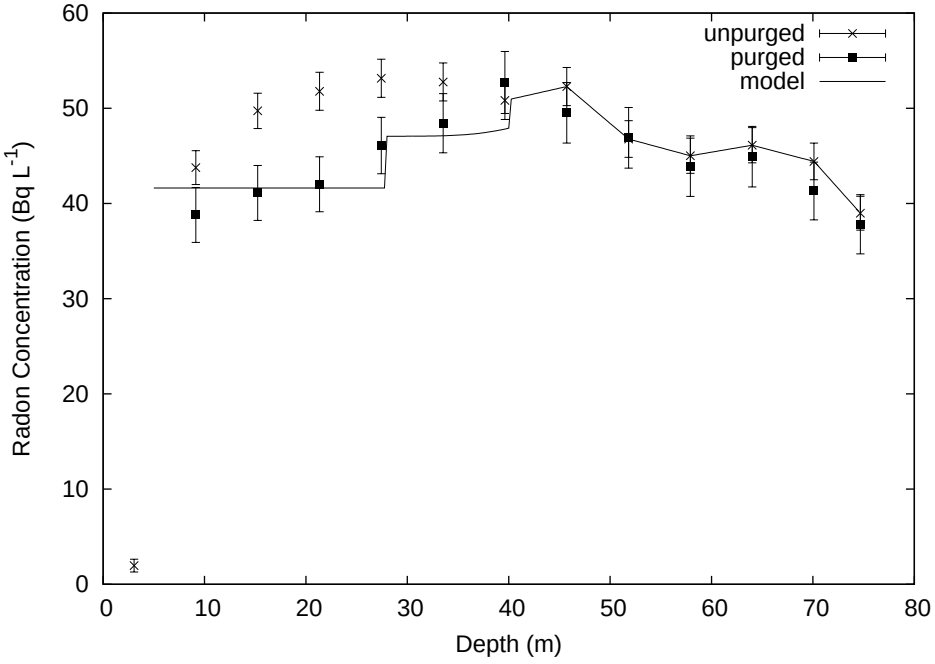

Figure 4.11: The unpurged and purged radon profiles in well RVR with a 2-σ measurement uncertainty. The solid line represents the purged radon profile replicated by the model.

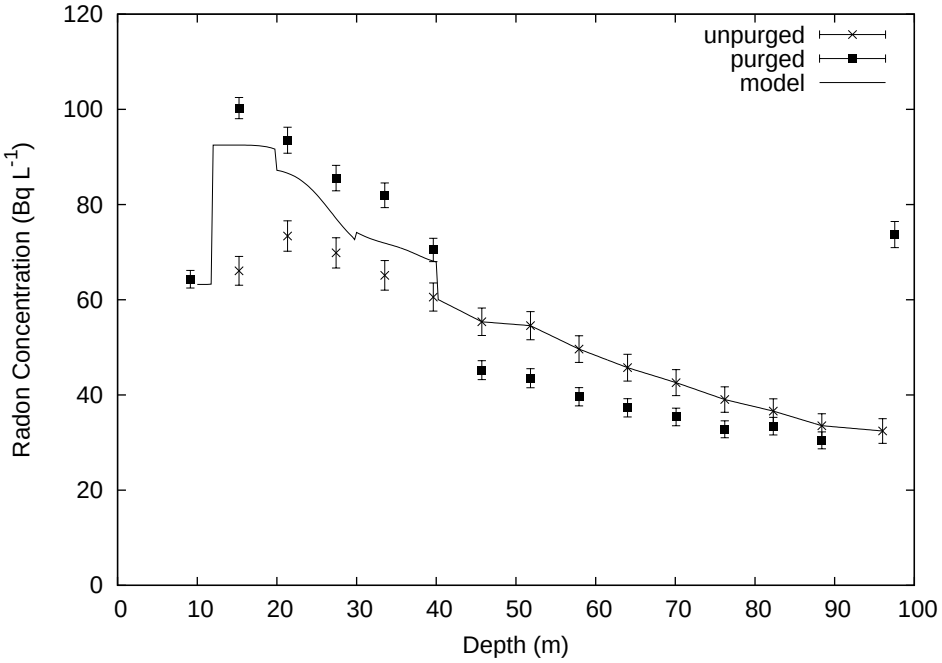

Figure 4.12: The unpurged and purged radon profiles in well AWA with a 2-σ measurement uncertainty. The solid line represents the purged radon profile replicated by the model.

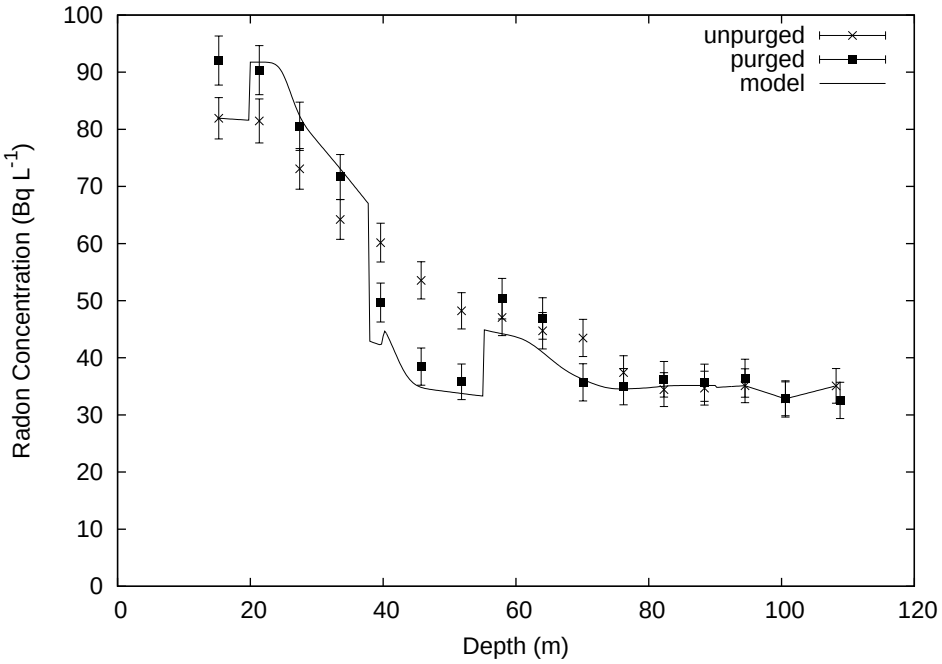

Figure 4.13: The unpurged and purged radon profiles in well AWC with a 2-σ measurement uncertainty. The solid line represents the purged radon profile replicated by the model.

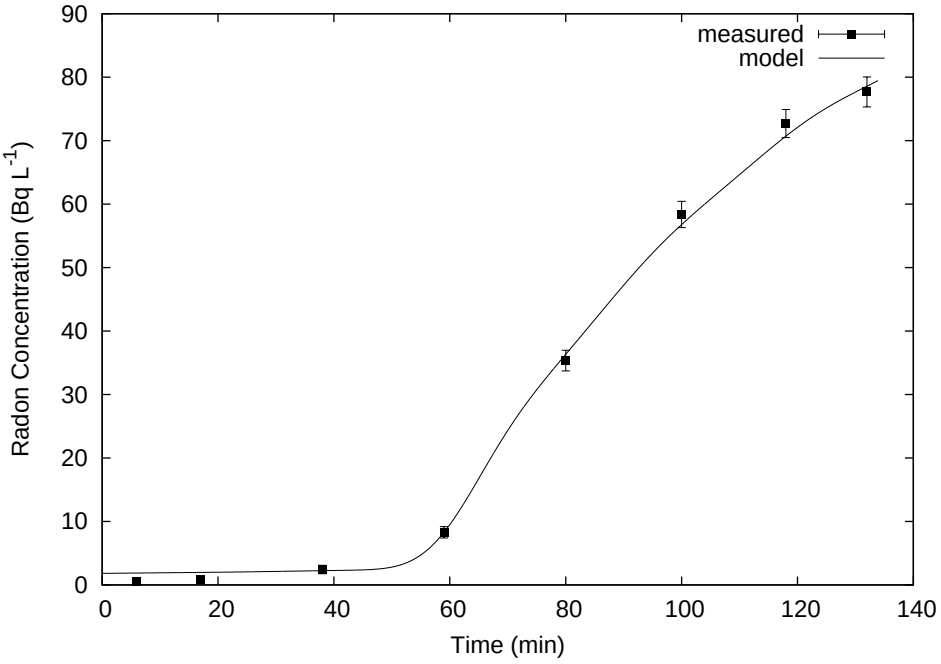

Figure 4.14: The radon concentrations in well STW while pumping from a 40 m depth with a 2-σ measurement uncertainty. The solid line represents the modeled fit to the measured radon concentrations.

quick radon increase to a steady concentration. The radon concentration did not vary in well RVR (Fig. 4.19). The radon concentration in well AWA (Fig. 4.20) remained relatively constant during pumping, but increased during the repeat and longer-pumped case (Fig. 4.21). Well AWC (Fig. 4.22) decreased in radon as the well was pumped, however when repeated (Fig. 4.23), the radon concentration increased after pumping over 150 min.

4.4.3 Borehole logging

The borehole geophysical logs (Figs. 4.24-4.29) illustrate the flow in the wells under pumping conditions, the diameter of the borehole, and the potential location of fractures, which were evident from spikes in the diameter. The flow was measured while pumping from the top of the well. The results generally indicated the pump-induced flow increased in a step-wise manner at inflow locations, with the greatest flow at the top. The flow of

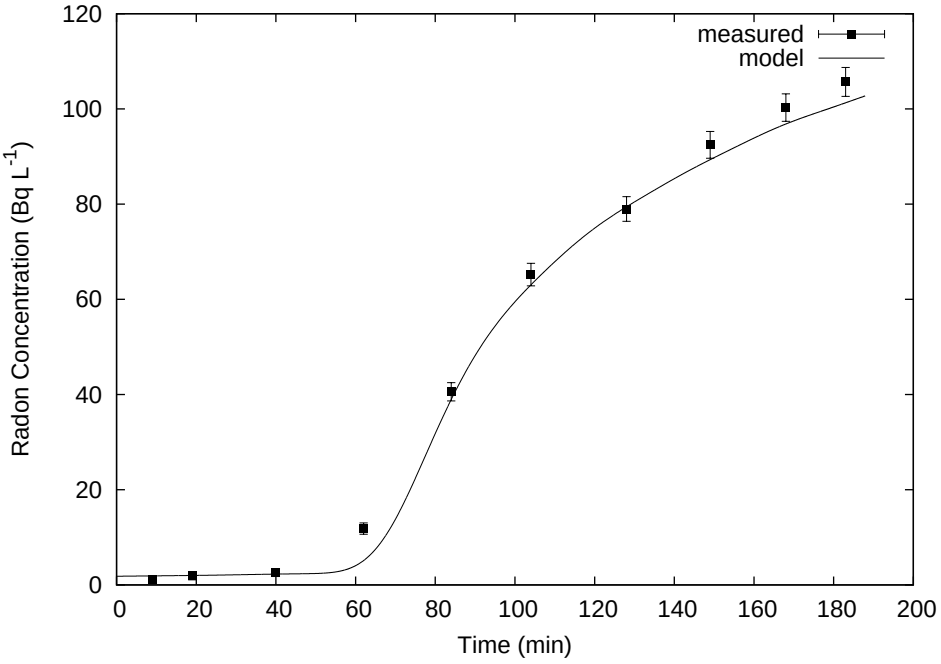

Figure 4.15: The radon concentrations during a repeat test of well STW while pumping from a 40 m depth with a 2-σ measurement uncertainty. The solid line represents the modeled fit to the measured radon concentrations of the original test.

wells STW, FWD, and FRW (Figs. 4.24, 4.25, 4.26) were above a major fracture location (22 , 22 m and 32 m, respectively) in the borehole. Below this point, there was negligible flow while pumping. Well RVR (Fig. 4.27) had some flow above the 28 m fracture but the majority of flow was below the casing at 4 m. The well AWA (Fig. 4.28) well had noticeable step-wise flow inputs beginning at 30 m with additional inputs at 20 m and 11 m. Well AWC flow log (Fig. 4.29) was noisy so inferred flow patterns and inflow locations were uncertain. At best, flow was evident throughout the entire length and step increases were evident at 90 m, 38 m. and 20 m. The only well with significant ambient flow was well RVR (Fig. 4.30). The flow is upward and ends at the uppermost fracture at 4 m.

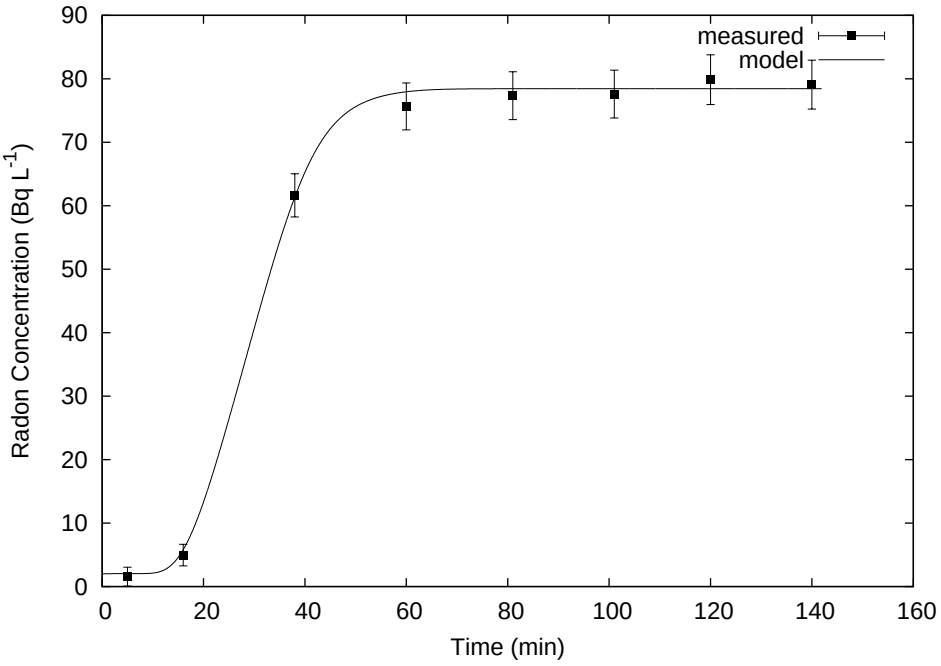

Figure 4.16: The radon concentrations in well FWD while pumping from a 40 m depth with a 2-σ measurement uncertainty. The solid line represents the modeled fit to the measured radon concentrations.

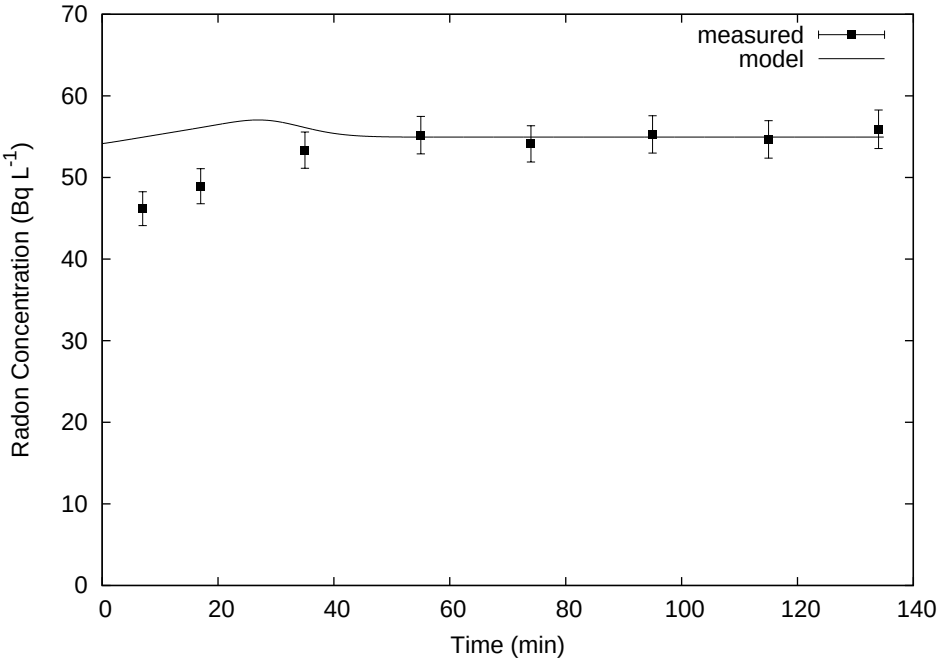

Figure 4.17: The radon concentrations in well FRW while pumping from a 40 m depth with a 2-σ measurement uncertainty. The solid line represents the modeled fit to the measured radon concentrations.

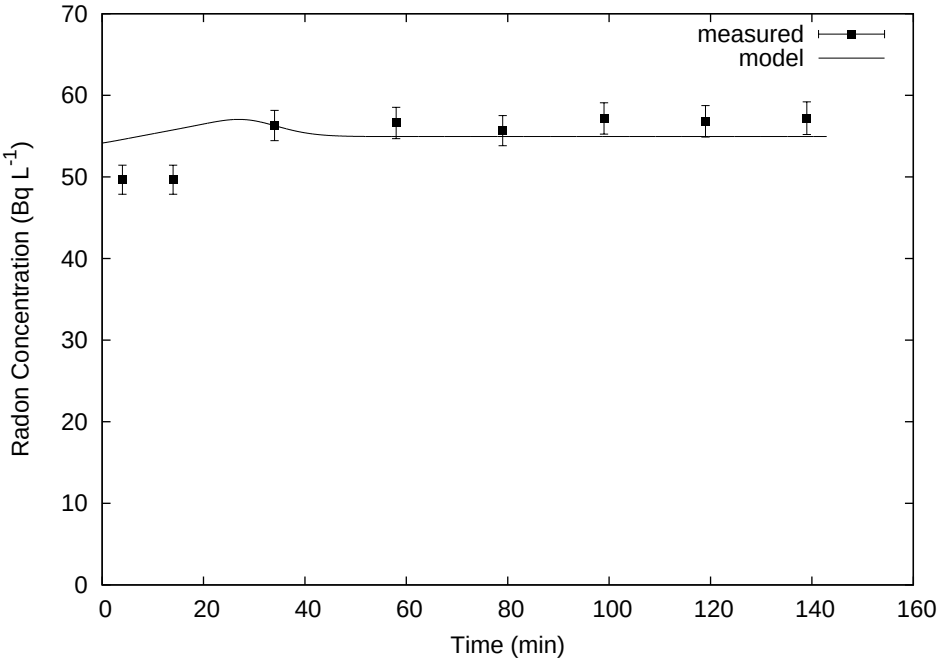

Figure 4.18: The radon concentrations during a repeat test of well FRW while pumping from a 40 m depth with a 2-σ measurement uncertainty. The solid line represents the modeled fit to the measured radon concentrations of the original test.

4.4.4 Rock chips

Five of the wells were measured for gamma-emitting nuclides of the uranium decay series near ^{222}Rn: ^{226}Ra, ^{214}Pb, and ^{214}Bi. A representative gamma log (Fig. 4.31) shows the contrast between the ^{226}Ra content of the rock surrounding the water in the well and the water's radon concentration (Fig. 4.9). The radium concentration was nearly constant throughout the length of the borehole. However, the radon concentration in the water was high for a short region of the well and near zero over the remaining regions. The other gamma logs are shown in Figs. B.12-B.15 in Appendix B.

The rock chips selected to determine the radon emanating-power are listed in Table 4.4. The radium concentration determined from the gamma counting was more than 25 times greater than the emanated radon in water concentration for the saturated rocks.

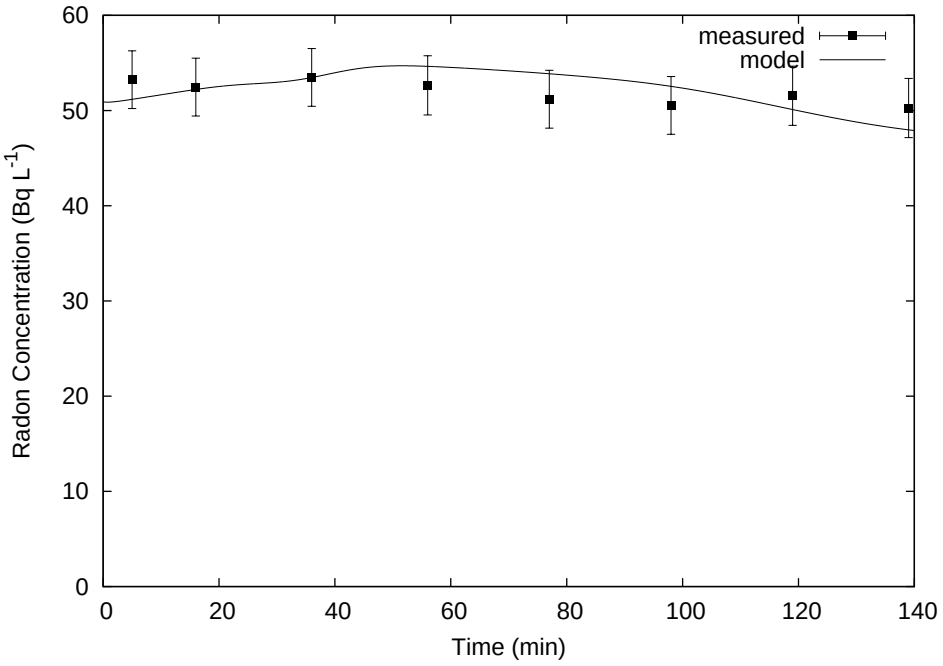

Figure 4.19: The radon concentrations in well RVR while pumping from a 40 m depth with a 2-σ measurement uncertainty. The solid line represents the modeled fit to the measured radon concentrations.

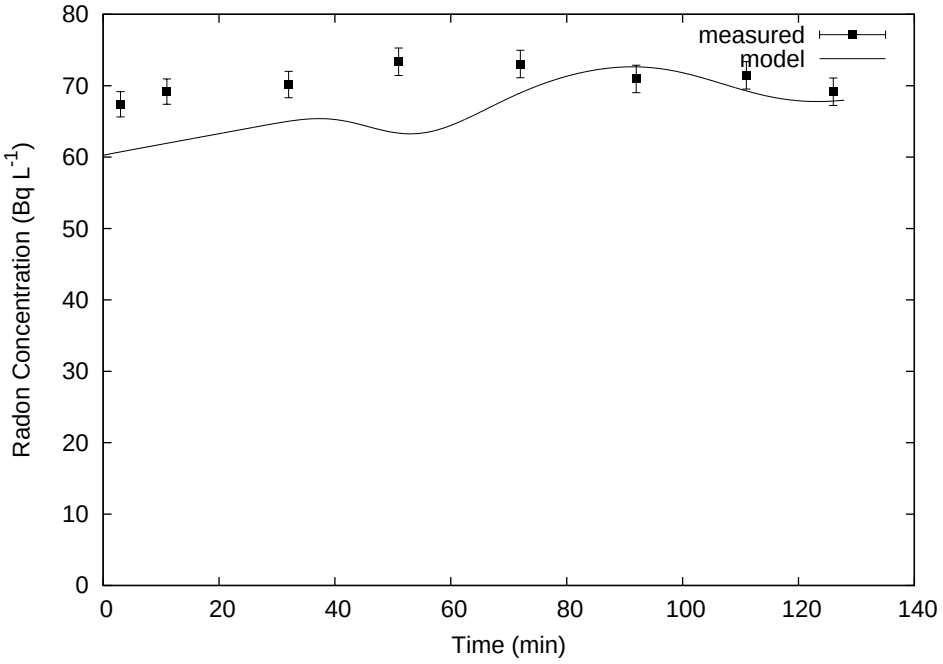

Figure 4.20: The radon concentrations in well AWA while pumping from a 40 m depth with a 2-σ measurement uncertainty. The solid line represents the modeled fit to the measured radon concentrations.

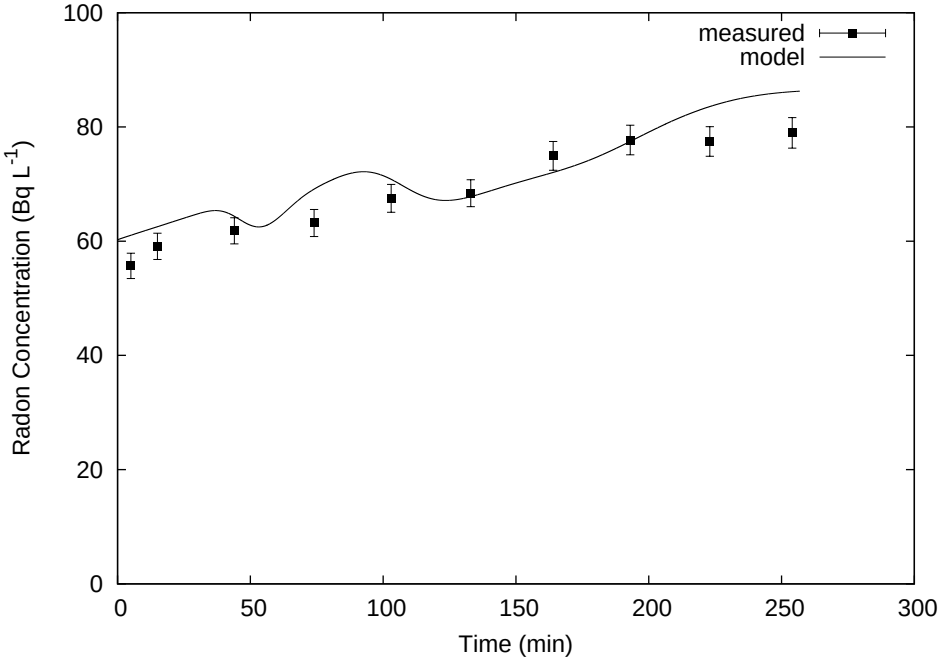

Figure 4.21: The radon concentrations during the repeat test of well AWA while pumping from a 40 m depth with a 2-σ measurement uncertainty. The solid line represents the modeled fit to the measured radon concentrations of the original test.

Table 4.4: The radium concentration and emanated radon concentration of a set of rock chips from the well drilling.

well sample	^{226}Ra conc. ($\mathrm{Bq\,kg^{-1}}$)	^{222}Rn conc. ($\mathrm{Bq\,kg^{-1}}$)
STW90	50.8 ± 6.7	1.2 ± 0.9
STW170	67.6 ± 7.1	1.2 ± 0.9
FRW90	71.8 ± 10.2	1.3 ± 1.2
FRW210	54.8 ± 5.5	1.5 ± 0.8
FRW110f	62.3 ± 7.7	2.2 ± 1.4
FRW195f	46.8 ± 4.2	1.7 ± 0.8
FWD70	62.7 ± 8.4	1.3 ± 0.8
FWD170	63.0 ± 5.6	0.91 ± 0.68
BRY80	43.7 ± 8.5	1.2 ± 0.7
BRY180	67.7 ± 6.5	1.9 ± 0.9

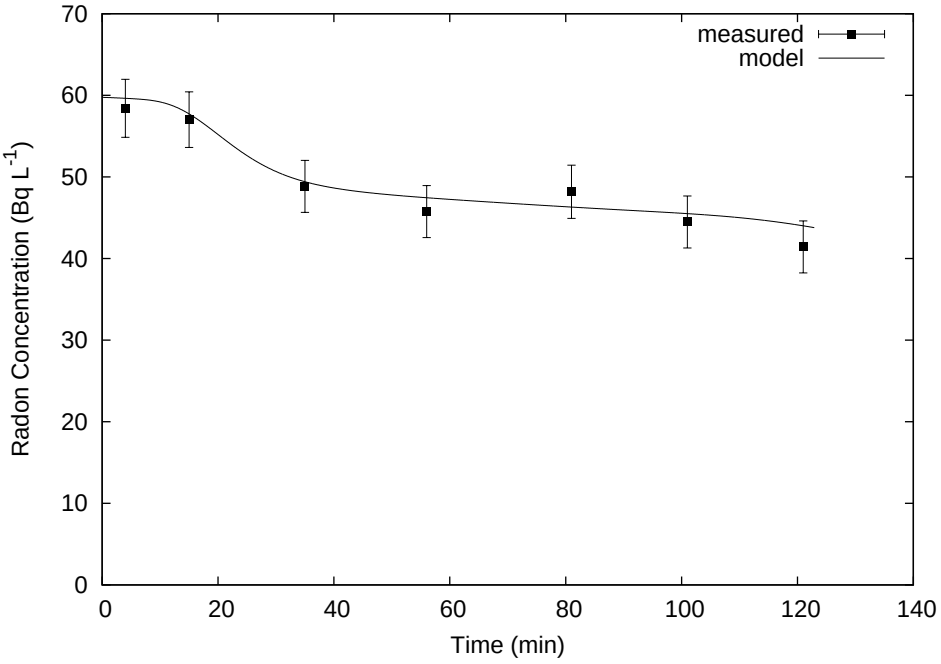

Figure 4.22: The radon concentrations in well AWC while pumping from a 40 m depth with a 2-σ measurement uncertainty. The solid line represents the modeled fit to the measured radon concentrations.

4.4.5 Modeling

Modeling of the inflows of ground water into the borehole while pumping the well enabled the determination of inflow rates of a certain radon concentration. The locations, radon concentrations and flow rates of the sources are listed in Table 4.5. For wells with multiple sources, the parameters for each source are listed. The flow rate of the water pumped out of each well is listed in Table 4.3. Only STW ($\alpha = 0.15 \pm 0.03$ m) and FWD ($\alpha = 0.15 \pm 0.09$ m) showed enough radon change over time to determine a dispersivity with a finite uncertainty. The modeling of the remaining wells used a standard dispersivity of 0.15 m. Well AWA parameters were estimated from the results but without model agreement, the uncertainties were not determined.

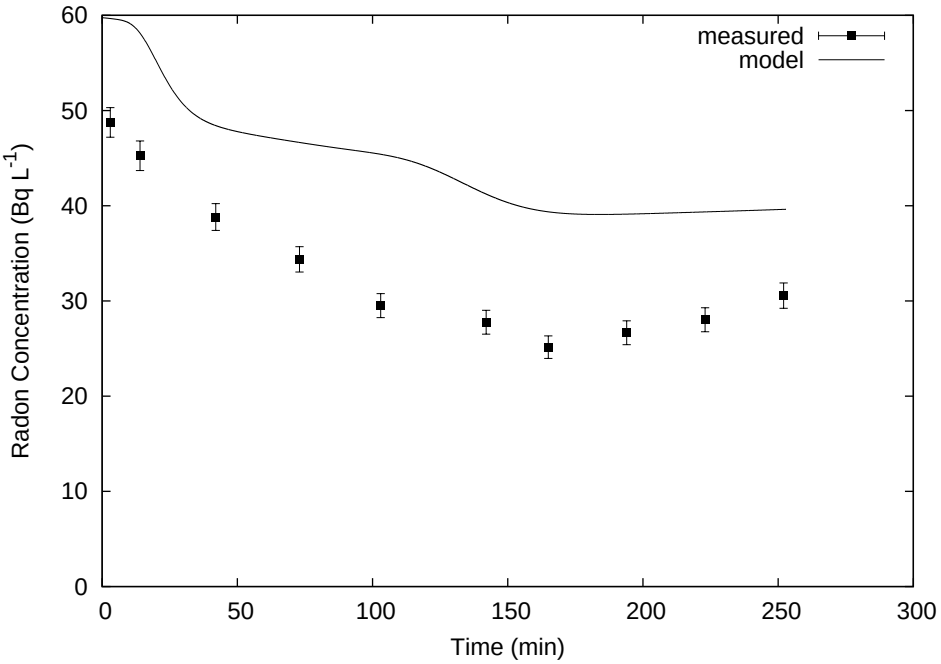

Figure 4.23: The radon concentrations during the repeat test of well AWC while pumping from a 40 m depth with a 2-σ measurement uncertainty. The solid line represents the modeled fit to the measured radon concentrations of the original test.

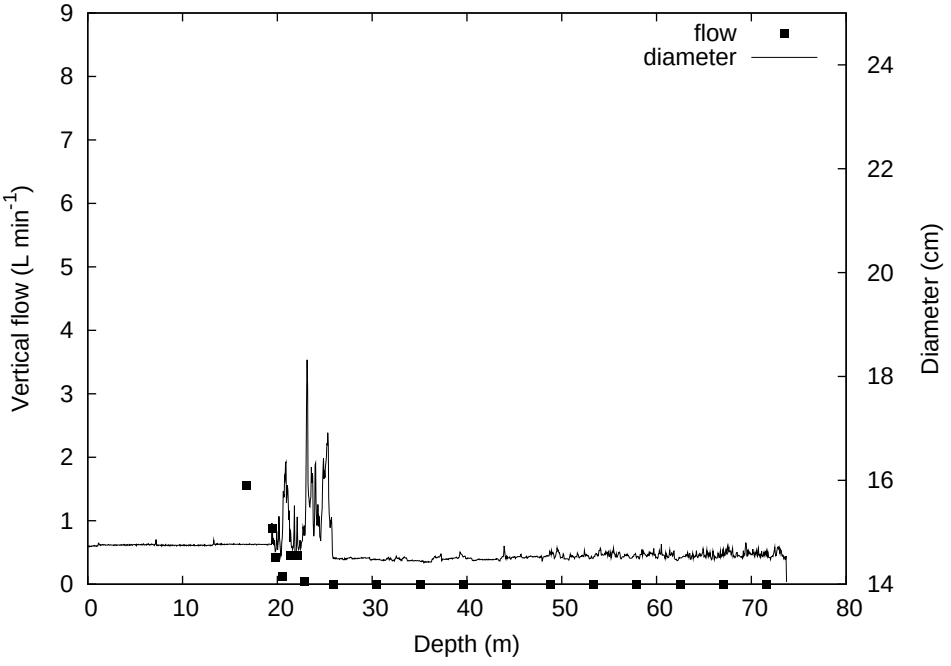

Figure 4.24: The pumped flow and caliper log for well STW (Rickert 2005).

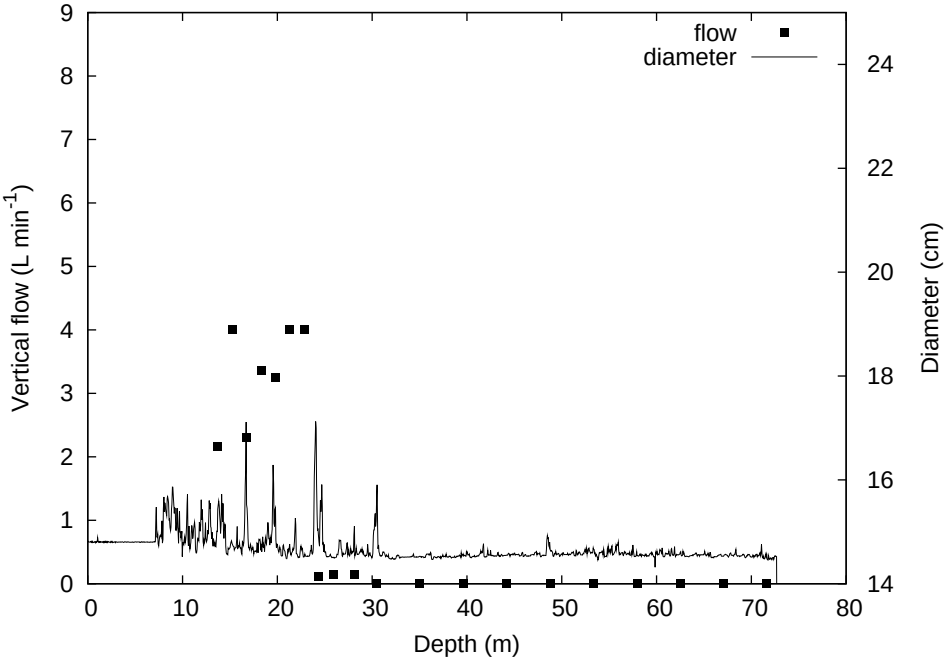

Figure 4.25: The pumped flow and caliper log for well FWD (Rickert 2005).

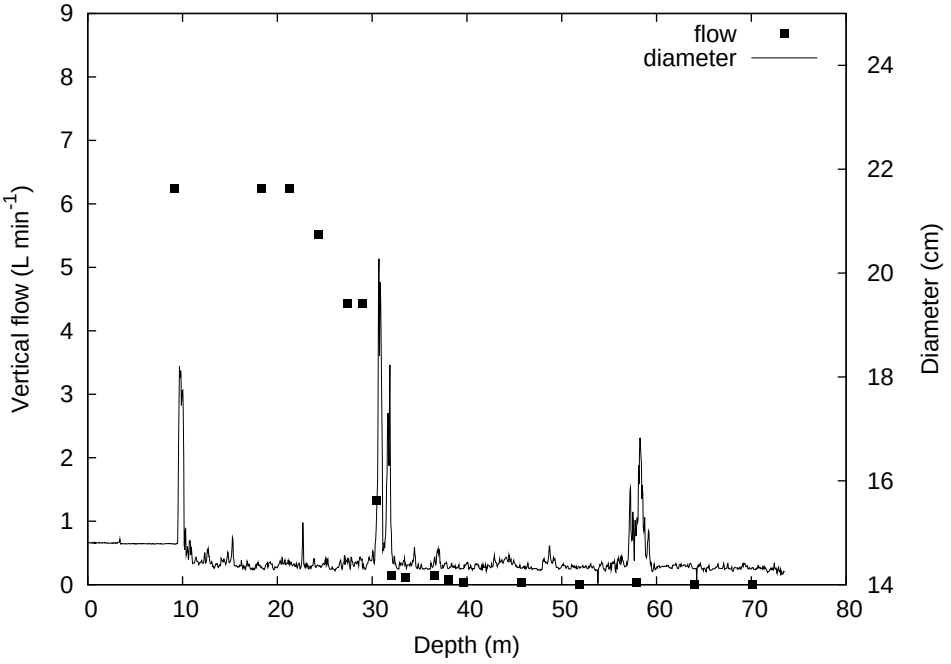

Figure 4.26: The pumped flow and caliper log for well FRW (Rickert 2005).

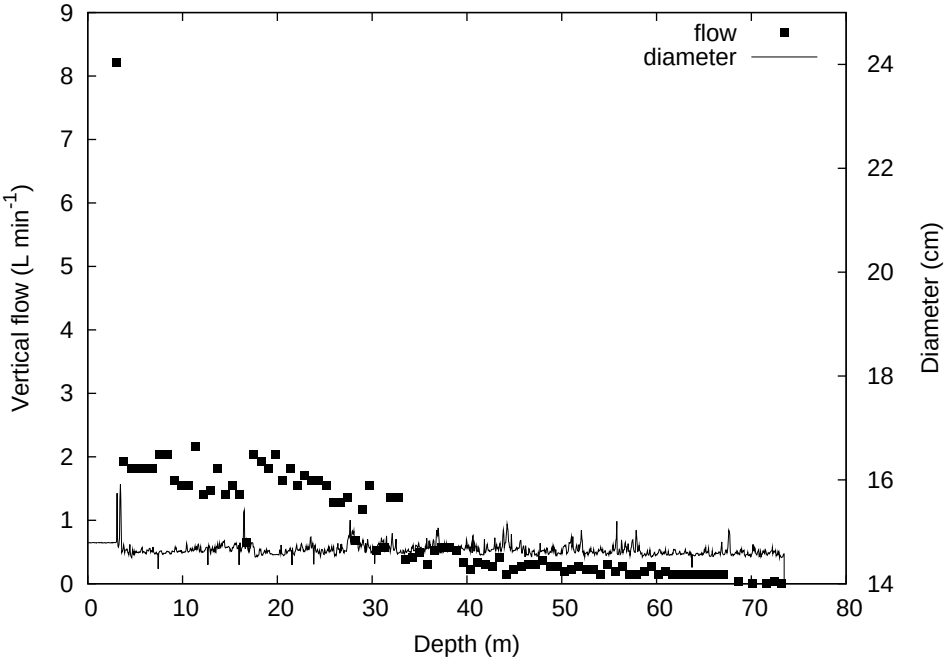

Figure 4.27: The pumped flow and caliper log for well RVR (Rickert 2005).

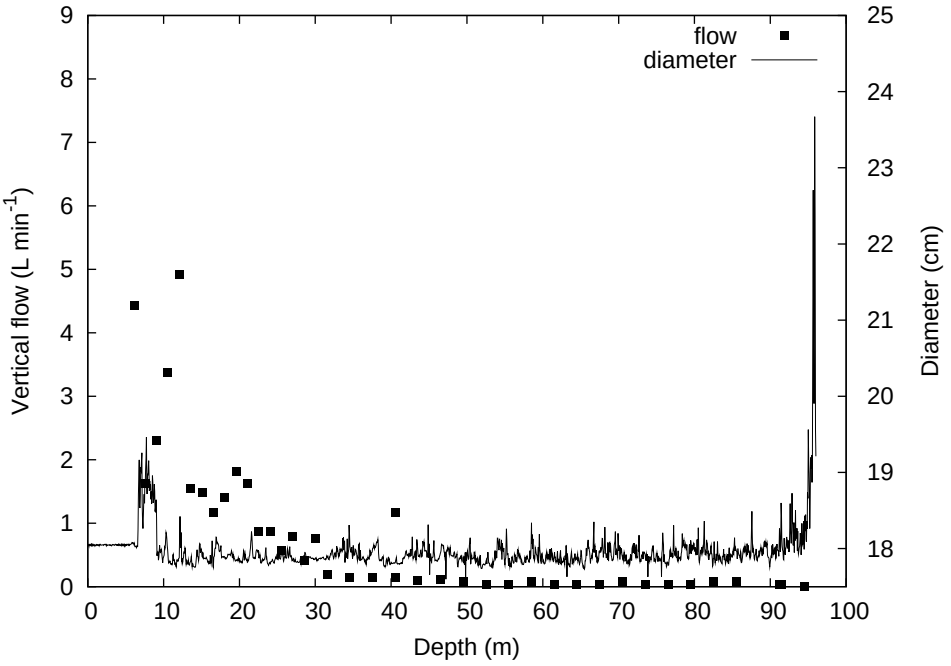

Figure 4.28: The pumped flow and caliper log for well AWA (Rickert 2005).

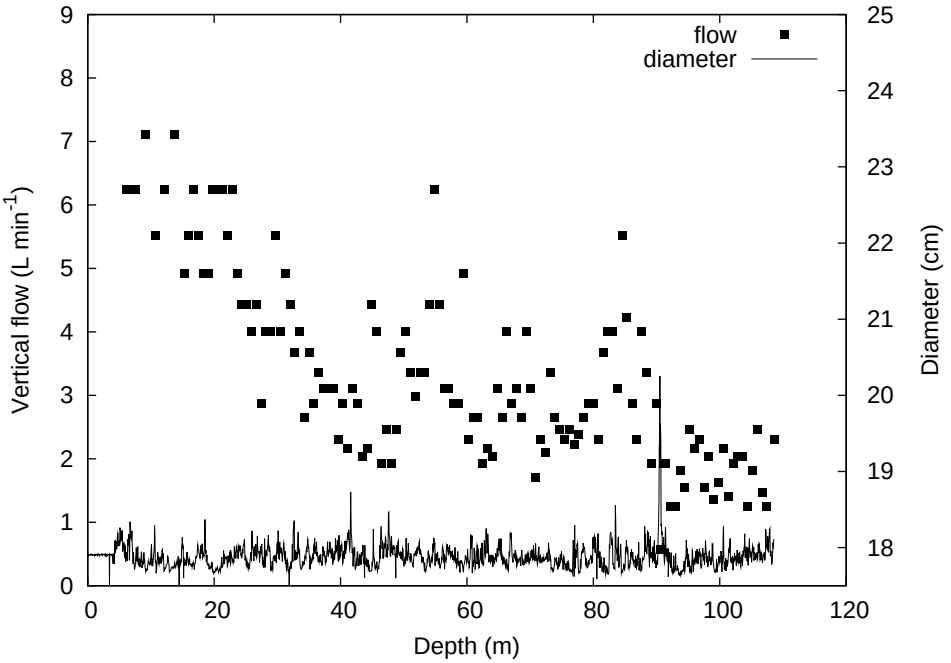

Figure 4.29: The pumped flow and caliper log for well AWC (Rickert 2005).

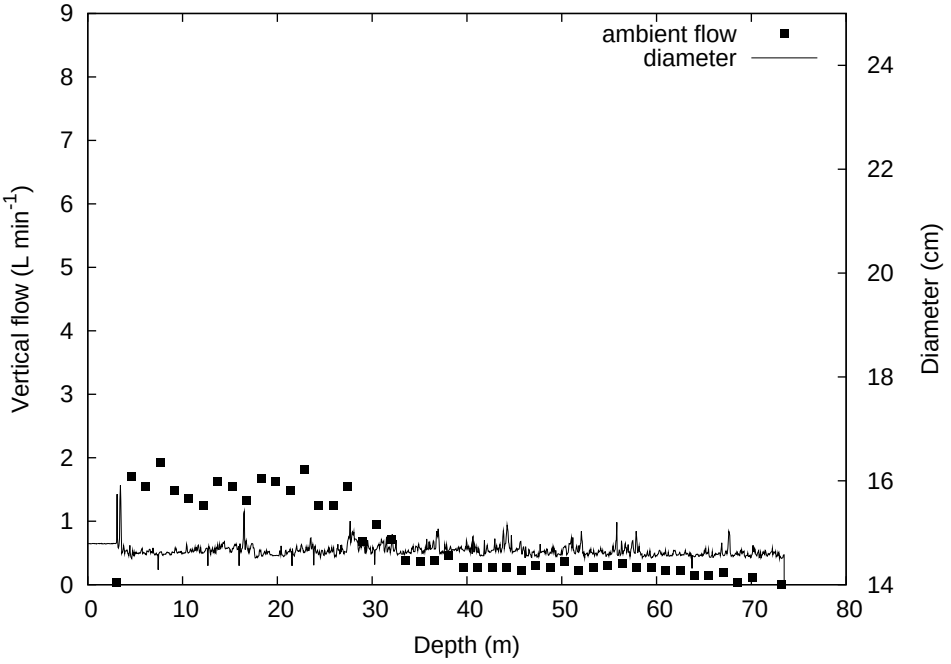

Figure 4.30: The ambient flow and caliper log for well RVR (Rickert 2005).

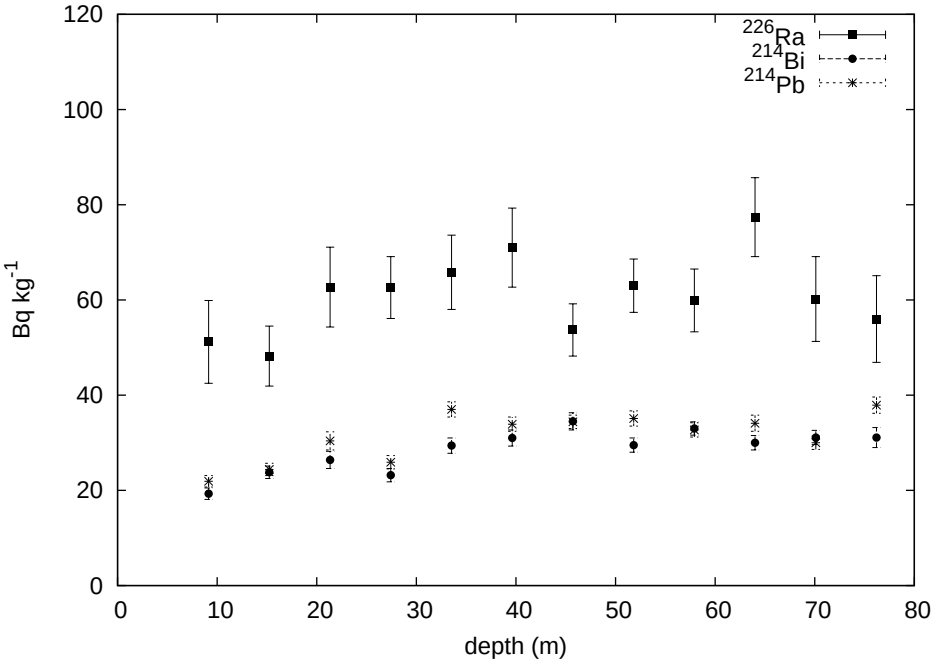

Figure 4.31: The concentration of ^{226}Ra, ^{214}Pb, and ^{214}Bi in the rock chips from the FWD well drilling. The uncertainties are a 1-σ counting uncertainty.

Table 4.5: The parameters used in the advection-dispersion model.

well	flow rate ($L\,min^{-1}$)	^{222}Rn conc. ($Bq\,L^{-1}$)	source depth (m)
STW	4.36 ± 0.02	120 ± 1	22
FWD	4.99 ± 0.17	78 ± 3	22
FRW	4.95 ± 2.48	55 ± 2	30
RVR	3.5 ± 0.2	41 ± 4	5
	1.5 ± 0.3	60 ± 2	28
AWA	2.8	93	12
	1.3	78	20
	1.0	81	30
AWC	1.3 ± 0.3	92 ± 5	20
	1.0 ± 0.3	13 ± 2	38
	1.0 ± 0.3	13 ± 9	55
	1.8 ± 0.3	35 ± 4	91

4.5 Discussion

The results demonstrate evidence of the causes of radon variation while pumping a well. Radon profiles have a major effect on the pumped radon concentration. For instance, the STW well unpurged radon profile has a low ($\sim$3 Bq L^{-1}) concentration throughout most of the borehole. However, after pumping the radon concentration increased over a length of the well, but only down to 40 m where the pump was located. As the well was pumped, the radon began at a low concentration and increased following a skewed "S" curve; a curve observed in Chapter 3 and noted by others (section 4.1.2.2). The increase was caused by water carrying a much higher radon concentration entering the well at a point above 40 m. The purged radon profile indicated the source of water with radon likely entered between 15-22 m and moved downward. The borehole logs indicate a large fracture between 20-26 m and vertical flow above 22 m depth. The model assumed the major flow into the well occurred at a 22 m depth and was the sole inflow location into the well.

The resulting modeled time-varying radon concentration agreed with measured values when reasonable values for the inflow rate and radon concentration were used. The radon concentration starts out low and slowly increased as a result of the low concentration water moving between 22 m and 40 m. Pumping initially removes stagnant water stored in the borehole. New ground water, enriched in radon, flows into the well as pumping continues and flows toward the pump. In addition, the water depth dropped during the pumping. Therefore, while radon was entering the well it was diluted with water already in the well above the inflow location. These two effects explain why the source radon concentration is actually higher than that observed in the inflow region of the purged radon profile in the borehole. The source radon concentration of the STW was the highest of all the sources in the collection of wells. The sole fracture in the well has a low transmissivity as evident in the flow logs and the substantial drop in water level while pumping. The pumping lowered

the head in the well enough to pull a significant amount of water out of pore space along the fracture. The pore space in rock would have the high radon concentrations due to its proximity and long residence time with radium on the rock surface.

When the pumping test was repeated for a longer pump time, the modeled results showed good agreement. The parameters of the model for the second run were based on the initial experiment (radon profiles were not measured for the repeat pumping tests) and therefore a limitation on the quality of the agreement is imposed. Regardless, the repeat test shows a similar response of an increasing radon concentration approaching a steady value of the inflow concentration. The radon concentration variation of well STW can be explained by a lone inflow above the pump location.

The response of well FWD was similar to STW, however the radon concentration in FWD was higher under ambient conditions. After pumping the radon concentration in FWD remained high and extended down to a depth of 40 m. This suggests that radon-rich water entered through the high-transmissivity fracture at 22 m, evident in the flow logs, and moved down to the pump during pumping. The pumped radon concentration started at a low concentration, consistent with the unpurged radon profile at 40 m depth, and steadily increased to a constant 78 $\mathrm{Bq\,L^{-1}}$ concentration. Similar to well STW, the model showed good agreement with the measured data for both the purged radon profile and the change in radon while pumping.

Radon concentrations in the bottom half of wells STW and FWD were nearly zero under ambient and pumped conditions. This suggests that even under pumping conditions, this region is hydraulically inactive. Radon has a half-life of 3.82 days and its aqueous concentration is affected by the elapsed time since isolation from radium. The metamorphic grade of bedrock surrounding these wells contains some radium due to natural uranium content and radon will exist the ground water. Water with a very low radon concentration, as in regions of the STW and FWD wells, must have isolated from radium for at least several half-lives. This low concentration was also used to determine the effect

of radium in the rock surrounding the water in the well. The radium logs from gamma counting indicate that the surrounding rock cannot be a significant source of the radon in well water. At most, the radium in the surrounding rock can only support radon concentrations at or below a concentration of 3 $\mathrm{Bq\,L^{-1}}$. This is low due to the low surface area of the rock walls per volume of water contained. Water in fractures have a higher radon concentration due to a greater rock surface area per contained water volume.

Well FRW shows little change in concentration while pumping, but it follows a flow pattern similar to STW and FWD. According to the flow log, the majority of the transmissivity in FWD occurs from the fracture at 32 m of depth, with a less transmissive fracture at 22 m. The maximum radon concentration occurs from 22 to 32 m in depth with little change in concentration across this region. When the model was run with an inflow at 22 m, agreement with the data was achieved only after 40 min of pumping (also true for the FRW repeat pumping). This discrepancy was likely caused by a change in the initial concentrations in the well during the 26 days between taking the unpurged radon profile and pumping the well. The first two measured radon concentrations during pumping were less than the initial concentration at 40 m on the unpurged radon profile. The model will not be able to predict a radon concentration initially with the measurements in this well. Further evidence of the change in the radon profile between the unpurged and purged radon profiles was evident in the bottom half of the well; without flow the radon profile was lower when purged than unpurged. Without any significant flow below 40 m, it is unlikely that the change was caused by pumping.

The only major sources of flow into the well occurred above 40 m, and there must be a source of radon for the water below this depth. Wells STW and FWD showed very low concentrations of radon below their major fracture supplying water to the well. In contrast, there is almost a steady unpurged radon profile throughout the entire depth of well FRW. If diffusion alone transported radon entering around 30 m depth to deeper depths, an exponential instead of constant radon concentration profile would be present.

Instead, the radon profile must be influenced by a slow ground water flow undetectable of the borehole geophysical flow logs.

Well RVR held at a steady radon concentration while pumping, though the radon profiles changed in concentration over the top half of the well. The flow logs indicated two fractures provided water to the well; one at 28 m and a larger contribution around 4 m. Water entering from the larger fracture at 4 m carried a lower radon concentration than the other at 28 m depth. The water entering through the top fracture has a concentration 41 $\mathrm{Bq\,L^{-1}}$ lower than the initial concentration in that region. This well has upward flow between the two fractures during ambient conditions. The water entering at 28 m of depth of a higher concentration, 60 $\mathrm{Bq\,L^{-1}}$, supplies the radon upward through the well. The radon found below 28 m must be supplied by trace vertical and horizontal ground-water flow.

The radon concentration of well AWA did not vary during pumping. Like the others, most of the vertical flow occurred over the top half of the well. The flow log indicated 3 major inflows above a depth of 30 m. This same region showed a increase in the radon profile after pumping. With three inflows, the parameters used in the model are less certain and with a steady concentration over time are based primarily on the change in radon profile. Water from the three fractures had concentrations greater than the initial radon pumped and given sufficient time (or pump rate) will raise the radon levels pumped out of the well. The repeat test if AWA showed this effect. The radon profile below 40 m depth did change slightly, but like the FRW well is also due to the change in the factors controlling the initial radon profile under ambient conditions and not the pumping of the well. This change in initial conditions was also evident in the pumped radon levels, which started off higher than the unpurged radon profile at the pump location.

Well AWC had the most erratic flow log. Looking past the noise in the data, there were definite locations where water-bearing fractures are likely: 91 m, 38 m, and 20 m depth. The radon profiles offer more guidance to the active zones in the well. The radon

increased in the uppermost portion supplied by the 20 m fracture. Just above the pump location there was a decrease in radon suggesting an inflow of a lower concentration. A lower concentration also occurred below the pump suggesting another inflow between 50-60 m depth. The final possible inflow at 91 m depth brings in water with a concentration nearly the same as the ambient concentration. There was good agreement with the model, especially with the pumped radon concentration. This well was the only one that showed a clear decrease in radon while pumping. The two inflows with low radon concentration near the pump caused this effect. However, with two other inflow at higher concentration in the well, the pumped radon levels should not continue to decrease much further. Pumping at well AWC was repeated using a longer pumping duration and an eventual increase in radon concentration was measured. The second test resulted in lower radon concentrations than the initial test and may be attributed to a different initial radon concentration profile.

For the wells where model agreement was high, the radon variation with time during pumping was caused by the details of where ground water entered the well. The flow logs verify that there was usually less than four hydraulically active fractures intersecting the well. While pumping the well, the volumetric flow rate, radon concentration of each source, and the location of the pump dictate the variation noted over time. For instance, a pumped radon concentration of a well with only one major source was linked to the location of the pump. Hypothetically, if the pump was located at a depth of 20 m in wells STW or FWD, near their major source of water, the response would be quite different. Instead of the observed slow and gradual increase towards a steady value, the radon concentration would increase much quicker whereas placing the pump deeper in the well would cause the response to be slower because more water had to be purged before the radon enriched ground water reached the pump. To specify a duration of pumping or volume of water purged as a moment in time of representative ground water sampling is inadequate. Neither a length of time nor volume of water that can be generally applied to ensure an

exclusive ground-water sample. Instead, the details of the sources of ground water in the well and the pump location cause the variation while pumping.

4.6 Summary and Conclusions

The series of measurements and experiments on bedrock wells at the University of Maine were conducted to determine the short-term variation in radon concentration while water is drawn from a well. Two of the nine wells showed variation over 80 $\mathrm{Bq\,L^{-1}}$, an additional two over 20 $\mathrm{Bq\,L^{-1}}$, and the remaining less than than 10 $\mathrm{Bq\,L^{-1}}$. A number of measurements were conducted to explain these variations. These included measuring the vertical radon profile in the well both before and after pumping, the flow during ambient and pumping conditions, the diameter in the borehole to identify fractures, the temperature of water during pumping, and the radium content in the rock surrounding the water column. Based on these observation, a model was used to replicate the measured radon concentration during and after pumping a well utilizing the location, flow rate, and radon concentration of the hydraulically active fractures that intersect the well.

The key conclusions from studying the wells are:

1. The vertical radon profile is not constant with depth.

2. The radium in the surrounding rock cannot explain this variation and can only support a radon concentration of 3 $\mathrm{Bq\,L^{-1}}$.

3. The radon profile changed after pumping.

4. Water-bearing zones determined by borehole logging also show a change in the radon profile. Except where ambient flow exists in the wells, the location of the greatest radon concentration with depth was a water inflow location. The regions with the lowest concentration usually signified a lack of inflow into the well.

5. Radon changes in concentration over time as water is pumped out of the well.

6. The movement of water in the well during pumping was replicated and fit to measurements through an advection-dispersion model.

7. The temporal variation of radon concentration is controlled by the relative locations and flow rates of the fractures and the pump.

8. The moment of representative ground water sampling based on radon cannot be generically determined by solely a duration of pumping, volumetric flow rate, or volume of water removed.

Chapter 5
SUMMARY AND CONCLUSIONS

5.1 Overview

This study represents a series of investigations dealing with waterborne radon. Terrestrial in origin, radon is found in ground water and can be released during water usage. Previous studies have attempted to calculate the amount of radon released when water is released at faucets in kitchen and bath locations. A model was introduced that predicts the amount of radon released when using water. An investigation at schools tested the model, which generally predicted a greater amount of released radon than measured. Three scenarios were investigated which could have an impact on the ability of using a model to predict the radon released during water usage. They are the accuracy of measuring radon in water, the nature of the spatial distribution of released radon in a room, and the temporal variations of the radon in water.

The accuracy of the methods and protocols of measuring radon in water was conducted through a laboratory intercomparison. The accuracy to measure radon in water was confirmed with agreement and consistency among four of nine participating laboratories. The remaining laboratories did not show inter-laboratory agreement or consistency.

Additional schools were studied to test the model and determine if a variation of radon existed. At the eight schools studied, all but one had measurements of released radon less than predicted. The lone school was complicated by an unusually low amount of water used for the duration of usage. Two of the schools were studied with multiple radon in air detectors in the kitchen to detect a variation in the spatial distribution. The variation was confirmed with ranges by a factor of 3.5 in radon concentration at one time.

During the school study, it was observed that the radon in water concentration increased while running water. The model assumed the radon concentration was constant and the precision of the model was limited by the amount of variation. Observation wells were studied to identify the causes and calibrate a model explain the variation. The variation was explained by the the locations and radon concentrations of ground water flow into to well and the movement of water through the well in relation to a pump. Knowledge of the hydraulic signature of a well would enable prediction of its temporal changes in radon concentration.

5.2 Conclusions

1. The ability to measure radon in water during this study should not be a cause of the disagreement between the model and measurement of radon release.

2. A nonuniform distribution of radon indicated that the room is not well mixed and not uniformly ventilated. The radon release model was not designed to handle such a variation.

3. Instead of assuming a constant concentration of waterborne radon, the radon release model needs to be adjusted to allow for changing radon concentration.

4. The short-term ground-water radon concentration variation from a well can be explained and predicted.

5.3 Future work

Future studies of waterborne radon release will benefit from the conclusions of this study. The intercomparison of radon in water measurements details the proper methods crucial to analytical accuracy. A modification of the current radon release model is needed to account for the temporal variations found and the heterogeneous distribution of radon.

Measurements of the air flow patterns in the room may assist this endeavor. The radon release model must be modified to account for a changing radon in water concentration. With detailed knowledge of the hydraulic activity of the well, the radon concentration change will be predictable.

REFERENCES

APPELO, C. A. J. AND POSTMA, D. 1996. Geochemistry, groundwater and pollution. A.A. Balkema, Rotterdam, Netherlands.

[ASTM] American Society for Testing and Materials 1998. Annual book of ASTM standards: Standard test method for radon in drinking water: Designation D 5072-98. American Society for Testing and Materials, Philadelphia, PA.

[AWWA] American Water Works Association 1996. Standard methods for the examination of water and wastewater: 7500-Rn radon. American Water Works Association and Public Health Association, Washington, DC.

BAUM, E. M., KNOX, H. D., AND MILLER, T. R. 2002. Nuclides and Isotopes: Chart of the Nuclides. Knolls Atomic Power Laboratory, Inc., sixteenth edition.

BRUTSAERT, W. F., NORTON, S. A., HESS, C. T., AND WILLIAMS, J. S. 1981. Geologic and hydrologic factors controlling radon-222 in ground water in Maine. *Ground Water* 19:407–417.

COOK, P. G., LOVE, A. J., AND DIGHTON, J. C. 1999. Inferring ground water flow in fractured rock from dissolved radon. *Ground Water* 37:606–610.

COUNTESS, R. J. 1978. Measurement of ^{222}Rn in water. *Health Physics* 34:390–391.

[CRCPD] Conference of Radiation Control Program Directors 2004. Technical white paper: Radon in drinking water regulation: A brief history. CRCPD Publication E-04-4, Frankfort, KY. Available at http://www.crcpd.org/Pubs/RadonInWaterE-29-Sept04.pdf.

CURRIE, L. A. 1968. Limits for qualitative detection and quantitative determination: Application to radiochemistry. *Analytical Chemistry* 40:586–593.

DAVIS, R. M. AND WATSON, JR., J. E. 1990. Influence of ^{226}Ra concentration in surrounding rock on ^{222}Rn concentration in ground water. *Health Physics* 58:369–371.

DOUGHTY, C. AND TSANG, C.-F. 2005. Signatures in flowing fluid electric conductivity logs. *Journal of Hydrology* 310:157–180.

DRANE, W. K., YORK, E. L., HIGHTOWER, III, J. H., AND WATSON, JR, J. E. 1997. Variation of ^{222}Rn in public drinking water supplies. *Health Physics* 73:906–911.

DUNCAN, D. L., GESELL, T. F., AND JOHNSON, R. H. 1977. Radon-222 in potable water. *In* Proceedings of the Tenth Midyear Topical Symposium of the Health Physics Society, pp. 340–357, Troy, NY. Rensselaer Polytechnic Institue Press.

EISENBUD, M. AND GESELL, T. F. 1997. Environmental radioactivity from natural, industrial, and military sources. Academic Press, San Diego.

ELLINS, K. K., ROMAN-MAS, A., AND LEE, R. 1990. Using ^{222}Rn to examine groundwater/surface discharge interactions in the Rio Grande de Manati, Puerto Rico. *Journal of Hydrology* 115:319–341.

[EPA] U.S. Environmental Protection Agency 1986. A citizen's guide to radon: What it is and what to do about it. OPA-86-004. U.S. EPA and U.S. Department of Health and Human Services.

[EPA] U.S. Environmental Protection Agency 1999. National promary drinking water regulations; radon-222; proposed rule: Federal Registry, 64(211). U.S. EPA.

FARAI, I. P. AND SANNI, A. O. 1992. ^{222}Rn in groundwater in Nigeria: A survey. *Health Physics* 62:96–98.

FITTS, C. R. 2002. Groundwater Science. Academic Press.

FOLGER, P. F., POETER, E., WANTY, R. B., FRISHMAN, D., AND DAY, W. 1996. Controls on ^{222}Rn variations in a fractured crystalline rock aquifer evaluated using aquifer tests and geophysical logging. *Ground Water* 34:250–261.

FREYER, K., TREUTLER, H. C., DEHNERT, J., AND NESTLER, W. 1997. Sampling and measurement of radon-222 in water. *Journal of Environmental Radioactivity* 37:327–337.

FUKUI, M. 1985. ^{222}Rn concentrations and variations in unconfined groundwater. *Journal of Hydrology* 79:83–94.

GALL, I. K., RITZI, JR., R. W., BALDWIN, JR., A. D., PUSHKAR, P. D., CARNEY, C. K., AND TALNAGI, JR., J. F. 1995. The correlation between bedrock uranium and dissolved radon in ground water of a fractured carbonate aquifer in Southwestern Ohio. *Ground Water* 33:197–206.

[GAO] General Accounting Office 2002. Revisions to EPA's cost analysis for the radon rule would improve its credibility and usefulness. Report to congressional committees. GAO-02-333. U.S. GAO.

GENEREUX, D. P., HEMOND, H. F., AND MULHOLLAND, P. J. 1993. Use of radon-222 and calcium as tracers in a three-end-member mixing model for streamflow generation on the West Fork of Walker Branch Watershed. *Journal of Hydrology* 142:167–211.

GESELL, T. F. AND PRICHARD, H. M. 1975. The technologically enhanced natural radiation environment. *Health Physics* 28:361–366.

GUNDERSEN, L. C. S. 1989. Anomalously high radon in shear zones. *In* Proceedings: The 1988 Symposium on Radon and Radon Reduction Technology - vol. 1. Symposium Oral Papers, Washington, DC. U.S. Environmental Protection Agency EPA/600/9-89/006a.

HESS, C. T. AND BEASLEY, S. M. 1990. Setting up a laboratory for radon in water measurements, pp. 193–202. *In* C. R. Cothern and P. A. Rebers (eds.), Radon, radium and uranium in drinking water. Lewis Publishers, Chelsea, MI.

HESS, C. T. AND HASKELL, L. E. 1994. A comparison of two pathways to human for radon from drinking water: Inhalation and ingestion, pp. 167–197. *In* R. G. M. Wang (ed.), Water contamination and health: Integration of exposure assessment, toxicology, and risk assessment. Marcel Dekker, Inc, New York.

HESS, C. T., MICHEL, J., HORTON, T. R., PRICHARD, H. M., AND CONIGLIO, W. A. 1985. The occurrence of radioactivity in public water supplies in the Unites States. *Health Physics* 48:553–586.

HESS, C. T., VIETTI, M. A., AND MAGE, D. T. 1987. Radon from drinking water, pp. 158–171. *In* D. D. Hemphill (ed.), Trace substances in environmental health – XXI. University of Missouri Press, Columbia, MO.

HESS, C. T., WEIFFENBACH, C. V., AND NORTON, S. A. 1982. Variations of airborne and waterborne Rn-222 in houses in Maine. *Environment International* 8:59–62.

HIGHTOWER, III, J. H. AND WATSON, JR., J. E. 1995. ^{222}Rn in water: A study of two sample collection methods, effects of mailing samples, and temporal variation of concentrations in North Carolina groundwater. *Health Physics* 69:219–226.

HOEHN, E. AND VON GUNTEN, H. R. 1989. Radon in groundwater: A tool to assess infiltration from surface waters to aquifers. *Water Resources Research* 25:1795–1803.

IGARASHI, G., SAEKI, S., TAKAHATA, N., SUMIKAWA, K., TASAKA, S., SASAKI, Y., TAKAHASHI, M., AND SANO, Y. 1995. Ground-water radon anomaly before the Kobe earthquake in Japan. *Science* 269:60–61.

KITTO, M. E., KUHLAND, M. K., AND DANSEREAU, R. E. 1996. Direct comparison of three methods for the determination of radon in well water. *Health Physics* 70:358–362.

KOTRAPPA, P. AND JESTER, W. A. 1993. Electret ion chamber radon monitors measure dissolved ^{222}Rn in water. *Health Physics* 64:397–405.

LACHAPELLE, E. B. 1988. A study of radon-222 from potable water sources to household air. Master's thesis, University of Maine.

LAWRENCE, E., POETER, E., AND WANTY, R. 1991. Geohydrologic, geochemical, and geologic controls on the occurance of radon in ground water near Conifer, Colorado, USA. *Journal of Hydrology* 127:367–386.

LEE, R. W. AND HOLLYDAY, E. F. 1993. Use of radon measurements in Carters Creek, Maury County, Tennessee, to determine location and magnitude of ground-water seepage, pp. 237–242. *In* L. C. S. Gundersen and R. B. Wanty (eds.), Field Studies of Radon in Rocks, Soils, and Water. C. K. Smoley, Boca Raton, Florida.

LUCAS, H. F. 1957. Improved low level alpha scintillation counter for radon. *Rev Scient Instrument* 28:680–683.

LUCAS, H. F. 1964. A fast and accurate survey technique for both radon-222 and radium-226, pp. 315–329. *In* J. A. S. Adams and W. M. Lowder (eds.), The Natural Radiation Environment. The University of Chicago Press, Chicago, IL.

MATHIEU, G. G., BISCAYE, P. E., LUPTON, R. A., AND HAMMOND, D. E. 1988. System for measurement of ^{222}Rn at low levels in natural waters. *Health Physics* 55:989–992.

MCHONE, N. W. AND SINISCALCHI, A. 1992. Temporal variations in bedrock well water radon and radium and water radon's effect on indoor air radon. *In* 1992 International Symposium on Radon and Radon Technology. Session XII Poster: Radon in Water, Minneapolis, MN. U.S. Environmental Protection Agency.

[NCRP] National Council of Radiological Protection and Measurements 1987. NCRP report 93: Ionizing radiation exposure of the population of the United States. National Council of Radiological Protection and Measurements, Bethasda, MD.

NELSON, P. H., RACHIELE, R., AND SMITH, A. 1983. Transport of radon in flowing boreholes at Stripa, Sweded. *Journal of Geophysical Research* 88:2395–2405.

NORRIS, M. J., GUISEPPE, V. E., AND HESS, C. T. 2004. Waterborne radon in seven Maine schools. *Health Physics* 86:528–535.

[NRC] National Research Council 1999a. Health effects of exposures to radon: BEIR VI. National Academy Press, Washington, DC.

[NRC] National Research Council 1999b. Risk assessment of radon in drinking water. National Academy Press, Washington, DC.

O'CONNELL, M. F. AND KAUFMANN, R. F. 1976. Radioactivity associated with geothermal waters in the Western United States: Basic data. Technial note ORP/LV-75-8A, U.S. Environmental Protection Agency, Office of Radiation Programs, Las Vegas, Nevada.

PARKER, L. V. AND CLARK, C. H. 2002. Study of five discrete interval-type groundwater sampling devices. Technical Report ERDC/CRREL TR-02-12, U.S. Army Corps of Engineers.

PARSA, B. AND HORTON, T. 1990. Radon-222 in drinking water: An NJDEP-EERF collaborative study. *Health Physics* 58:209–212.

PRICHARD, H. M. AND GESELL, T. F. 1977. Rapid measurements of ^{222}Rn concentrations in water with a commercial liquid scintillation counter. *Health Physics* 33:577–581.

PRICHARD, H. M. AND GESELL, T. F. 1981. An estimate of population exposures due to radon in public water supplies in the area of Houston, Texas. *Health Physics* 41:599–606.

PROSCHAN, F. 1952. Rejection of outlying observations. *American Journal of Physics* 21:520–525.

QUET, C., ROUSSEAU-VIOLET, J., AND BUSSIÈRE, P. 1975. Recoil emanating power and specific surface area of solids labelled by radium recoil atoms. I. Theory for single solid particles. *Radiochem. Radioanal. Lett.* 23:359–368.

RICKERT, E. A. 2005. Hydrologic and borehole geophysical investigation of bedrock observation wells at the University of Maine. Master's thesis, University of Maine.

SENIOR, L. A., SLOTO, R. A., AND REIF, A. G. 1997. Hydrogeology and water quality of the West Valley Creek Basin, Chester County Pennsylvania. U.S. Geological Survey Water-Resources Investigations Report 94-4137, United States Geological Survey.

SLOTO, R. A. 2000. Naturally occurring radionuclides in the ground water of Southeastern Pennsylvania. U.S. Geological Survey Fact Sheet 012-00, U.S. Geological Survey.

STATE OF MAINE 1993. Air and water radon service provider registration rules. *In* Rule Chapters for Part of the Department of Health and Human Services, chapter 224. State of Maine. Available at http://www.maine.gov/sos/cec/rules/10/chaps10.htm.

TANNER, A. B. 1964. Radon mitigation in the ground: A review, pp. 161–191. *In* J. A. S. Adams and W. M. Lowder (eds.), The Natural Radiation Environment. University of Chicago Press.

TANNER, A. B. 1980. Radon mitigation in the ground: A supplementary review. *In* T. F. Gesell and W. M. Lowder (eds.), Natural Radiation Environment III, volume 1. Technical Information Center/U.S. Department of Energy, Houston, Texas.

TORGERSON, T., BENOIT, J., AND MACKIE, D. 1992. Lithological control of groundwater ^{222}Rn concentration in fractured rock media, pp. 263–283. *In* Isotopes of Noble Gases as Tracers in Environmental Studies. International Atomic Energy Agency, Vienna.

VEEGER, A. I. AND RUDERMAN, N. C. 1998. Hydrogeologic controls on radon-222 in a buried valley-fractured bedrock aquifer system. *Ground Water* 36:596–604.

VITZ, E. 1991. Toward a standard method for determining waterborne radon. *Health Physics* 60:817–829.

WANTY, R. B. AND NORDSTROM, D. K. 1993. Natural radionuclides, pp. 423–441. *In* W. M. Alley (ed.), Regional Ground-water quality. Van Nostrand Reinhold, New York.

WHITTAKER, E. L., AKRIDGE, J. D., AND GIOVINO, J. 1987. Two test procedures for radon in drinking water. Publication EPA/600/2-87/082, U.S. Environmental Protection Agency, Las Vegas, Nevada.

WOOD, W. W., KRAEMER, T. F., AND SHAPIRO, A. 2004. Radon (^{222}Rn) in ground water of fractured rocks: A diffusion/ion exchange model. *Ground Water* 42:552–567.

YONEDA, M., INOUE, Y., AND TAKINE, N. 1991. Location of groundwater seepage points into a river by measurement of ^{222}Rn concentration in water using activated charcoal passive collectors. *Journal of Hydrology* 124:307–316.

Appendix A
SUPPLEMENTAL DATA FOR CHAPTER 3

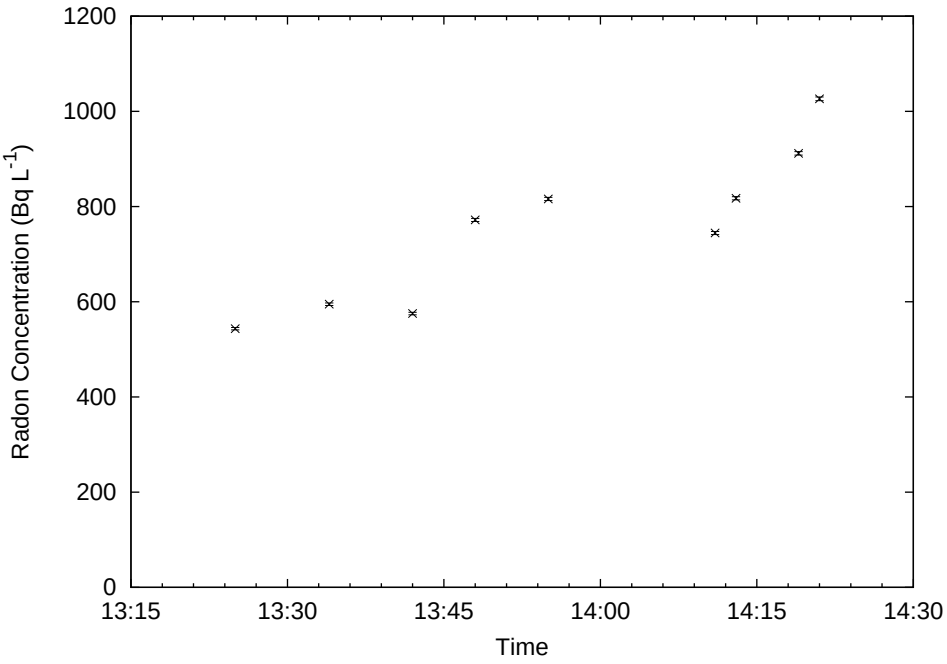

Figure A.1: The radon in water during water usage at school SL.

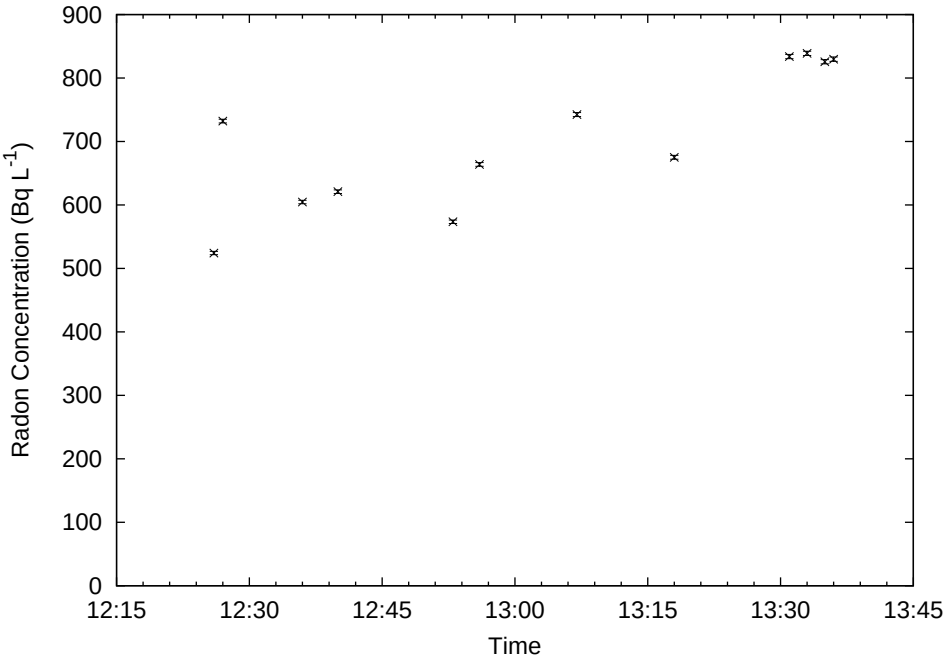

Figure A.2: The radon in water during water usage at school CR.

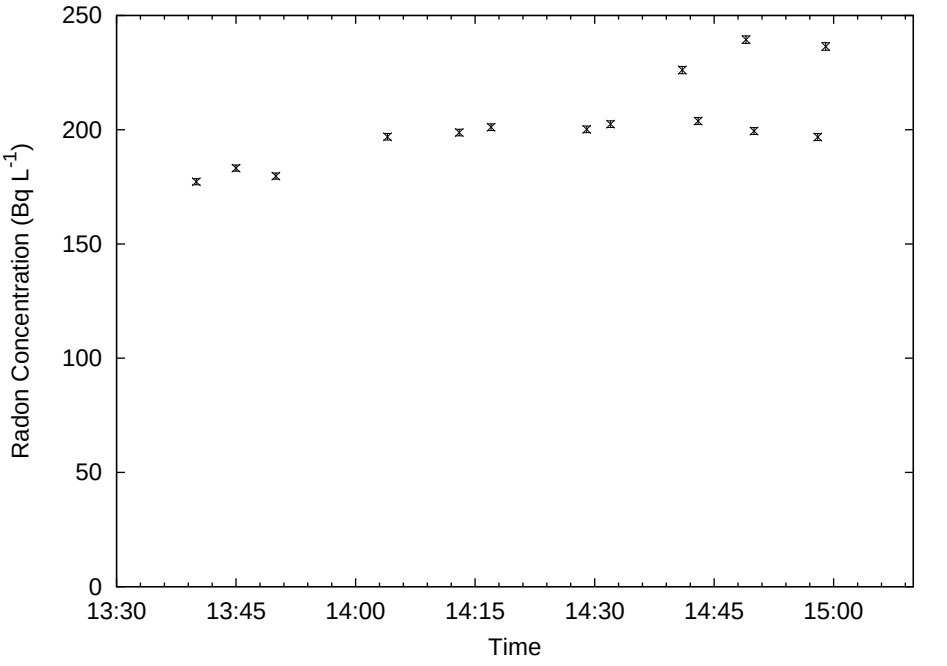

Figure A.3: The radon in water during water usage at school DM.

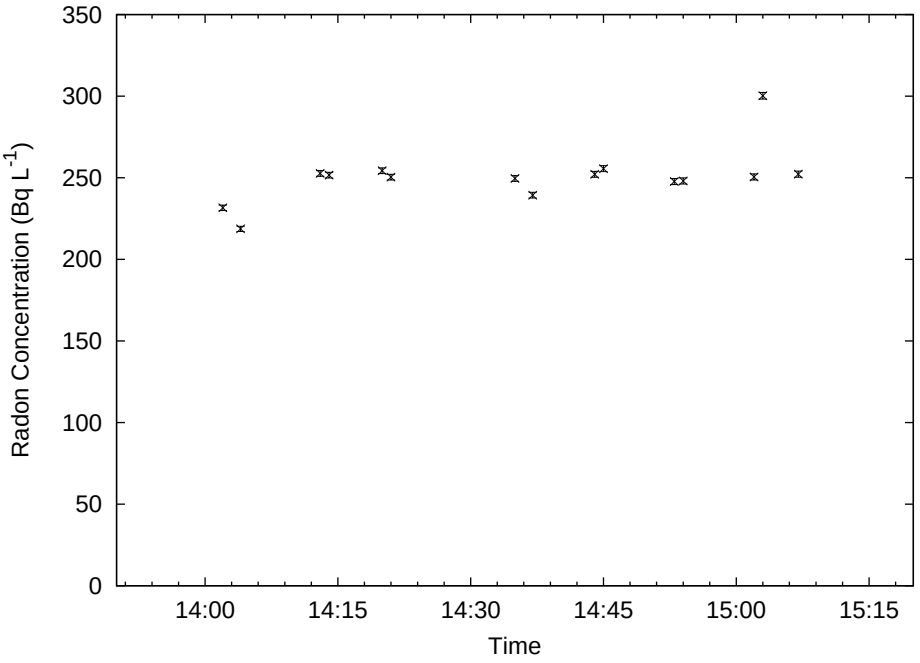

Figure A.4: The radon in water during water usage at school BR.

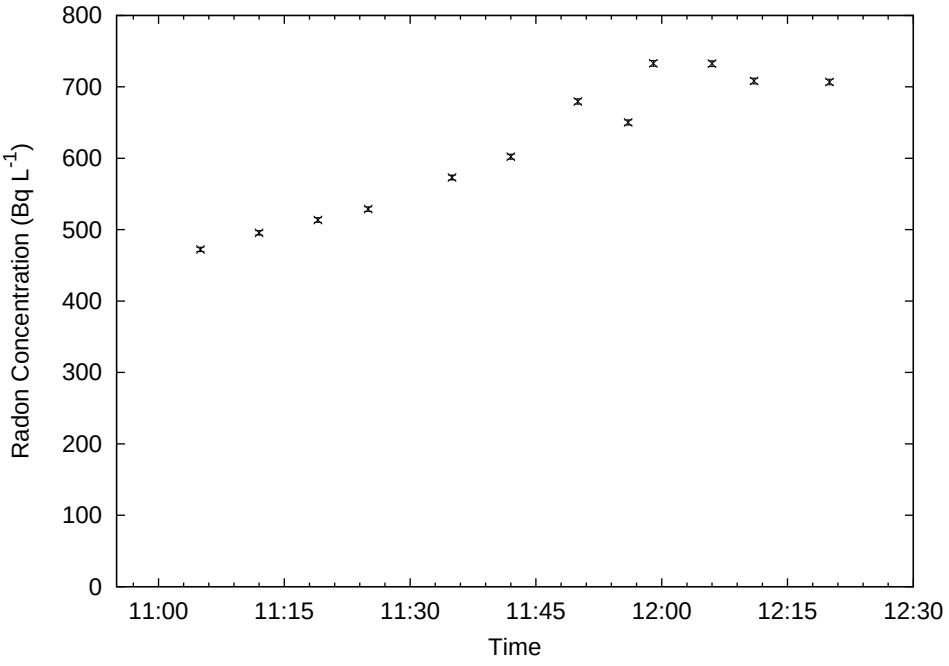

Figure A.5: The radon in water during water usage at school MR.

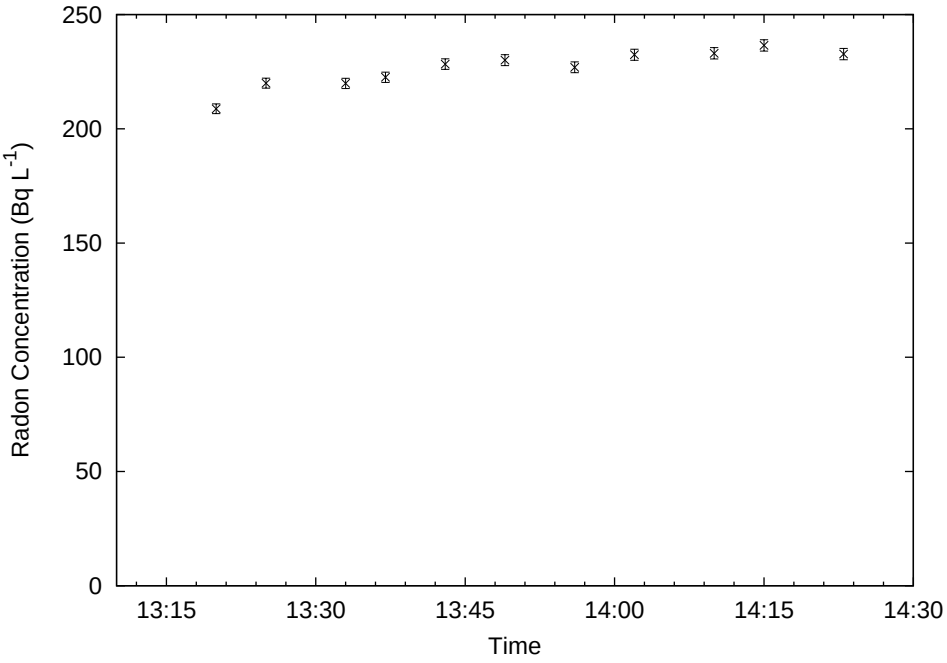

Figure A.6: The radon in water during water usage at school BL.

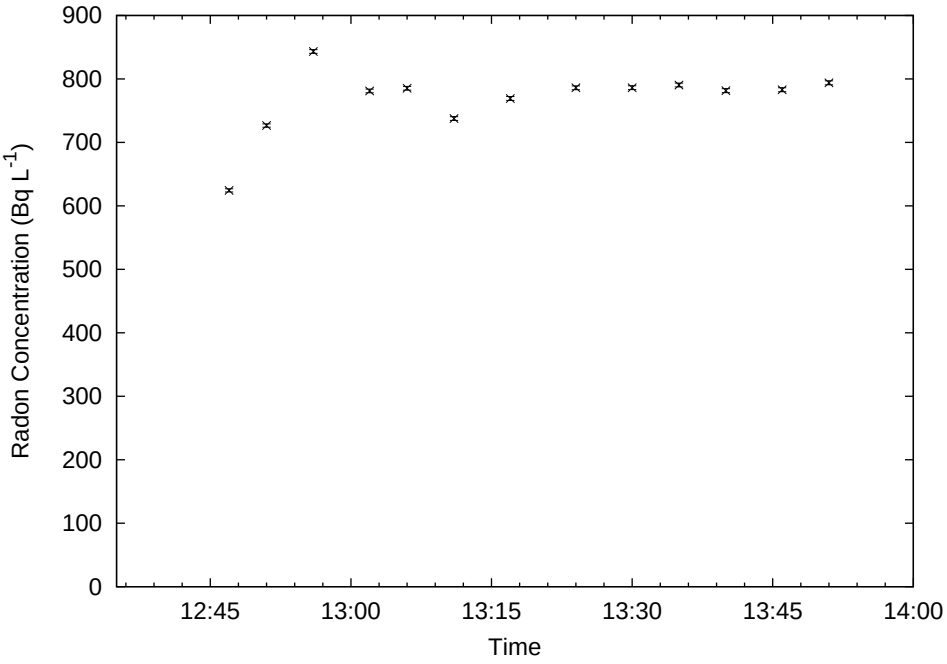

Figure A.7: The radon in water during water usage at school LS.

Appendix B
SUPPLEMENTAL DATA FOR CHAPTER 4

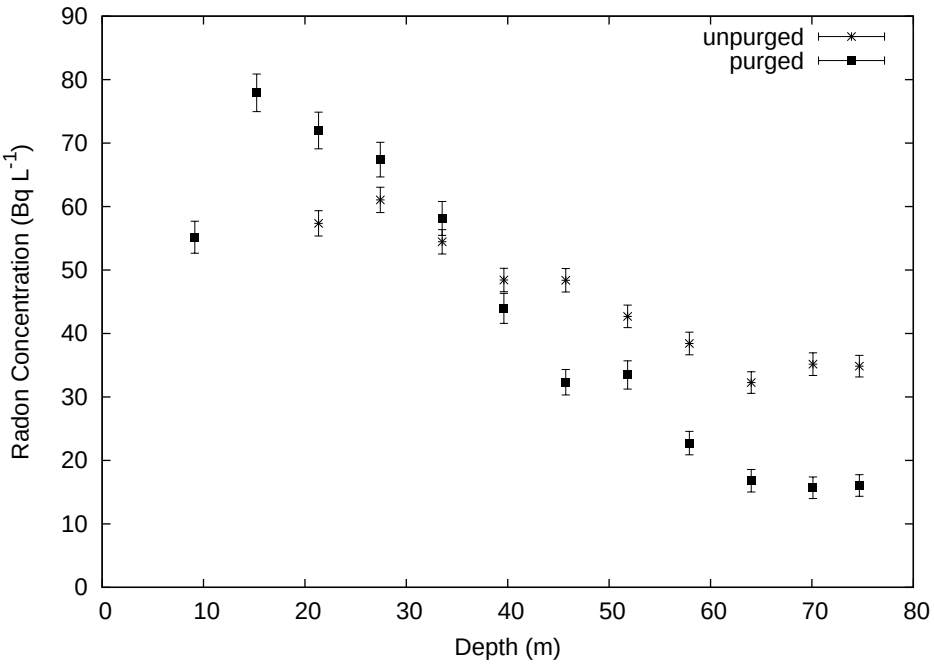

Figure B.1: The unpurged and purged radon profiles in well BRY with a 2-σ measurement uncertainty.

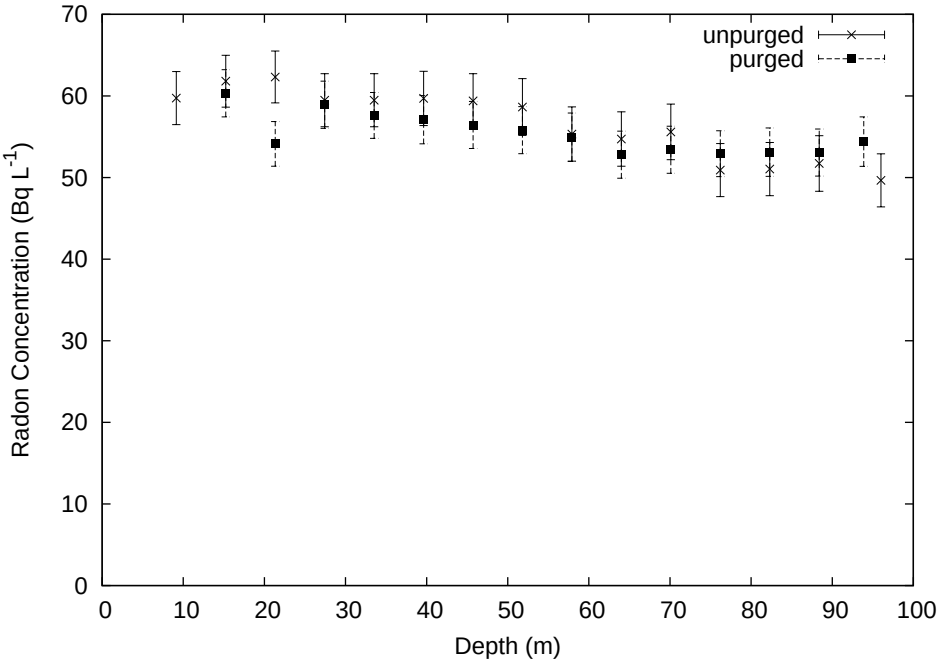

Figure B.2: The unpurged and purged radon profiles in well AWB with a 2-σ measurement uncertainty.

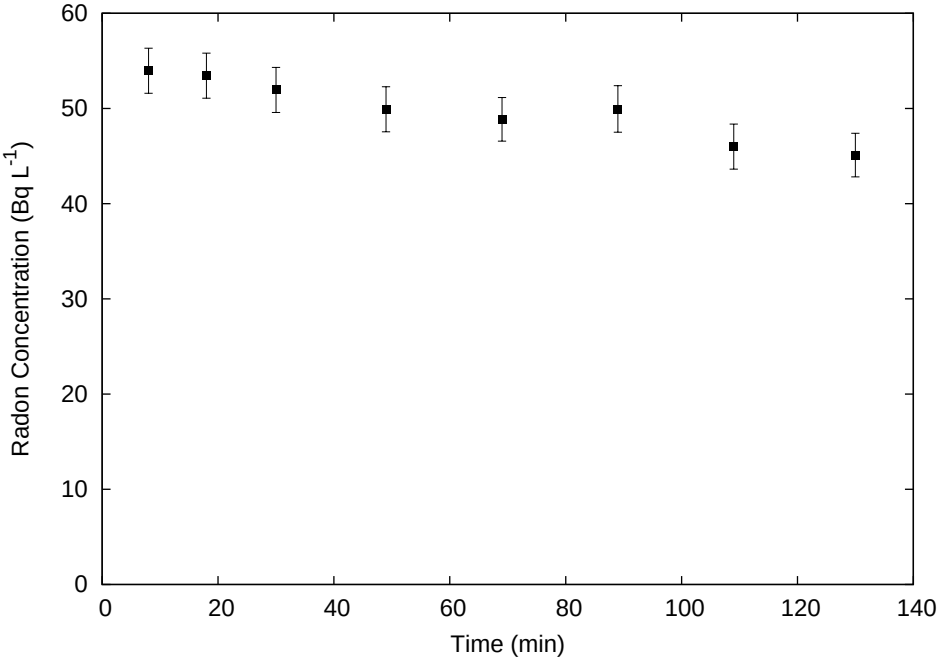

Figure B.3: The radon concentrations in well BRY while pumping from a 40 m depth with a 2-σ measurement uncertainty.

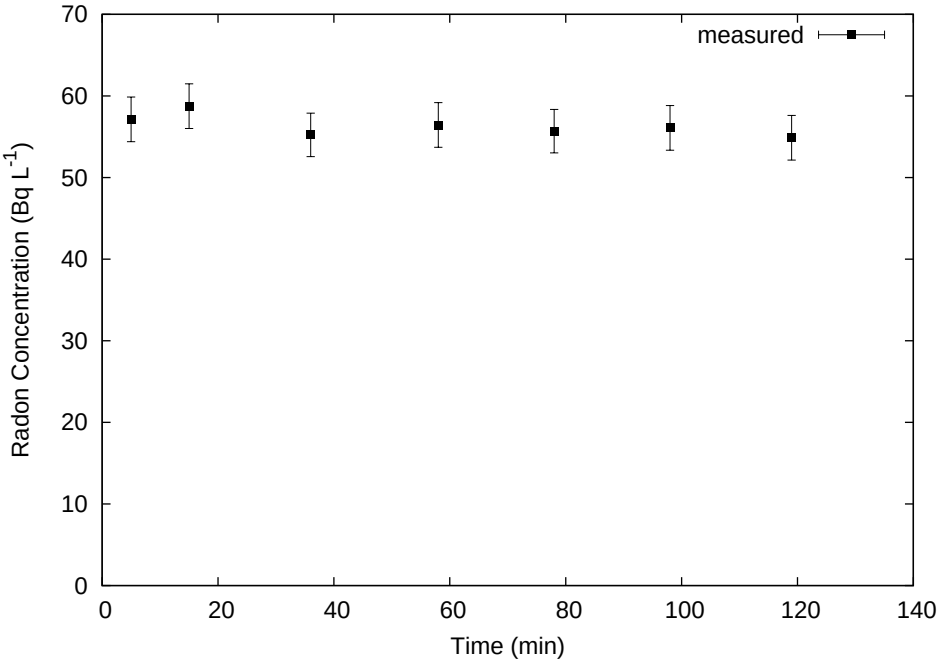

Figure B.4: The radon concentrations in well AWB while pumping from a 40 m depth with a 2-σ measurement uncertainty.

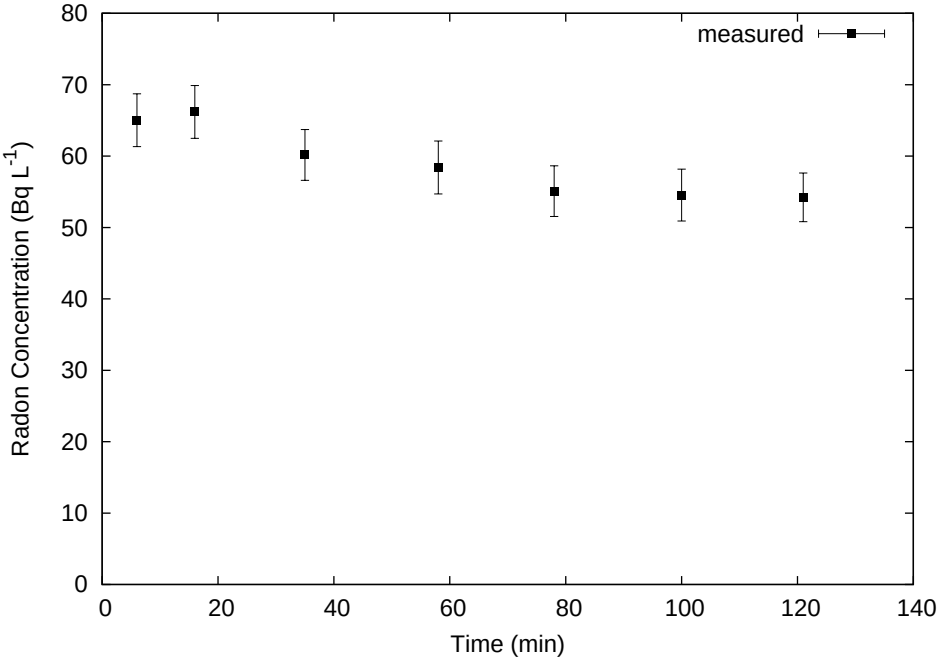

Figure B.5: The radon concentrations in well AWD while pumping from a 40 m depth with a 2-σ measurement uncertainty.

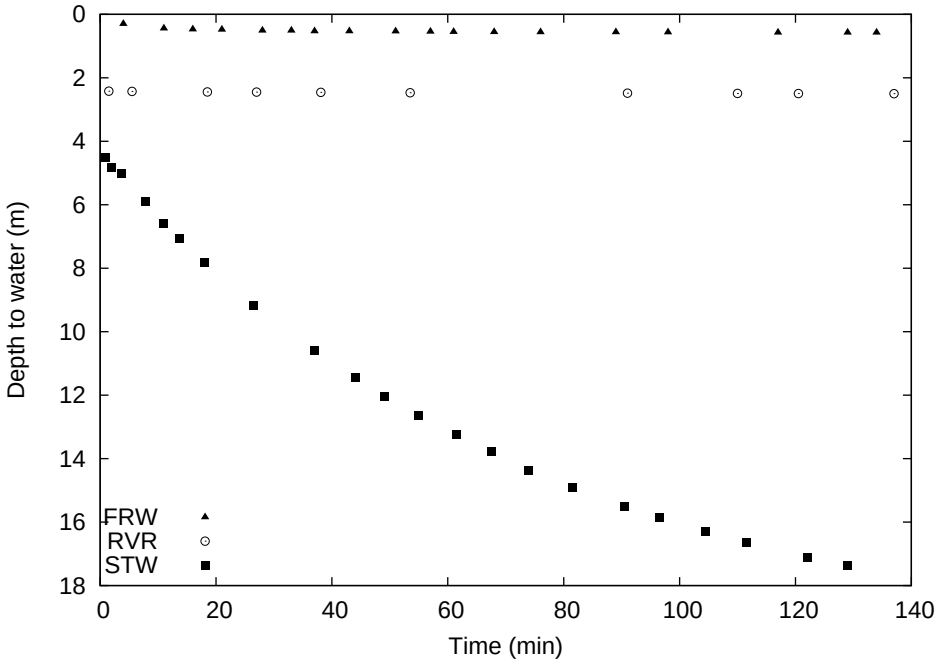

Figure B.6: The measured depth to water in the FRW, RVR, and STW wells while pumping.

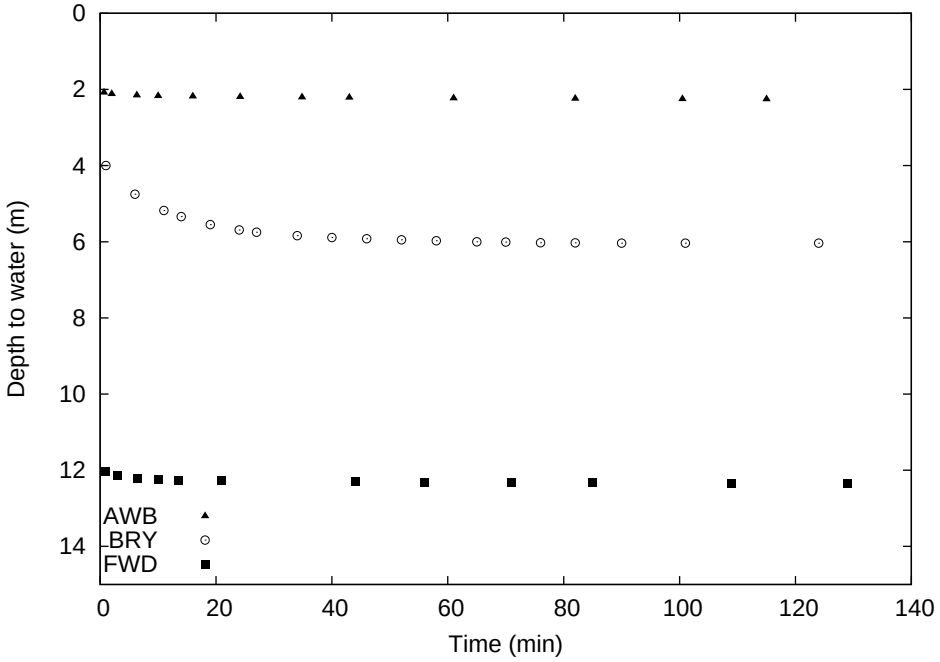

Figure B.7: The measured depth to water in the AWB, BRY, and FWD wells while pumping.

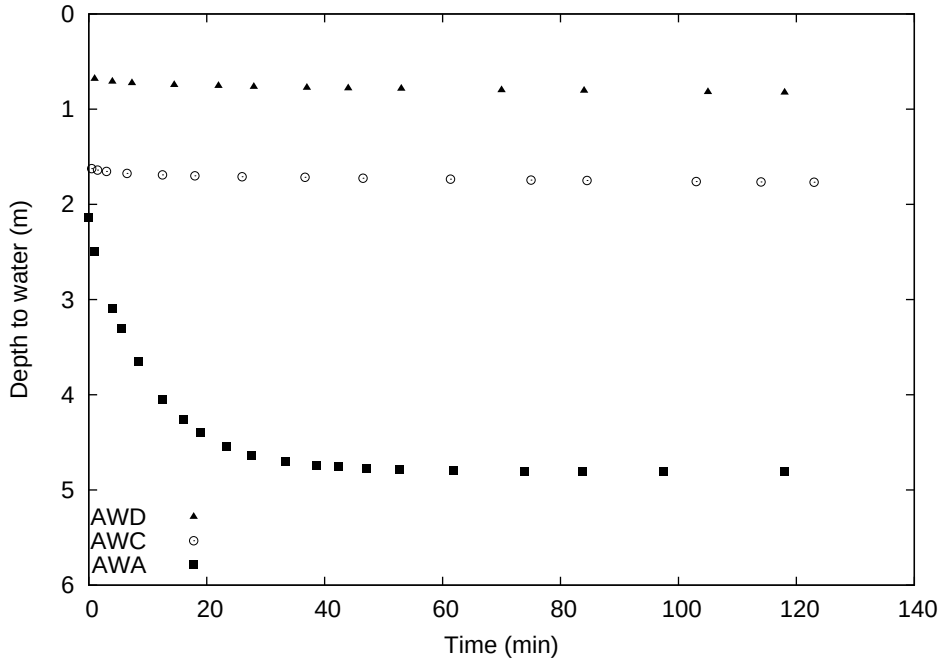

Figure B.8: The measured depth to water in the AWD, AWC, and AWA wells while pumping.

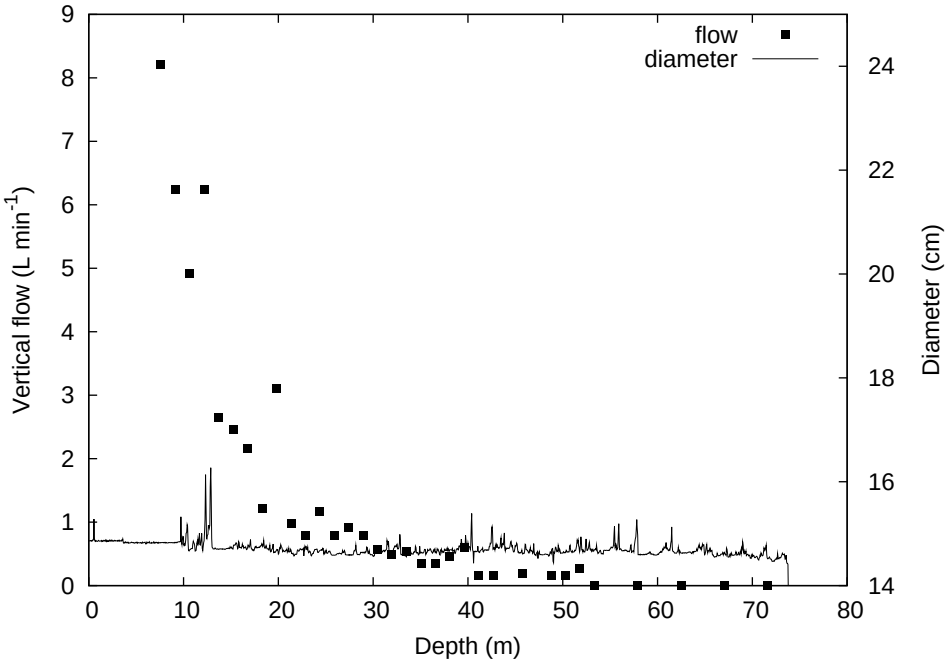

Figure B.9: The pumped flow and caliper log for well BRY (Rickert 2005).

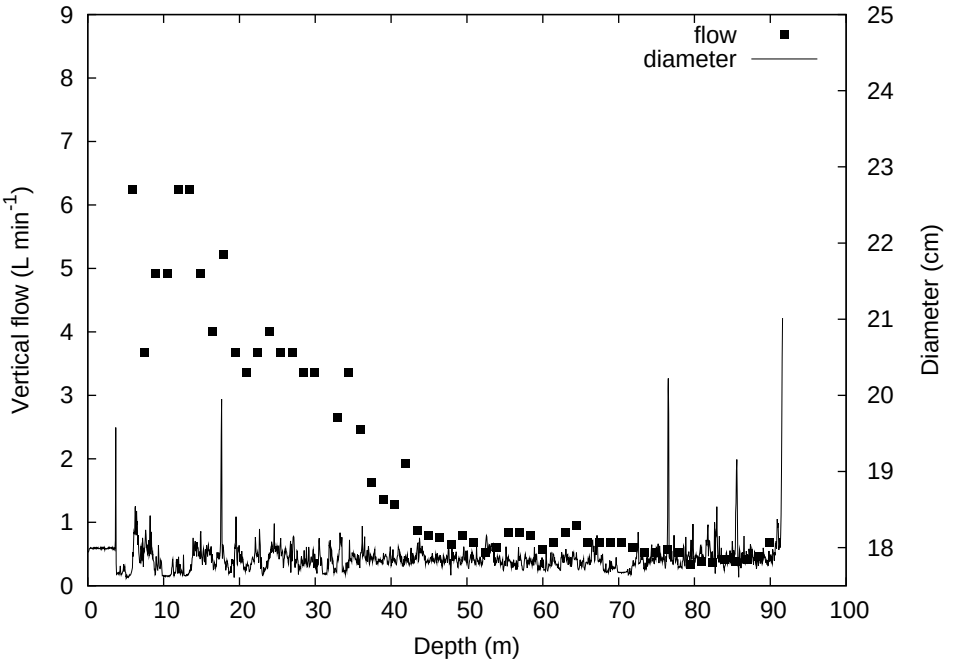

Figure B.10: The pumped flow and caliper log for well AWB (Rickert 2005).

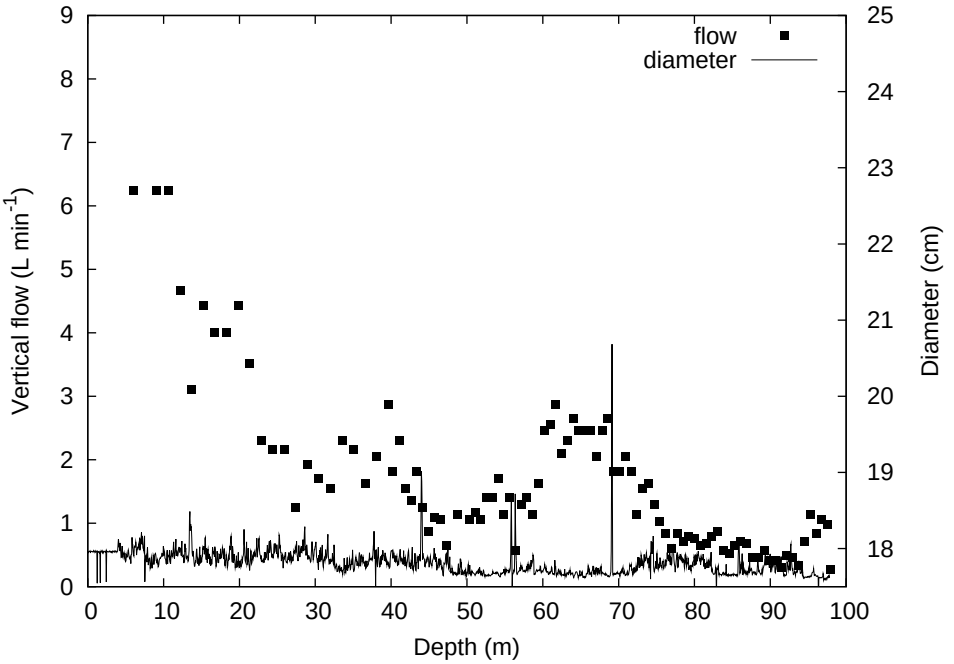

Figure B.11: The pumped flow and caliper log for well AWD (Rickert 2005).

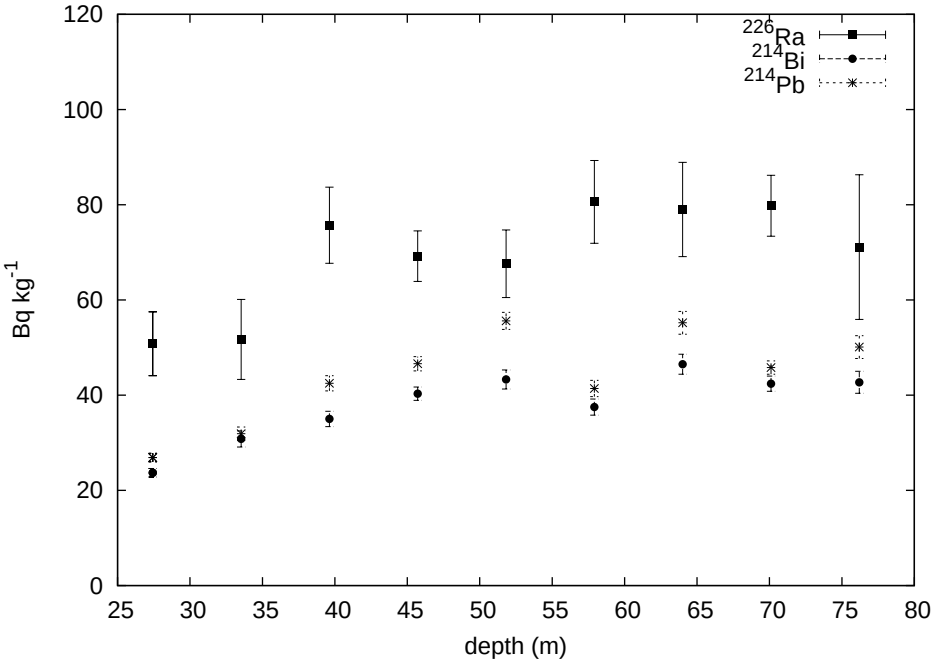

Figure B.12: The concentration of ^{226}Ra, ^{214}Pb, and ^{214}Bi in the rock chips from the STW well drilling with a 1-σ counting uncertainty.

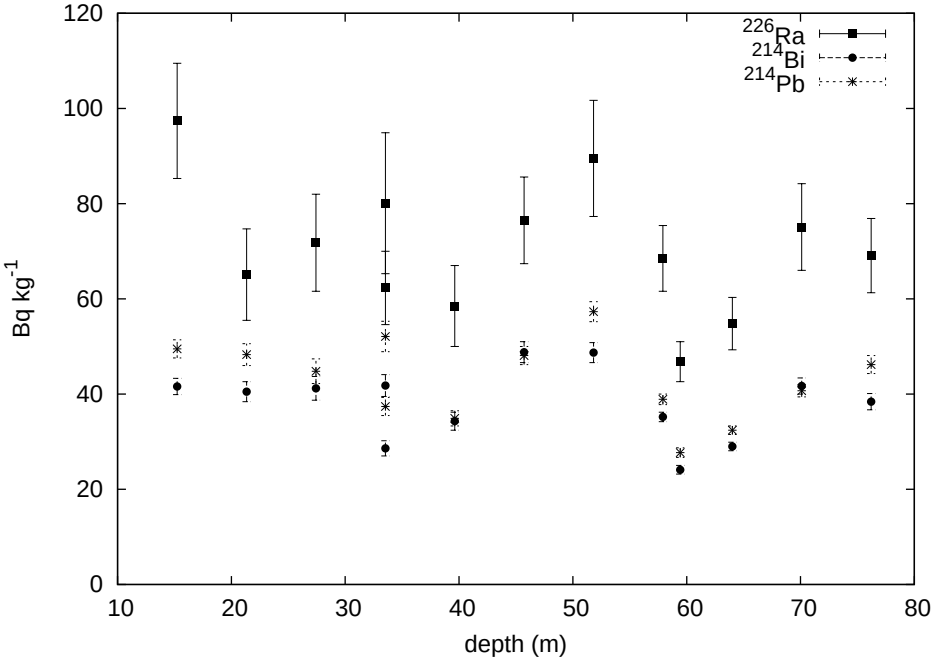

Figure B.13: The concentration of ^{226}Ra, ^{214}Pb, and ^{214}Bi in the rock chips from the FRW well drilling with a 1-σ counting uncertainty.

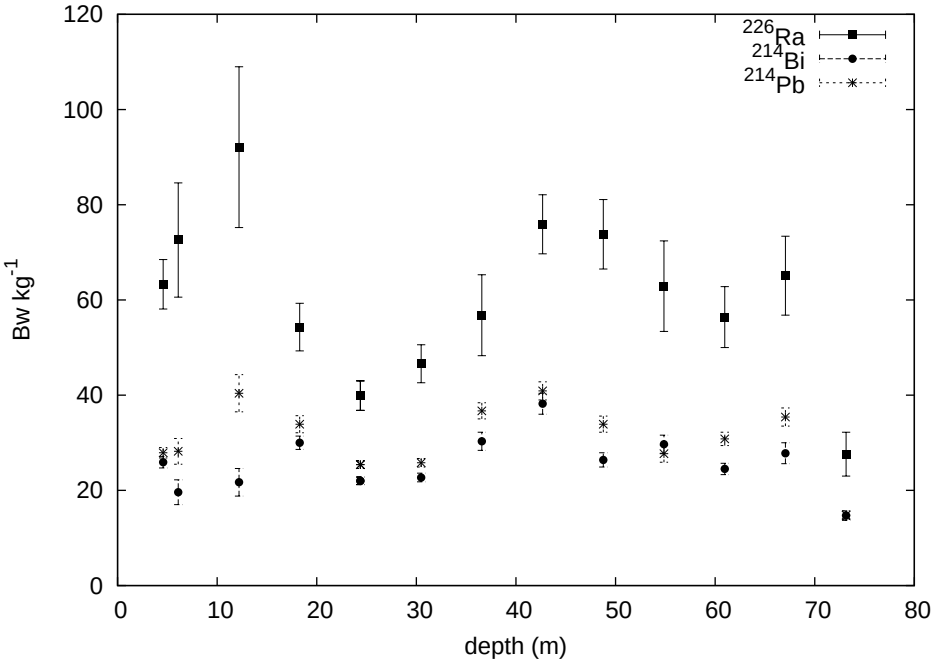

Figure B.14: The concentration of ^{226}Ra, ^{214}Pb, and ^{214}Bi in the rock chips from the RVR well drilling with a 1-σ counting uncertainty.

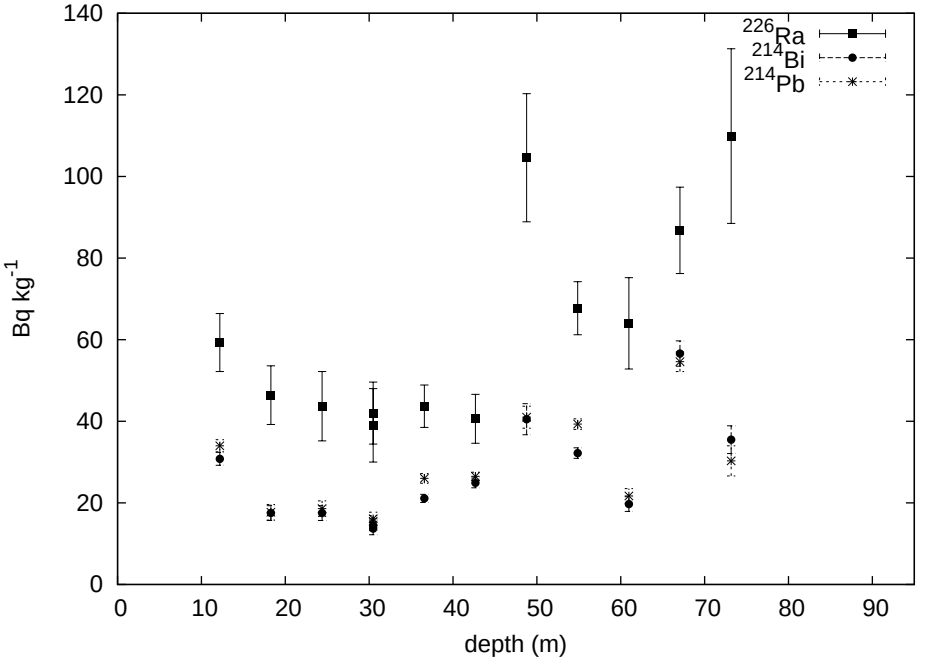

Figure B.15: The concentration of ^{226}Ra, ^{214}Pb, and ^{214}Bi in the rock chips from the BRY well drilling with a 1-σ counting uncertainty.

Appendix C
COMPUTER CODE

Finite difference advection-dispersion C++ code

```
#include<fstream>
#include<iostream>
#include<vector>
#include<string>
#include<iomanip>
#include<math.h>
using namespace std;

// Finite difference code of advection-dispersion equation
//
// At locations of source and sinks, a modified fd
// code keeps the fluxes right. This way, a far distance with
// C=0 is not needed. Works with multiple sources -by specifying
// fluxes at those locations. There is no dispersion across flux
// boundaries.
// Give initial and final conditions and all parameters as
// separate file passed as command line argument. Reports when
// the model exceeds 2-sigma of the measured Rn vs time data,
// used for sensitivity analysis of uncertainty and calculates
// chi-squared. Works with dropping head as additional velocity
// above "start" - need to provide the *.head.new file as a 2nd
// argument.
//
// Vince Guiseppe
// v 1.3
// Sep. 2006
//
// usage %> ade.x well.in [well.head]

int main(int argc, char *argv[]){
// output file for debugging
ofstream tempfile ("tempfile");

// defs.
int xmax;  // maximum or total depth [m]
int tmax;  // maximum time [min]
double begin;  // domain begin
double dx;  // space step [m]
```

```
double dt;  // time step [min]
int x_steps, t_steps;  //number of space and time steps
double dtmax, vmax;  // stability condition
double a;  // dispersivity [m]
double A=1;  // area needed?
double xin[5];  // inflow locations [m]
double vin[5];  // inflow velocities [m/min]
double Cin[5];  // inflow concentrations [pCi/L]
char name[20];  // well name
int ni, ns, nf, nh;  //number of initial concentrations,
                     // sources, final concs, head meas.
double Ci[20], xi[20],  // initial conc., locations
       Cf[20], Cfe[20],  // final conc. and meas. error
       head[50], htime[50],  // meas. head, time
       scale;  // scale initial conc.
int tf[20];  // final rn conc time

//get parameters from file
string temp, st1="steps", st2="disp", st3="source",
       st4="initial", st5="final", st6="time";
ifstream infile (argv[1]);
if (infile.is_open()){
  infile >> name;
  while(temp !=st1){
    infile >> temp;
    if(temp==st1){
      infile >> temp >> temp >> temp >> temp;
      infile >> dx >> dt >> xmax >> tmax >> begin;
      break;}}
  while(temp!=st2){
    infile >> temp;
    if(temp==st2){
      infile >> a;
      break;}}
  while(temp!=st3){
    infile >> temp;
    if(temp==st3){
      infile >> ns >> temp >> temp >> temp;
      for(int k=0;k<ns;k++){
        infile >> xin[k] >> vin[k] >> Cin[k];}
      break;}}
  while(temp !=st4){
    infile >> temp;
    if(temp==st4){
      infile >> ni >> scale >> temp >> temp;
      for (int j=0;j<ni;j++){
```

```
        infile >> xi[j] >> Ci[j];
        xi[j]=xi[j]*0.3048;}
      break;}}
  while(temp!=st5){
    infile >> temp;
    if(temp==st5){
      infile >> nf >> temp >> temp >> temp;
      for(int f=0;f<nf;f++){
        infile >> tf[f] >> Cf[f] >> Cfe[f];}
      break;}}
  infile.close();}
else{ cout << "could not open " << argv[1] << endl; exit(1);}
cout << ns << " source(s)" << endl;

if (argc==3){
  ifstream headfile (argv[2]);
  if (headfile.is_open()){
    while(temp!=st6){
      headfile >> temp;
      if(temp==st6){
        headfile >> nh;
        for(int h=0;h<nh;h++){
        headfile >> head[h] >> temp >> htime[h];}
        break;}}}
  headfile.close();}

// check stability
vmax=0;
for(int k=0;k<ns;k++){
  vmax+=vin[k];}
cout << "vmax= " << vmax << endl;
dtmax=1/(2*(a*vmax/dx/dx+vmax/dx));
cout << "dt must be less than " << dtmax << endl;

//number of steps
x_steps=int(xmax/dx);
t_steps=int(tmax/dt);
cout << x_steps << "<-x t->" << t_steps << endl;

double C[x_steps][t_steps]; //Concentration 2-d array
double v[x_steps]; // velocity array
double vh[t_steps];
double k1, k2, k3, k4;
int start, next, a2, stop;

//zero out arrays
```

```
for(int i=0;i<x_steps;i++){
  for(int m=0;m<t_steps;m++){
    C[i][m]=0;}
  v[i]=0;}

//set falling head velocities
for (int m=0;m<t_steps;m++){
  vh[m]=0;}
if(argc==3){
  int h1,h2;
  double hslope;
  for(int h=0;h<nh-1;h++){
    h1=int(ceil(htime[h]/dt));
    h2=int(htime[h+1]/dt);
    hslope=(head[h+1]-head[h])/(htime[h+1]-htime[h]);
    for (int z=h1;z<h2+1;z++){
      vh[z]=hslope;}}
  for (int z=0;z<int(ceil(htime[0]/dt));z++){
    vh[z]=(head[1]-head[0])/(htime[1]-htime[0]);}
  for (int m=0;m<t_steps;m++){
    tempfile << m*dt << "\t" << vh[m] << endl;}}

//initial concentrations
int delta, d1,d2;
for(int j=0;j<ni-1;j++){
  d1=int((xi[j+1]/dx));
  d2=int(ceil(xi[j]/dx));
  double slope=(Ci[j+1]-Ci[j])/(xi[j+1]-xi[j]);
  for(int y=d2;y<d1+1;y++){
    C[y][0]=scale*(Ci[j]+(y*dx-xi[j])*slope);}}
for(int y=0;y<int(ceil(xi[0]/dx));y++){
  C[y][0]=scale*(Ci[0]+(y*dx-xi[0])*(Ci[1]-Ci[0])/
    (xi[1]-xi[0]));}
for(int m=1;m<t_steps;m++){
  C[int(begin/dx)-1][m]=C[int(begin/dx)-1][0];}

//go!
if(ns==1){  // one source, above pump
  start=int(xin[0]/dx);
  stop=int(40/dx);
  double s1=Cin[0];
  for(int i=start;i<stop+1;i++){
    v[i]=vin[0];}
  for(int m=0;m<t_steps-1;m++){
    for(int i=int(begin/dx);i<x_steps-1;i++){
      if(i<start-1){
```

```
        k1=(a-dx/2+vh[m]*dt/2)*vh[m]*dt/dx/dx;
        k2=vh[m]*dt/dx;
        C[i][m+1]=C[i][m]+k1*(C[i+1][m]-2*C[i][m]+C[i-1][m])-
          k2*(C[i][m]-C[i-1][m]);}
      else if(i==start-1){
        k2=vh[m]*dt/dx;
        C[i][m+1]=C[i][m]-k2*(C[i][m]-C[i-1][m]);}
      else if(i==start){
        k2=vh[m]*dt/dx;
        k3=(v[i]-vh[m])*dt/dx;
        if(k3<0){k3=0;}
        k4=v[i]*dt/dx;
        C[i][m+1]=C[i][m]+k2*C[i-1][m]+k3*s1-k4*C[i][m];}
      else if(i==stop){
        k2=v[i]*dt/dx;
        C[i][m+1]=C[i][m]-k2*(C[i][m]-C[i-1][m]);}
      else{
        k1=(a-dx/2+v[i]*dt/2)*v[i]*dt/dx/dx;
        k2=v[i]*dt/dx;
        C[i][m+1]=C[i][m]+k1*(C[i+1][m]-2*C[i][m]+C[i-1][m])
          -k2*(C[i][m]-C[i-1][m]);}}}}
else if(ns==2){  // two sources, both above pump
  //source locations and velocities
  start=int(xin[0]/dx);
  next=int(xin[1]/dx);
  stop=int(40/dx);
  double s1=Cin[0];         //first source
  double s2=Cin[1];        //2nd source
  for(int i=start;i<stop+1;i++){
    v[i]=vin[0];}         //set velocities, v1 [m/min]
    for(int i=next+1;i<stop+1;i++){
    v[i]=vin[0]+vin[1];}  //set velocities, v1+v2 [m/min]
  for(int m=0;m<t_steps-1;m++){
    for(int i=1;i<x_steps-1;i++){
      k1=(a-dx/2+v[i]*dt/2)*v[i]*dt/dx/dx;
      k2=v[i]*dt/dx;
      k3=(v[i+1]-v[i])*dt/dx;
      k4=v[i+1]*dt/dx;
      if(i<start){
        k1=(a-dx/2+vh[m]*dt/2)*vh[m]*dt/dx/dx;
        k2=vh[m]*dt/dx;
        C[i][m+1]=C[i][m]+k1*(C[i+1][m]-2*C[i][m]+C[i-1][m])-
          k2*(C[i][m]-C[i-1][m]);}
      else if(i==start){
        k2=vh[m]*dt/dx;
        k3=(v[i]-vh[m])*dt/dx;
```

```
        if(k3<0){k3=0;}
        k4=v[i]*dt/dx;
        C[i][m+1]=C[i][m]+k2*C[i-1][m]+k3*s1-k4*C[i][m];}
      else if(i==next){
        C[i][m+1]=C[i][m]+k2*C[i-1][m]+k3*s2-k4*C[i][m];} //2nd
      else if(i==stop){
        C[i][m+1]=C[i][m]-k2*(C[i][m]-C[i-1][m]);}
      else if(i==next-1){
        C[i][m+1]=C[i][m]-k2*(C[i][m]-C[i-1][m]);}
      else{
        C[i][m+1]=C[i][m]+k1*(C[i+1][m]-2*C[i][m]+C[i-1][m])-
          k2*(C[i][m]-C[i-1][m]);}}}}
else if(ns==3){ // 3 sources, one above, two below pump
  //source locations and velocities
  start=int(xin[0]/dx);
  int b1=int(xin[1]/dx);
  int b2=int(xin[2]/dx);
  stop=int(40/dx);
  double s1=Cin[0],
  s2=Cin[1],
  s3=Cin[2];
  for(int i=start;i<stop+1;i++){
    v[i]=vin[0];}
  for(int i=stop+1;i<b1+1;i++){
    v[i]=vin[1]+vin[2];}
  for(int i=b1+1;i<b2+1;i++){
    v[i]=vin[2];}
  for(int i=0;i<x_steps;i++){
    tempfile << i*dx << "\t" << v[i] << endl;}
  for(int m=0;m<t_steps-1;m++){
    for(int i=int(begin/dx);i<x_steps-1;i++){
      k1=(a-dx/2+v[i]*dt/2)*v[i]*dt/dx/dx;
      k2=v[i]*dt/dx;
      k3=(v[i]-v[i+1])*dt/dx;
      k4=v[i+1]*dt/dx;
      if (i<start-1){
        k1=(a-dx/2+vh[m]*dt/2)*vh[m]*dt/dx/dx;
        k2=vh[m]*dt/dx;
        C[i][m+1]=C[i][m]+k1*(C[i+1][m]-2*C[i][m]+C[i-1][m])
          -k2*(C[i][m]-C[i-1][m]);}
      else if(i==start-1){
        k2=vh[m]*dt/dx;
        C[i][m+1]=C[i][m]-k2*(C[i][m]-C[i-1][m]);}
      else if(i==start){
        k2=vh[m]*dt/dx;
        k3=(v[i]-vh[m])*dt/dx;
```

```
        if(k3<0){k3=0;}
        k4=v[i]*dt/dx;
        C[i][m+1]=C[i][m]+k2*C[i-1][m]+k3*s1-k4*C[i][m];}
      else if(i==stop){
        C[i][m+1]=C[i][m]-k2*C[i][m]-k4*C[i][m]+k2*C[i-1][m]+
          k4*C[i+1][m];}
      else if(i==b1){
        C[i][m+1]=C[i][m]+k4*C[i+1][m]+k3*s2-k2*C[i][m];}
      else if(i==(b1+1)){
        C[i][m+1]=C[i][m]-k2*(C[i][m]-C[i+1][m]);}
      else if(i==b2){
        C[i][m+1]=C[i][m]-k2*(C[i][m]-s3);}
      else if(i>stop and i!=b1 and i!=b1+1 and i!=b2){
        C[i][m+1]=C[i][m]+k1*(C[i+1][m]-2*C[i][m]+C[i-1][m])-
          k2*(C[i][m]-C[i+1][m]);}
      else{
        C[i][m+1]=C[i][m]+k1*(C[i+1][m]-2*C[i][m]+C[i-1][m])-
          k2*(C[i][m]-C[i-1][m]);}}}}
else if(ns==4){ // 4 sources, 2 above, 2 below
  //source locations and velocities
  start=int(xin[0]/dx);
  next=int(xin[1]/dx);
  int b1=int(xin[2]/dx);
  int b2=int(xin[3]/dx);
  stop=int(40/dx);
  double s1=Cin[0],
  s2=Cin[1],
  s3=Cin[2],
  s4=Cin[3];
  for(int i=start;i<next+1;i++){
    v[i]=vin[0];}
  for(int i=next+1;i<stop+1;i++){
    v[i]=vin[0]+vin[1];}
  for(int i=stop+1;i<b1+1;i++){
    v[i]=vin[2]+vin[3];}
  for(int i=b1+1;i<b2+1;i++){
    v[i]=vin[3];}
  for(int i=0;i<x_steps;i++){
    tempfile << i*dx << "\t" << v[i] << endl;}
  for(int m=0;m<t_steps-1;m++){
    for(int i=int(begin/dx);i<x_steps-1;i++){
      k1=(a-dx/2+v[i]*dt/2)*v[i]*dt/dx/dx;
      k2=v[i]*dt/dx;
      k3=(v[i]-v[i+1])*dt/dx;
      k4=v[i+1]*dt/dx;
      if(i<start-1){
```

```
      k1=(a-dx/2+vh[m]*dt/2)*vh[m]*dt/dx/dx;
      k2=vh[m]*dt/dx;
      C[i][m+1]=C[i][m]+k1*(C[i+1][m]-2*C[i][m]+C[i-1][m])-
        k2*(C[i][m]-C[i-1][m]);}
    else if(i==start-1){
      k2=vh[m]*dt/dx;
      C[i][m+1]=C[i][m]-k2*(C[i][m]-C[i-1][m]);}
    else if(i==start){
      k2=vh[m]*dt/dx;
      k3=((vin[0]+vin[1])-vh[m])*(vin[0]/(vin[0]+vin[1]))*
        dt/dx;
      if(k3<0){k3=0;}
      k4=(vh[m]+(vin[0]+vin[1]-vh[m])*
        vin[0]/(vin[0]+vin[1]))*dt/dx;
      C[i][m+1]=C[i][m]+k2*C[i-1][m]+k3*s1-k4*C[i][m];}
    else if(i==next-1){
      k2=(vh[m]+(vin[0]+vin[1]-vh[m])*
        vin[0]/(vin[0]+vin[1]))*dt/dx;
      C[i][m+1]=C[i][m]-k2*(C[i][m]-C[i-1][m]);}
    else if(i==next){
      k3=((vin[0]+vin[1])-vh[m])*(vin[1]/(vin[0]+vin[1]))*
        dt/dx;
      if(k3<0){k3=0;}
      C[i][m+1]=C[i][m]+k2*C[i-1][m]+k3*s2-k4*C[i][m];}
    else if(i==stop){
      C[i][m+1]=C[i][m]-k2*C[i][m]-k4*C[i][m]+k2*C[i-1][m]+
        k4*C[i+1][m];}
    else if(i==b1){
      C[i][m+1]=C[i][m]+k4*C[i+1][m]+k3*s3-k2*C[i][m];}
    else if(i==(b1+1)){
      C[i][m+1]=C[i][m]-k2*(C[i][m]-C[i+1][m]);}
    else if(i==b2){
      C[i][m+1]=C[i][m]-k2*(C[i][m]-s4);}
    else if(i>stop and i!=b1 and i!=b1+1 andi!=b2
      and i!=next-1 and i!=next){
      C[i][m+1]=C[i][m]+k1*(C[i+1][m]-2*C[i][m]+C[i-1][m])-
        k2*(C[i][m]-C[i+1][m]);}
    else{
      if(i<next-1){
        k2=(vh[m]+(vin[0]+vin[1]-vh[m])*
          vin[0]/(vin[0]+vin[1]))*dt/dx;
        k1=(a-dx/2+v[i]*dt/2)*v[i]*dt/dx/dx;}
      C[i][m+1]=C[i][m]+k1*(C[i+1][m]-2*C[i][m]+C[i-1][m])-
        k2*(C[i][m]-C[i-1][m]);}}}}
else if(ns==5){  // 5 sources, 3 above, 2 below
  //source locations and velocities
```

```
start=int(xin[0]/dx);
next=int(xin[1]/dx);
a2=int(xin[2]/dx);
int b1=int(xin[3]/dx);
int b2=int(xin[4]/dx);
stop=int(40/dx);
double s1=Cin[0],
s2=Cin[1],
s3=Cin[2],
s4=Cin[3],
s5=Cin[4];
for(int i=start;i<next+1;i++){
  v[i]=vin[0];}
for(int i=next+1;i<a2+1;i++){
  v[i]=vin[0]+vin[1];}
for(int i=a2+1;i<stop+1;i++){
  v[i]=vin[0]+vin[1]+vin[2];}
for(int i=stop+1;i<b1+1;i++){
  v[i]=vin[3]+vin[4];}
for(int i=b1+1;i<b2+1;i++){
  v[i]=vin[4];}
for(int m=0;m<t_steps-1;m++){
  for(int i=int(begin/dx);i<x_steps-1;i++){
    k1=(a-dx/2+v[i]*dt/2)*v[i]*dt/dx/dx;
    k2=v[i]*dt/dx;
    k3=(v[i]-v[i+1])*dt/dx;
    k4=v[i+1]*dt/dx;
    if(i<start-1){
      k1=(a-dx/2+vh[m]*dt/2)*vh[m]*dt/dx/dx;
      k2=vh[m]*dt/dx;
      C[i][m+1]=C[i][m]+k1*(C[i+1][m]-2*C[i][m]+C[i-1][m])-
        k2*(C[i][m]-C[i-1][m]);}
    else if(i==start-1){
      k2=vh[m]*dt/dx;
      C[i][m+1]=C[i][m]-k2*(C[i][m]-C[i-1][m]);}
    else if(i==start){
      k2=vh[m]*dt/dx;
      k3=((vin[0]+vin[1]+vin[2])-vh[m])*
       (vin[0]/(vin[0]+vin[1]+vin[2]))*dt/dx;
      if(k3<0){k3=0;}
      k4=(vh[m]+(vin[0]+vin[1]+vin[2]-vh[m])*
        vin[0]/(vin[0]+vin[1]+vin[2]))*dt/dx;
      C[i][m+1]=C[i][m]+k2*C[i-1][m]+k3*s1-k4*C[i][m];}
    else if(i==next-1){
      k2=(vh[m]+(vin[0]+vin[1]+vin[2]-vh[m])*
        vin[0]/(vin[0]+vin[1]+vin[2]))*dt/dx;
```

```
          C[i][m+1]=C[i][m]-k2*(C[i][m]-C[i-1][m]);}
        else if(i==next){
          k3=((vin[0]+vin[1]+vin[2])-vh[m])*
            (vin[1]/(vin[0]+vin[1]+vin[2]))*dt/dx;
          if(k3<0){k3=0;}
          C[i][m+1]=C[i][m]+k2*C[i-1][m]+k3*s2-k4*C[i][m];}
        else if(i==a2-1){
          k2=(vh[m]+(vin[0]+vin[1]+vin[2]-vh[m])*
            vin[0]/(vin[0]+vin[1]+vin[2]))*dt/dx;
          C[i][m+1]=C[i][m]-k2*(C[i][m]-C[i-1][m]);}
        else if(i==a2){
          k3=((vin[0]+vin[1]+vin[2])-vh[m])*
            (vin[2]/(vin[0]+vin[1]+vin[2]))*dt/dx;
          if(k3<0){k3=0;}
        C[i][m+1]=C[i][m]+k2*C[i-1][m]+k3*s3-k4*C[i][m];}
        else if(i==stop){
          C[i][m+1]=C[i][m]-k2*C[i][m]-k4*C[i][m]+k2*C[i-1][m]+
            k4*C[i+1][m];}
        else if(i==b1){
          C[i][m+1]=C[i][m]+k4*C[i+1][m]+k3*s4-k2*C[i][m];}
        else if(i==(b1+1)){
          C[i][m+1]=C[i][m]-k2*(C[i][m]-C[i+1][m]);}
        else if(i==b2){
          C[i][m+1]=C[i][m]-k2*(C[i][m]-s5);}
        else if(i>stop and i!=b1 and i!=b1+1 and
          i!=b2 and i!=next-1 and i!=next){
        C[i][m+1]=C[i][m]+k1*(C[i+1][m]-2*C[i][m]+C[i-1][m])-
            k2*(C[i][m]-C[i+1][m]);}
        else{
          if(i<next-1){
            k2=(vh[m]+(vin[0]+vin[1]+vin[2]-vh[m])*
              vin[0]/(vin[0]+vin[1]+vin[2]))*dt/dx;
            k1=(a-dx/2+v[i]*dt/2)*v[i]*dt/dx/dx;}
          C[i][m+1]=C[i][m]+k1*(C[i+1][m]-2*C[i][m]+C[i-1][m])-
            k2*(C[i][m]-C[i-1][m]);}}}}
  else{ cout << "too many sources" << endl; exit(1);}

double res[nf];  // residuals
double chi=0;  // chi-squares
for(int f=0;f<nf;f++){
  res[f]=(C[stop][int(tf[f]/dt)]-Cf[f]);
  cout << res[f] << "\t" << Cfe[f]*2;
  if (res[f]>Cfe[f]*2){
    cout << "----------> overshot at # "
      << f+1 << ", t=" << tf[f] << endl;}
  else if (res[f]<Cfe[f]*-2){
```

```
    cout << "----------> undershot at # "
      << f+1 << ", t=" << tf[f] << endl;}
  else{cout << endl;}
chi+=pow((res[f]/Cfe[f]/2),2);
cout << "chi=" << chi/nf << endl;

//log file
char dist[20], time[20];
strcpy(dist,name);
strcat(dist,".dist");
ofstream outfile (dist);  // vs. x
outfile.setf(ios::fixed);
for(int i=int(begin/dx);i<int(xi[ni-1]/dx)+1;i++){
  outfile << i*dx << "\t" << C[i][int(0/dt)] << "\t" <<
    C[i][int(tmax/dt)-1] << endl;}
outfile.close();
strcpy(time,name);
strcat(time,".time");
ofstream logfile (time); // vs. t
logfile.setf(ios::fixed);
for(int m=1;m<t_steps;m++){
  logfile << m*dt << "\t" << setprecision(3) <<
    (C[stop][m]) << endl;}
logfile.close();
tempfile.close();

return 0;}
```

Radon in water analysis PERL code

```
#!/usr/bin/perl
#############################################################
#
# This is the standard script used to reduce the data
# from the liquid scint. detector (LSD) in Bennett 11
# A Packard 1500 with RS232 output enabled
# connected to a linux PC running minicom to capture
# the raw output
#
#############################################################
#
# Instructions:
# Capture the LSD output into a file named HH-MM_DD-mon-YY.txt
# Where HH is 24 hour, MM is minute, DD is day, mon is 3 letter
# month and YY is two digit year when LSD was started.
```

```
#
# Another file is made separately named HH-MM_DD-mon-YY.dat
# listing, in the order in the detector, the following:
# sample \tab HH-MM \tab DD-mon-YY
#
# The pump test option is used for samples taken at intervals
# from a pumped water source, such as pumping from a well. This
# enables the elapsed times to be presented in the output.
#
#############################################################

#get modules with perl -MCPAN -e "shell"
use Statistics::Descriptive;
use Time::Piece;
use strict;
my $run, @lines, $line,@temp,$sample,@cpm,@time, $bg, @cpmc;
my @jizz, $index, $jndex, @sum, @ave, $stat, @cpms, $source;
my @name, @starttime, $startdate, $shour, $sminute, @rows;
my $row, @location, @tmp, @sampletime, @eltime, @temptime;
my $timeon, %pumptime=(), $pump_flag, $depth, $pump, $z;
my $code, @realtime, @activity, @specs, $spec,@deviation;
my @amatrix, $staty, $flag=0,@umatrix;

# module used to find calibration factor bewteen
# counts/min and pCi/L
$stat = Statistics::Descriptive::Full->new();
$stat->add_data(118440,59220,11844,0);
#ONLY USING 3 STANDARDS HERE AND WINDOW A

# ask user for base name of data files
print "what base name of date files? (HH-MM_DD-mon-YY)\n";
chomp($source=<STDIN>);
open(OUT,">$source.out"); # output
open(DATA,"$source.dat"); # sample names,collection dates/times
open(FILE,"$source.txt"); # raw output from LSD
chomp(@lines = <FILE>);
close(FILE);
$run=0;

# pull count rate and elapsed time data from LSD data.
STEP: foreach $line(@lines){
  if ($line=~/nuclide/){
    $run++} # nuclide is used once at the start of every run
  if ($line=~/[A-Za-z]/or $line eq ""){  # ignore blank lines
    next STEP}
  if ($line!~/[0-9]/){
```

```
    next STEP}
  @temp=split ' ',$line;
  $cpm[$run-1][$temp[2]-1]=$temp[4];
  $time[$run-1][$temp[2]-1]=$temp[12];}
$index=$#cpm;  # number of runs -1
$jndex=$#{$cpm[0]};  # number of samples -1
for(my $i=0;$i<$index+1;$i++){#find bg from 1 and 5 sample
  $bg+=$cpm[$i][0]+$cpm[$i][4];}
$bg=$bg/(2*($index+1));
printf "background=%.2f cpm\n",$bg;
print "runs=".($index+1)."\nsamples=".($jndex+1)."\n";
for(my $i=0;$i<$index+1;$i++){  #subtract bg
  for(my $j=0;$j<$jndex+1;$j++){
    $cpmc[$i][$j]=$cpm[$i][$j] - $bg;}}
for(my $j=1;$j<4;$j++){ #find K from 2,3,4 sample in LSD tray
  for(my $i=0;$i<$index+1;$i++){
    $sum[$j-1]+=$cpmc[$i][$j];}
  $ave[$j-1]=$sum[$j-1]/($index+1);}

# find slope of line standards concentration vs. count rate
@jizz=$stat->least_squares_fit($ave[0],$ave[1],$ave[2],0);
printf "Calibration=%.2f pCi/L/cpm\n",$jizz[1];
my $lld=(($bg*55)**(1/2))/55*3.3*$jizz[1];
printf "LLD=%.0f pCi/L\n", $lld;

# do indice change to get first sample (6th in tray) to j=0
for(my $j=5;$j<$jndex+1;$j++){
  for(my $i=0;$i<$index+1;$i++){
    $cpms[$i][$j-5]=$cpmc[$i][$j];}}  #cpm of samples

# get start time date from base name of files
@name=split /_/,$source;
@starttime=split /-/,$name[0];
$shour=$starttime[0];
$sminute=$starttime[1];
$startdate=$name[1];
$timeon=Time::Piece->strptime("$startdate\t$shour\t$sminute",
  "%d-%b-%y\t%H\t%M");
chomp(@rows=<DATA>);
close(DATA);
my $k=0;

# get sample collection times from .dat file
foreach $row(@rows){
  @tmp=split /\t/, $row;
  $location[$k]=$tmp[0];
```

```
  $eltime[$k]=$tmp[3];
  $temptime[$k]=Time::Piece->strptime("$tmp[2]_$tmp[1]",
    "%d-%b-%y_%H:%M"); #time of sampling
  $sampletime[$k]=($timeon-$temptime[$k])/60;
  # minutes from sampling to start of counter
  $k++;}
print "Detector started $timeon\n";

# after first run, LSD output only counts elasped time from
# start of run
# following will correct time for additional runs beyond run 1
for(my $i=1;$i<$index+1;$i++){
  for(my $j=0;$j<$jndex+1;$j++){
      $time[$i][$j]+=$time[$i-1][$jndex];}}
for(my $i=0;$i<$index+1;$i++){
  for (my $j=5;$j<$jndex+1;$j++){
      $realtime[$i][$j-5]=$time[$i][$j]+$sampletime[$j-5];}}
      # minutes from sampling to counting

# do a indice transpose and calculate rn concentration and
# uncertainty
for(my $j=0;$j<$jndex-4;$j++){
  for(my $i=0;$i<$index+1;$i++){ #transpose happens here
    $amatrix[$j][$i]=$cpms[$i][$j]*$jizz[1]*exp(0.693/5500*
      $realtime[$i][$j]); # the rn concentration
    # alternative rn calculation calculation below,
    # based on integrated counts over the counted time interval
    # $amatrix[$j][$i]=$jizz[1]*(-.693/5500)*($cpms[$i][$j]*55)/
    # (exp(-0.693/5500*($realtime[$i][$j]+55))-exp(-0.693/5500*
    # ($realtime[$i][$j])));
    if ($cpm[$i][$j+5]==0){next;}
    print "$cpm[$i][$j+5]\t";
    # prints original gross sample count rates to screen
    $umatrix[$j][$i]=$amatrix[$j][$i]*((($cpm[$i][$j+5]+$bg)*55)
      **(1/2))/($cpms[$i][$j]*55);} # uncertainty
  print "\n"; # calculate mean and std. dev. of multile runs.
  my $staty=Statistics::Descriptive::Sparse->new();
  $staty->add_data(@{$amatrix[$j]}[0 .. $index]);
  $deviation[$j]=$staty->standard_deviation();
  $activity[$j]=$staty->mean;}

# option to print all runs, average always gets reported
print "List each run separately? (y/n)\n";
chomp($flag=<STDIN>);
my $j=0;
```

```
# start output report
print OUT "# Detector started $timeon\n# runs=".($index+1).
  "\tsamples=".($jndex+1)."\t";
printf OUT "background=%.2f cpm\n# efficiency=%.2f pCi/L/cpm\t",
  $bg,$jizz[1];
printf OUT "LLD = %.0f pCi/L\n",$lld;
print OUT "# sample\ttime\tdate";

# optional pumping test routine, calculates elapsed time
# from pump start
print "pumping test? (y/n)\n";
chomp ($pump_flag=<STDIN>);
if ($pump_flag eq "y"){
  print "How many pump test in this data? ";
  chomp ($z=<STDIN>);
  for (my $p=1;$p<=$z;$p++){
    print "For what sample code? ";
    chomp ($code=<STDIN>);
    print "Pump on time? (hh-min_dd-mon-yy)\n";
    chomp ($pump=<STDIN>);
    $pumptime{$code}=Time::Piece->strptime("$pump",
      "%H-%M_%d-%b-%y");
    print "Pump on at $pumptime{$code} for the $code well\n";}
  print OUT "\textra";}
  if ($flag eq "y"){
    for (my $i=0;$i<=$index;$i++){
    print OUT "\trun ".($i+1)."\t+/-";}}
print OUT "\taverage\tstdev\n";

# get  elapsed time and depth
foreach $row(@rows){
  print OUT "$row\t";
  if ($pump_flag eq "y"){
    if ($pumptime{$location[$j]}){
      print OUT (($temptime[$j]-$pumptime{$location[$j]})/60).
        "\t";}
    else{
      $depth=substr $location[$j], 3;
      print OUT "$depth\t";}}
  if ($flag eq "y"){
    for (my $i=0;$i<=$index;$i++){
      printf OUT "%.0f\t%.0f\t",$amatrix[$j][$i],
        $umatrix[$j][$i];}}
  printf OUT "%.0f\t%.0f\n",$activity[$j],$deviation[$j];
  $j++;}
close (OUT);
```

BIOGRAPHY OF THE AUTHOR

Vincente Guiseppe was born in West Reading, Pennsylvania on October 14, 1976. He was raised in Plowville, Pennsylvania and graduated from Twin Valley High School in 1995. He attended Millersville University of Pennsylvania and graduated in 1999 with a Bachelor's degree in Physics and a minor in Mathematics. He moved north and entered the Physics graduate program at The University of Maine in the fall of 2000. There he conducted research within the Environmental Research Laboratory.

Upon completion of his degree, Vincente will be a Postdoctoral Research Associate at Los Alamos National Laboratory in New Mexico where he will work on the Majorana experiment. Vincente is a candidate for the Doctor of Philosophy degree in Physics from the University of Maine in December, 2006.